

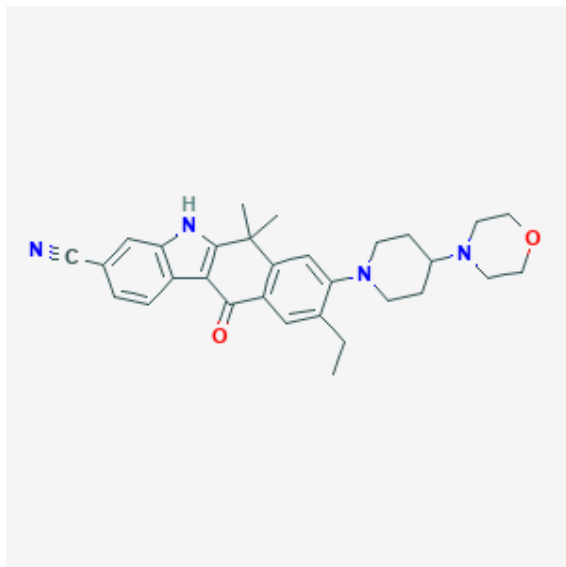
CHAPTER-3: IMPURITY PROFILING, ISOLATION, CHARACTERISATION AND DEGRADATION KINETICS OF IMPURITIES IN ALECTINIB

3.1 INTRODUCTION AND SELECTION OF DRUG

Cancer is the second leading cause of death worldwide according to the World Health Organization data of the year 2018. The most common type of human cancer is lung cancer with estimated 1.76 million deaths in 2018 [1]. About 85% cases of lung carcinoma are from non-small-cell lung cancer (NSCLC) as its dominant type [2]. Platinum-based chemotherapy had been the first-line treatment of this condition. However, severe adverse effects and increased resistance of cancer cells led to various novel therapeutic activities with higher safety and efficacy [3]. Initially, for novel treatment of NSCLC, the first generation of tyrosine kinase inhibitors were used which were not successful in inhibiting the kinase activity of fusion protein, generated between protein echinoderm microtubule-associated protein-like 4 (EML4) and anaplastic lymphoma kinase (ALK). Therefore, recent studies have focused on the discovery and development of new alternative drugs for the treatment of NSCLC including patients with EML4-ALK fusion proteins [4]. Subsequently, crizotinib was the first-generation drug that can be used in the treatment of ALK-positive NSCLC. However, since more and more patients were found to be resistant to this drug, second-generation ALK inhibitors such as ceritinib, alectinib and brigatinib were developed [4]. Amongst these drugs, alectinib (Alecensa) is a second-generation, orally active, potent, and highly selective inhibitor of ALK. In December 2015, alectinib got accelerated approval from the Food and Drug Administration for the treatment of ALK-positive NSCLC and later got regular approval in November, 2017 [5]. Alectinib has been approved for the treatment of ALK fusion-gene positive, unresectable, advanced or recurrent NSCLC in Japan, where it has been given orphan drug designation [6]. International Conference on Harmonization (ICH) has recommended Q1A (R2) and Q1B guidelines to perform forced degradation studies on drug substances to generate all possible degradation products to establish its stability attributes [7-9]. ICH has also recommended Q3A (R2) and Q3B (R2) guidelines to provide requirements of characterization of impurities present at higher than the identification threshold in a drug substance or product [10-12].

3.2 DRUG PROFILE [23-24]:

Molecular structure



IUPAC Name:

9-ethyl-6,6-dimethyl-8-(4-morpholin-4-ylpiperidin-1-yl)-11-oxo-5H-benzo[b]carbazole-3-carbonitrile

Molecular formula:

C₃₀H₃₄N₄O₂

Molecular weight:

482.6

Exact mass: 482.26817634

Monoisotopic mass: 482.26817634

pKa: 7.05

Commercial formulation: Alecensa as 150 mg capsules from Chugai Pharmaceutical Co. Japan which is part of the Hoffmann-La Roche group.

3.3 LITERATURE REVIEW

The literature mentions a validated RP-HPLC method and its validation for the estimation of alectinib in bulk and in pharmaceutical dosage form [13, 14]. The HPLC-PDA (photodiode array) method for the determination of alectinib concentrations in the plasma of adolescent and LC-MS/MS method for estimation of alectinib in human plasma were also reported [15, 16]. None of these methods has employed forced degradation study of alectinib and thereby none of them is capable of estimating alectinib in presence of its degradation products. Hence, the main objective of the current research work was to develop a chromatographic stability indicating method which is efficient to capture alectinib and its degradation products through a well resolved chromatogram and yet having sufficiently less run time. Moreover, it was planned to characterize the generated degradation products by using various sophisticated spectroscopic techniques as no literature was found on the detailed structure elucidation of the degraded products of alectinib which is one of the crucial reasons of the present research work. Hence this analytical method has vast applicability in the pharmaceutical industry for quality control testing of alectinib and its related substances. The method would be extremely helpful to the pharmaceutical industries and academic scientists to identify any of the stated degradants in their drug substance [17-20].

3.4 SECTION-A: ANALYTICAL METHOD DEVELOPMENT AND VALIDATION FOR ESTIMATION OF ALECTINIB IN PRESENCE OF ITS DEGRADATION PRODUCTS BY HPLC.

3.4.1 FORCED DEGRADATION STUDY AND ANALYTICAL METHOD DEVELOPMENT

The forced degradation experiments were performed according to ICH Q1B guidelines to test the stability of alectinib under the following conditions: acidic and alkaline hydrolysis, oxidation, heat and light.

3.4.1.1 EXPERIMENTAL

3.4.1.1.1 Chemicals, reagents and materials

The active pharmaceutical ingredient alectinib was generously provided by Sun Pharmaceuticals Industries Limited., Vadodara, India. Milli-Q water was obtained from the Milli-Q ®Integral water purification system. H₂O₂ 30% (Perhydrol®) for analysis EMSURE® ISO, Merck), HCl 34-37% (Trace Metal grade, Fischer Scientific, UK), NaOH pellets (AR grade, Rankem, Mumbai, India) was utilized for stress degradation studies [21]. Formic acid 98-100% (analytical reagent grade, Rankem, Thane, India) was used for dilution.

3.4.1.1.2 Instruments:

3.4.1.1.2.1 High performance liquid chromatography

The HPLC system (Waters Alliance 2695) equipped with a PDA detector and with the Empower 3.0 software was used for chromatographic studies. The pH of the buffer solution was adjusted using Eutech (Model: PH-510) pH meter. Ultrasonic cleaner (Leelasonic-500) was used for degassing the mobile phase and other solutions.

3.4.1.1.3 Solutions preparation under various degradation conditions for forced degradation study

The sample solutions used for forced degradation study were having concentration of 0.3mg/mL in diluent. The diluent used was a mixture of 0.05 % formic acid (98-100%) in water and acetonitrile in the ratio of 80:20.

3.4.1.1.3.1 Acidic condition

Approximately 3 mg of alectinib was accurately weighed and transferred into 10

mL of volumetric flask; 5mL of 5M HCl solution in water was added. The solution was heated at 60°C for 30 minutes and neutralized with 5M NaOH solution before injection. Finally, the solution was diluted up to the mark with diluent. A blank solution was also prepared under identical conditions omitting the sample in preparation.

3.4.1.1.3.2 Alkali condition

For alkali degradation, approximately 3 mg of alectinib was accurately weighed and transferred into a 10 mL volumetric flask. It was observed that the substance was not completely soluble even in 0.5 mL of 5M NaOH solution. The solution was therefore prepared by adding 0.3mL of formic acid (98.0-100%) to 0.5mL of 5M NaOH solution. The solution was then kept in the water bath at 60 °C for 30 min, again added 1 to 1.5 mL formic acid (98-100%) solution to dissolve the precipitates. The solution was then neutralized with 5M HCl solution and finally diluted up to the mark with diluent before injection. A blank was also prepared under similar conditions omitting the sample in preparation.

3.4.1.1.3.2 Oxidation condition

Approximately 3 mg of alectinib was accurately weighed and transferred into a 10 mL volumetric flask, followed by the addition of 2mL of 30 % H₂O₂ solution. The solution was heated in water bath for 30 minutes at 60°C temperature and diluted up to the mark with diluent. A blank was also prepared under the same condition omitting the sample in preparation.

3.4.1.1.3.3 Preparation of solutions for oxidative degradation for HRMS study:

The HRMS detailed mass analysis study was performed in oxidative degradation condition where 300µg/mL solutions of alectinib were exposed to varied concentration of 1mL of 30% H₂O₂ solutions at 70°C temperature for 30 minutes. Similarly blank and as such sample was also prepared and run in the HRMS instrument system.

3.4.1.1.3.4 Photolytic condition

Approximately 3 mg of alectinib was accurately weighed and transferred into a 10 mL volumetric flask and diluted up to the mark with diluent. Moreover, 50 mg of alectinib was exposed directly to UV-visible light in the photo-stability cabinet for 4 hours duration. Similarly, the blank was also prepared in the same condition omitting the sample in preparation.

3.4.1.1.3.5 Thermal condition

Approximately 3 mg of alectinib was accurately weighed and transferred into a 10 mL volumetric flask, diluted up to the mark with diluent, and exposed to heating at 80 °C for 2 hours. Similarly, the blank was also prepared in the same condition omitting sample in preparation.

Similarly, degradation was also performed with synthetic mixture solution by taking 6.14 mg weight of alectinib synthetic mixture. All the degradation samples were then injected in HPLC system after analytical method development trials and finalization of the analytical conditions and recorded the chromatograms with all the degradation products if generated.

When analytical method development was initiated for alectinib and its degradation products, efforts were made to develop the method on HPLC equipped with UV-PDA detector. However, it was thought that, at first, mobile phase and other conditions which are compatible with MS detector should be used. If satisfactory development achieved with MS compatible method, the same method could be used for later study on structure elucidation. It happens sometimes for complex projects that MS compatible conditions do not serve the purpose of impurities separation. In such cases separate method for LC-UV and LC-MS are developed. In alectinib, however, all the impurities separation was satisfactorily achieved in the method developed with LC-UV-PDA detector as well as for MS detector. Following sections are for experimental and results and discussion of method development trials for LC-UV-PDA method which have been used later in LC-MS and HRMS studies as well:

MS compatible LC method was developed which was started with sample solution

preparation, wavelength maximum selection, stationary phase selection, followed by mobile phase and diluent optimization and peak symmetry optimization. The details are as mentioned below:

3.4.1.1.4 Solutions used for method development

For initial developmental trials, 1000 μ g/mL solution of alectinib was prepared by accurately weighing 10mg of alectinib and transferring into 10mL volumetric flask. It was dissolved in 5 mL of diluent of 0.05% formic acid in the mixture of water and acetonitrile in the ratio of 80:20 and then diluted up to the mark with diluent. However, in the subsequent trial experiments, the concentration of alectinib solution was reduced to 300 μ g/mL by diluting 3mL of 1000 μ g/mL solution up to 10mL with diluent.

The sample solutions were also prepared from synthetic mixture prepared in laboratory as the commercial formulation was not available [23]. The list of excipients used for preparation of synthetic mixture has been shown in Table-3.1. Placebo without active ingredient was also run in the system to check if any peaks were observed with placebo ingredients.

Table-3.1: List of ingredients added for preparation of synthetic mixture[23]

| Sr No. | Ingredient | mg/Capsule |
|--------|-----------------------------------------------|------------|
| 1 | Alectinib Hydrochloride | 161.33 |
| 2 | Lactose Monohydrate | 33.67 |
| 3 | Hydroxypropyl cellulose (HPMC) (Hypromellose) | 15.00 |
| 4 | Sodium Lauryl Sulfate | 75.00 |
| 5 | Carboxymethylcellulose Calcium | 43.55 |
| 6 | Magnesium Stearate | 1.65 |
| | Total weight | 330.2 |

3.4.1.1.5 Analytical wavelength selection

When alectinib degradation solution was run in the PDA detector, the wavelength maxima of alectinib and its major degradation products was acquired from the range of 200-400nm. The peak purity of alectinib was also obtained which showed good level of purity of main peak suggesting no any interference peaks in the main

peak.

3.4.1.1.6 Stationary phase selection:

Initially standard Thermo column Hypersil BDS C18 (250x4.6)mm, 5 μ was used but the peak shape of alectinib obtained was slightly broad. Hence, it was thought to try other brands of C18 column, out of all available columns of Waters, Agilent and Kromasil make, Kromasil C18 (250x4.6)mm, 5 μ was found appropriate when multiple injections of solutions of alectinib was injected and run in the system.

3.4.1.1.7 Mobile phase and diluent optimization:

The physicochemical parameters of alectinib suggest that the pKa value of alectinib is 7.05. Hence it was thought to keep the buffer pH of the mobile phase to 7.00. The first target was to develop MS analytical compatible method so that it would be easy to identify all the degradation products peaks in MS detector at later stage of structure elucidation. Out of all the volatile buffers which could have pH of 7.00, ammonium formate buffer was selected as it can give the neutral pH with formic acid easily. The physicochemical parameters of alectinib suggest that alectinib is poorly soluble in aqueous medium. Hence it was tried to dissolve in acidic medium. To formulate the diluent with acidic medium with MS compatible mobile phase, initially it was thought to take 0.1% formic acid in the mixture of water and acetonitrile in the ratio of 50:50. But it was decided to reduce the formic acid and acetonitrile concentration in the mixture as minimum as possible. With this in mind, when tried, it was found that it was freely soluble in the solution of 0.05% formic acid in the mixture of water and acetonitrile in the ratio of 80:20. At the later stage of LC chromatography development, it was also noticed that proper peak symmetry was observed with this diluent.

3.4.1.1.7.1 Trial-1

Experimental trial-1 was initiated with mobile phase-A as buffer solution (10mM ammonium formate of pH adjusted to 7.00 with 0.25 % ammonia solution in water) and mobile phase-B as acetonitrile and 1000 μ g/mL solution of alectinib was run with gradient run starting with 0.0% of Mobile phase-B to 100% of Mobile phase-B at 50 minutes with flow rate of 1.0 mL/min. The injection volume was kept at 20 μ l and the column was selected as Kromasil C18 (250x4.6)mm, 5 μ (Make: Akzonobel).

3.4.1.1.7.2 Trial-2

Since the peak of alectinib was eluted very late in the chromatogram, gradient was modified to start at 50% of mobile phase-B and reaching at 100% of mobile phase-B at 50 minutes with flow rate of 1.0 mL/min.

3.4.1.1.7.3 Trial-3

Even though alectinib peak was eluted at around 15 minutes which is acceptable but some impurities peaks observed after degradation were found merged between 5-10 minutes duration. For better separation of these impurities and improvement in peak shape of alectinib, mobile phase-A composition was optimized to a mixture of buffer (10mM ammonium formate of pH adjusted to 7.00 with 0.25 % ammonia solution in water) and acetonitrile in the ratio of 95:5. Mobile phase-B composition was optimized to a mixture of buffer (10mM ammonium formate of pH adjusted to 7.00 with 0.25 % ammonia solution in water) and acetonitrile in the ratio of 25:75. The gradient program was kept as same, linear as mentioned in trial-2 experiment but the total run time was reduced to 35 minutes by increasing the flow rate from 1.0 mL/minutes to 1.5 mL/minutes.

3.4.1.1.8 Peak symmetry optimization:

For further improvement of peak sharpness, column temperature was tried to increase to 50°C. Moreover, due to overshooting of the alectinib solution of 1000µg/mL, it was decided to reduce the concentration of alectinib to 300µg/mL so that its response can be accommodated in the chromatogram and linearity at higher level (150% level) can be satisfactorily achieved.

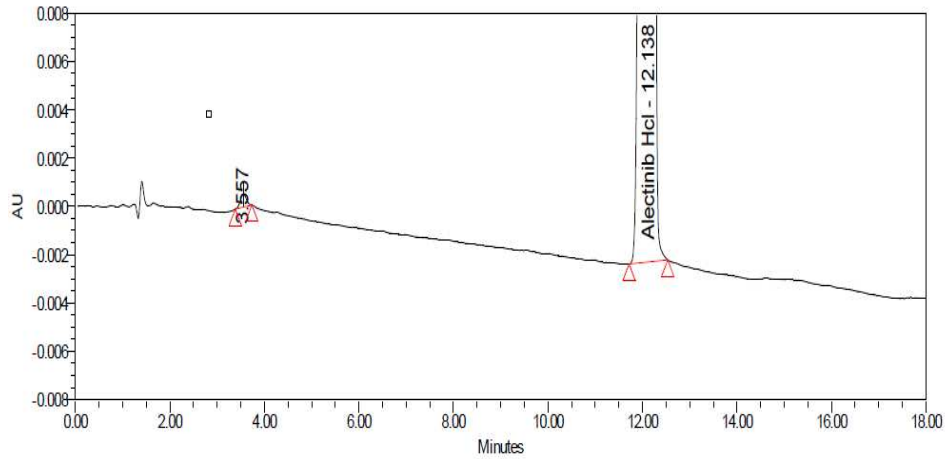
3.4.1.2 RESULTS AND DISCUSSION:

Alectinib was found to be stable in all the degradation conditions except oxidation. Oxidative stress degradation generated four degradation products which were isolated by preparative-HPLC and then efforts were made to elucidate their structure by studying various spectroscopic data (Figure-3.1-A to 3.1-G).

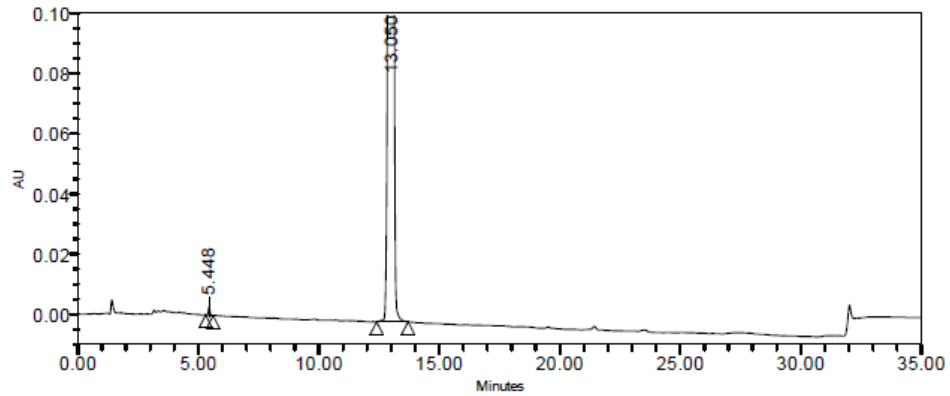
The chromatogram of standard alectinib sample showed a peak at RT 3.557 minutes (Figure-3.1-A). Except oxidation degradation condition, alectinib drug was found to be stable in all the other conditions.

Figure -3.1(A) to 3.1(G). Chromatograms of alectinib under forced degradation conditions such as acid (B), alkali (C), oxidative (D), photolytic (E, F), and thermal (G)

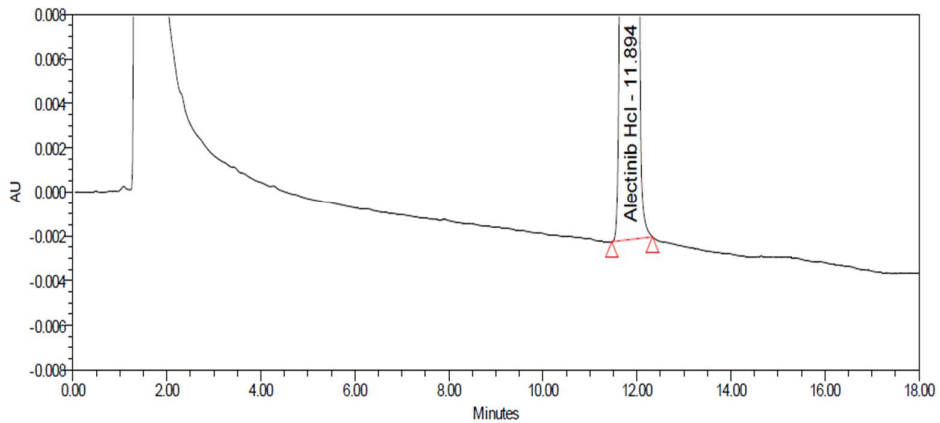
A. Alectinib chromatogram



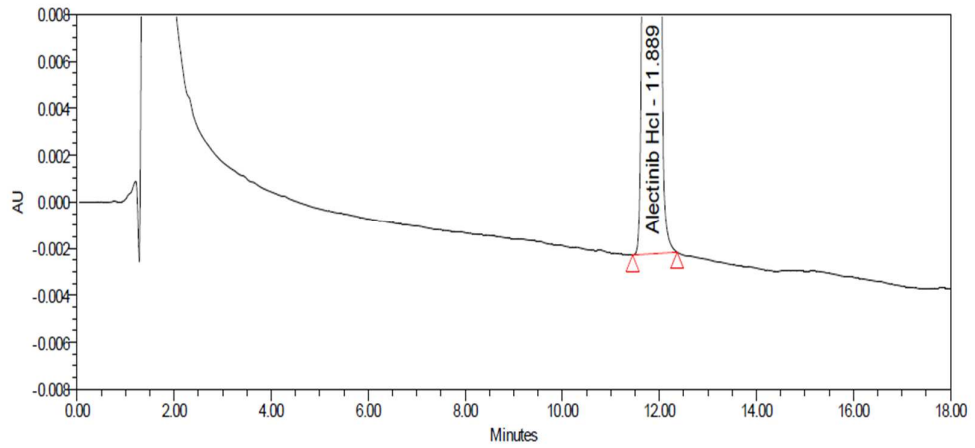
A. Chromatogram of alectinib synthetic mixture containing other excipients



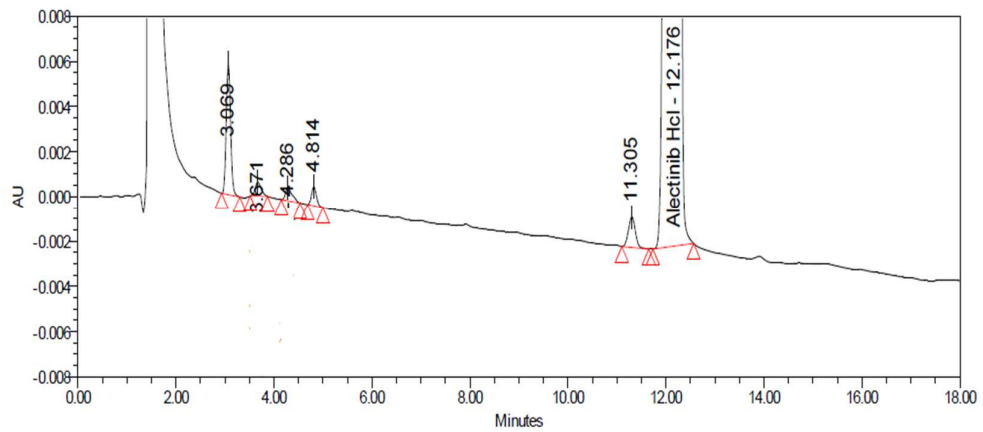
B. Acid degradation



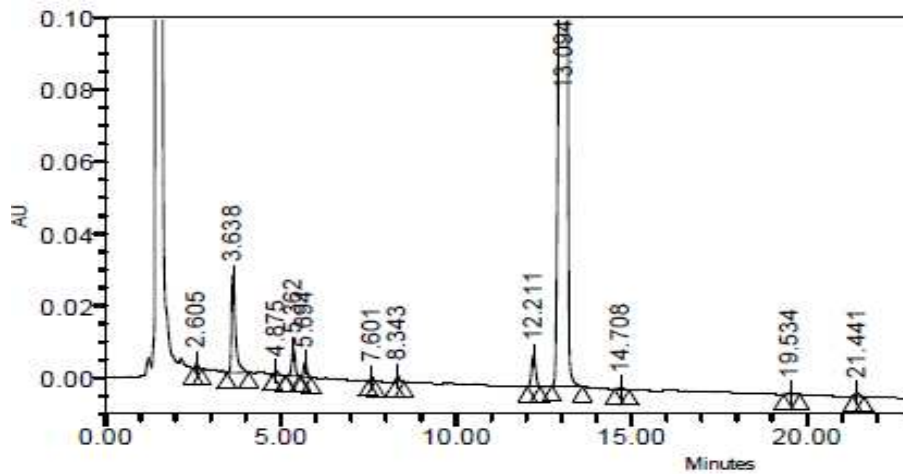
C. Alkali degradation



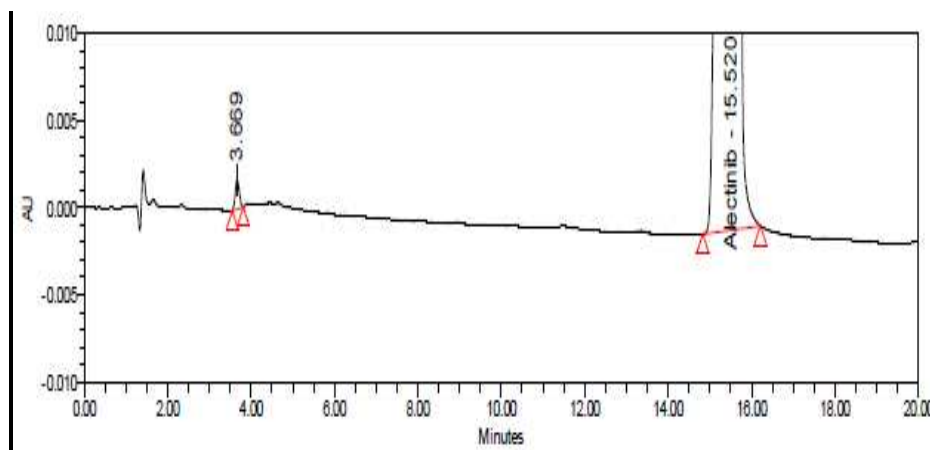
D. Oxidative degradation



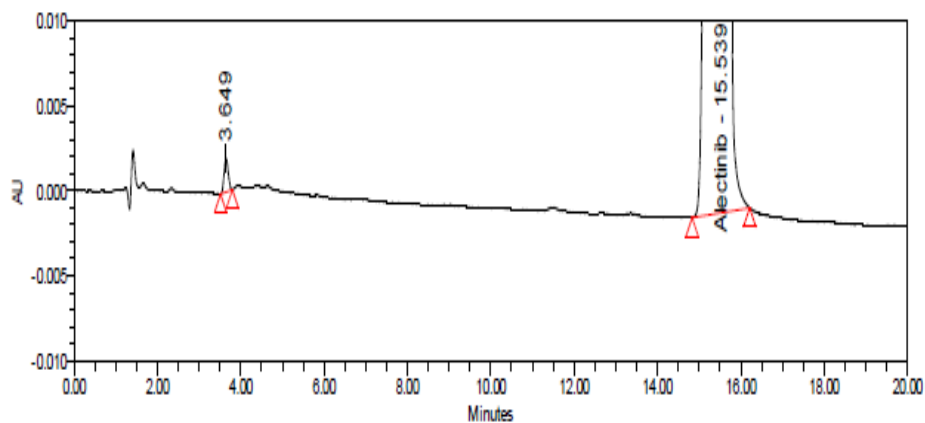
D1. Synthetic mixture in oxidative degradation condition



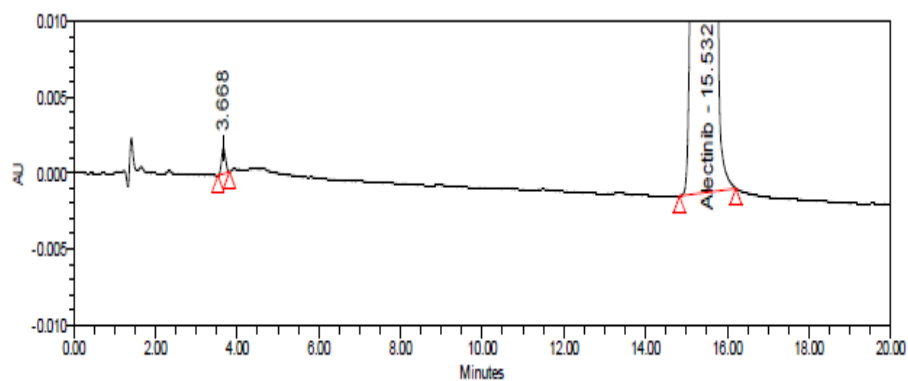
E. Photolytic degradation: direct drug substance



F. Photolytic degradation: Sample solution



G. Thermal degradation



The summary of degradation study is shown in Table-3.2. In oxidative degradation condition, it gets degraded in the range of 2% to 63.69% depending on the

exposure to H₂O₂ and time duration at heating. However, with optimized degradation condition, four major degradation products were observed in the chromatogram (Figure-3.1-D) at RT about 3.069, 4.286, 4.814, and 11.305 minutes. Similar degradation products generation was also noted with synthetic mixture of alectinib with other excipients. Out of these four, major degradation products, DP at 3.069 and 11.035 are most prominent and easily generated degradation products. All of these four degradation products were characterized and discussed in individual sections in this chapter.

Table-3.2: Degradation products summary of DPs initially identified through LCMS and NMR based study

| Degradation products | RT of Impurity | RRT | Observed molecular ion peak (m/z) | % observed |
|----------------------------|----------------|------|-----------------------------------|--------------|
| DP-1 (N-oxide) | 4.65 | 0.30 | 499.15 | 0.11 |
| DP-2 (Epoxide) | 14.27 | 0.91 | 499.26 | 9.86 |
| DP-3 (N-hydroxy) | 3.17 | 0.20 | 499.19 | 8.83 |
| DP-4 (Amide) | 3.63 | 0.23 | 501.27 | 1.84 |
| alectinib | 15.63 | 1.00 | 483.32 | 70.17 |
| Other degradation products | | | | 8.83 |
| Mass balance | | | | 99.64 |

Following is the results and discussion obtained from method development trial experiments and then final analytical conditions for LC-MS, HRMS and NMR instrument methods.

3.4.1.2.1 Analytical wavelength selection:

The λ_{\max} of alectinib was found to be 230nm whereas the λ_{\max} of degradation products were near to 230nm. Hence based on this, the final wavelength of the analytical method was set as 230nm for better UV response in the chromatogram.

3.4.1.2.2 Mobile phase and diluent optimization:

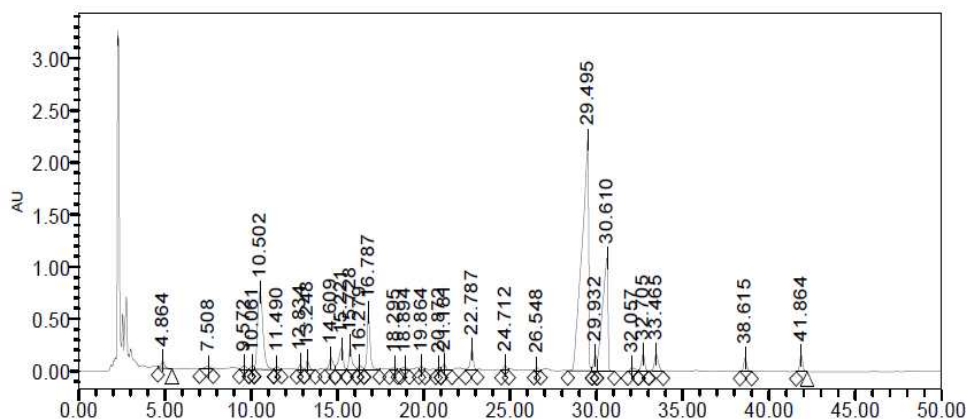
After a number of preliminary trials, gradient elution using mobile phase-A and mobile phase-B were finalized. The linear gradient used was the gradient program

with 50% of mobile phase-B increasing to 100% of mobile phase-B at 30 minutes.

3.4.1.2.2.1 Trial-1:

The initial trial experiment was linear gradient program starting with 0.0% of mobile phase-B (acetonitrile) to 100% of mobile phase-B (acetonitrile) at 50 minutes and it was run to check the elution of alectinib in the chromatogram and take the base for further optimization. Mostly, any organic compound elution pattern can be checked with this trial so that its elution behavior can be preliminary identified. As shown in Figure-3.2 Chromatogram of trial-1, alectinib was eluted very late at around 29.495 minutes. This suggests that the organic ratio in the chromatogram run should be increased so that its elution can be earlier in the chromatogram.

Figure-3.2: Chromatogram of trial-1 experiment showing very late elution of alectinib peak



Chromatographic conditions:

Column: Kromasil C18 (250x4.6)mm, 5 μ (Make: Akzonobel).

Mobile phase: Mobile phase-A as buffer solution (10mM ammonium formate of pH adjusted to 7.00 with 0.25 % ammonia solution in water) and mobile phase-B as acetonitrile

Detection wavelength: 230nm

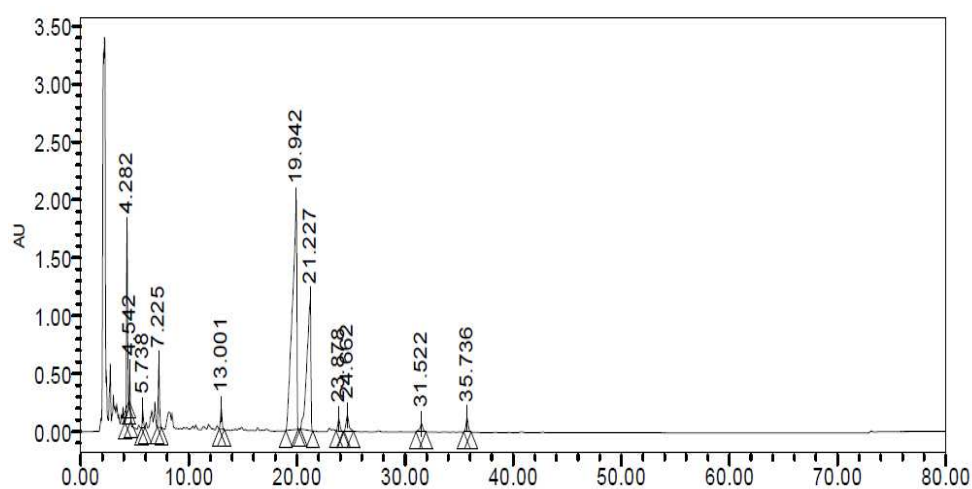
Gradient and flow rate: Gradient run starting with 0.0% of Mobile phase-B to 100% of Mobile phase-B at 50 minutes with flow rate of 1.0 mL/min

3.4.1.2.2.2 Trial-2:

Mobile phase-A continued as buffer solution (10mM ammonium formate of pH adjusted to 7.00 with 0.25 % ammonia solution in water) and mobile phase-B as

acetonitrile. Based on the observation from trial-1, when gradient was started with 50% of mobile phase-B (acetonitrile) and going with the same gradient pattern, it improved the retention time of alectinib. However, at the same time the impurity profile of other impurities in the chromatogram should not be ignored hence it was reviewed and found that the impurities between 5-10 minutes were not well separated with this gradient and peak shapes of alectinib and other degradation products were also slightly broad. (Figure-3.3) This suggests further improvement in mobile phase and gradient program.

Figure-3.3: Chromatogram of trial-2 experiment showing alectinib elution at around 15 minutes but other impurities peaks get merged between 5-10 minutes.



Chromatographic conditions:

Column: Kromasil C18 (250x4.6)mm, 5 μ (Make: Akzonobel).

Mobile phase: Mobile phase-A as buffer solution (10mM ammonium formate of pH adjusted to 7.00 with 0.25 % ammonia solution in water) and mobile phase-B as acetonitrile

Detection wavelength: 230nm

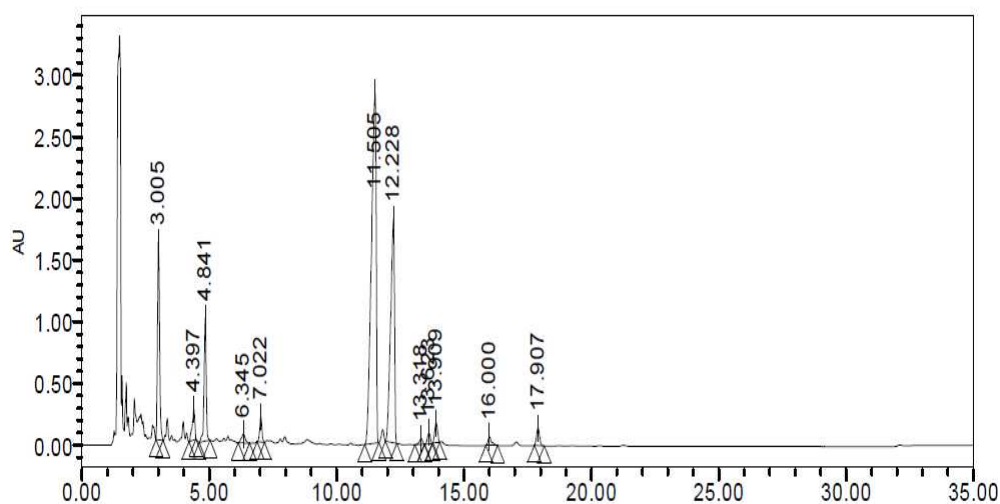
Gradient and flow rate: Gradient run starting with 50.0% of Mobile phase-B to 100% of Mobile phase-B at 50 minutes with flow rate of 1.5 mL/min

3.4.1.2.2.3 Trial-3:

Based on the observation from trial-2 experiment, it was thought to mix the buffer and acetonitrile in the composition of mobile phase-A (a mixture of buffer (10mM ammonium formate of pH adjusted to 7.00 with 0.25 % ammonia solution in water) and acetonitrile in the ratio of 95:5) and mobile phase-B (a mixture of buffer

(10mM ammonium formate of pH adjusted to 7.00 with 0.25 % ammonia solution in water) and acetonitrile in the ratio of 25:75). as it always gives better separation when a mixture of buffer and acetonitrile is chosen instead of only buffer or only acetonitrile as the mobile phase. As shown in Figure-3.4, this composition of mobile phase and gradient program have not only improved the peak shape and resolution between degradation products and alectinib but also reduced the total run time.

Figure-3.4: Chromatogram of trial-3 experiment showing proper elution pattern of the alectinib and its degradation products.



Chromatographic conditions:

Column: Kromasil C18 (250x4.6)mm, 5 μ (Make: Akzonobel).

Mobile phase: Mobile phase-A as buffer solution (10mM ammonium formate of pH adjusted to 7.00 with 0.25 % ammonia solution in water) and mobile phase-B as acetonitrile

Detection wavelength: 230nm

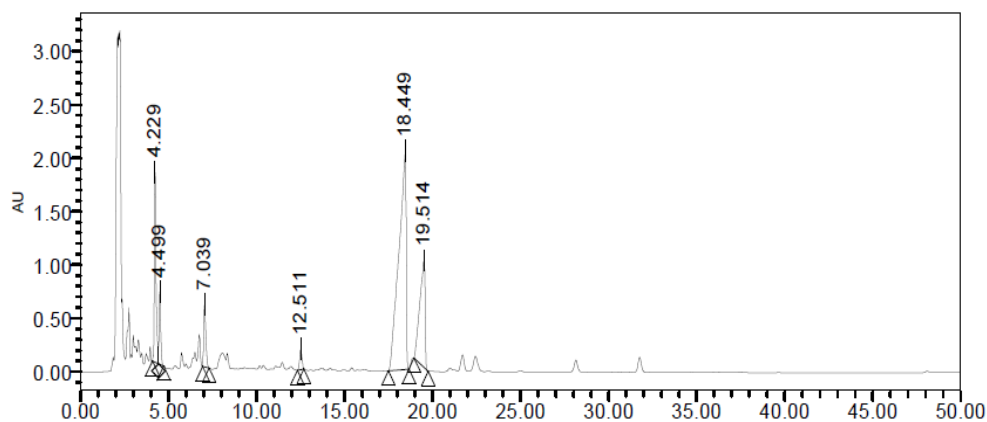
Gradient and flow rate: Gradient run starting with 50.0% of Mobile phase-B to 100% of Mobile phase-B at 25 minutes with flow rate of 1.5 mL/min

3.4.1.2.2.4 Peak symmetry optimization:

The peak response of 1000 μ g/mL of alectinib solution was large and peak height reached beyond 1.0 AU. While the alectinib concentration was reduced to 300 μ g/mL, it gave proper response in the range of chromatographic height range so that linearity and recovery at 150% level would be observed satisfactory at the later stage of method validation. Moreover, the effect of column temperature on chromatogram is shown in Figure-3.5 and 3.6. The peak shape with column at room temperature was broad whereas the peak shape with column at 50°C column

temperature was found sharp and appropriate with increased theoretical plates and other peak symmetry parameters.

Figure-3.5: Broad peak shape with column at RT



Chromatographic conditions:

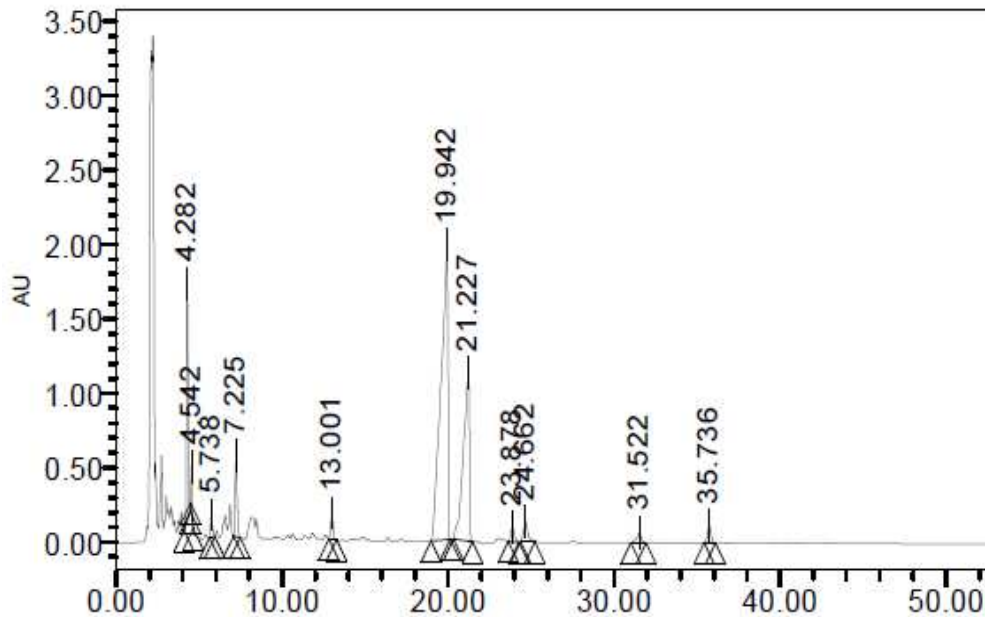
Column: Kromasil C18 (250x4.6)mm, 5 μ (Make: Akzonobel).

Column temperature: RT

Mobile phase: Mobile phase-A (a mixture of buffer (10mM ammonium formate of pH adjusted to 7.00 with 0.25 % ammonia solution in water) and acetonitrile in the ratio of 95:5) and mobile phase-B (a mixture of buffer (10mM ammonium formate of pH adjusted to 7.00 with 0.25 % ammonia solution in water) and acetonitrile in the ratio of 25:75).

Gradient and flow rate: Gradient run starting with 0.0% of Mobile phase-B to 100% of Mobile phase-B at 50 minutes with flow rate of 1.0 mL/min

Figure-3.6: Improved peak shape with column at 50°C



Chromatographic conditions:

Column: Kromasil C18 (250x4.6)mm, 5 μ (Make: Akzonobel).

Column temperature: 50°C

Mobile phase: Mobile phase-A (a mixture of buffer (10mM ammonium formate of pH adjusted to 7.00 with 0.25 % ammonia solution in water) and acetonitrile in the ratio of 95:5) and mobile phase-B (a mixture of buffer (10mM ammonium formate of pH adjusted to 7.00 with 0.25 % ammonia solution in water) and acetonitrile in the ratio of 25:75).

Gradient and flow rate: Gradient run starting with 0.0% of Mobile phase-B to 100% of Mobile phase-B at 50 minutes with flow rate of 1.0 mL/min

3.4.1.2.5 Final analytical conditions for HPLC-UV-PDA method which is also MS compatible

Kromasil C18 (250 X 4.6) mm, i.d., 5 μ (Make: Akzonobel) column was maintained at 50 °C temperature during analysis. The mobile phase-A was composed of 10mM ammonium formate buffer (the pH was adjusted to 7.00 with 0.25 % ammonia solution in water) and acetonitrile in the ratio of 95:05. The mobile phase-B was a mixture of 10mM ammonium formate buffer (the pH was adjusted to 7.00 with 0.25 % ammonia solution in water) and acetonitrile in the ratio of 25:75. The gradient program was planned as a linear gradient program (Time/%B) which was set at 0.00/50, 25.0/100, 30.0/100, 30.1/50, 35.0/50. The injection volume and flow rate were set as 20 μ l and 1.5mL/min respectively. The appropriate response of alectinib and its degradation products were observed at a

detection wavelength of 230nm. The chromatographic conditions in both HPLC and LC-MS/MS studies were identical as the conditions were compatible with LC-MS/MS instrument. Mass spectrometric conditions were set as: capillary voltage: 3.5kV, cone voltage: 15V and 30V, extractor voltage: 1.00 V, RF lens: 0.4V, source temperature: 110°C, desolvation temperature: 350°C, cone gas flow: 25 L/Hr, desolvation gas flow: 650 L/Hr, collision energy: 2.0eV.

3.4.2 ANALYTICAL METHOD VALIDATION

Method validation experiments were conducted as per ICH guideline Q2 (R1) [13] and parameters such as linearity, sensitivity, accuracy, method precision, robustness and specificity were performed.

3.4.2.1 EXPERIMENTAL

The experimental details of each of the method validation parameters are as follows:

3.4.2.1.1 Linearity

Linearity is the first most parameter to check whether developed LC method is giving linear response of alectinib or not. Linearity of the developed method was determined by preparing the different concentrations of alectinib solutions in the range of 75µg/mL to 450µg/mL. All the experiments were performed in triplicate. Calibration curve was plotted between the area response observed and the concentration. Correlation coefficient was calculated from the calibration curve. For good linear calibration curve, correlation coefficient should be more than 0.99.

3.4.2.1.2 Sensitivity

Limit of detection (LOD) is defined as the lowest possible concentration of the sample which can be detected by the specified analytical method. Limit of quantitation (LOQ) is defined as the lowest possible concentration which can be reliably quantified by the specified analytical method. Theoretically based on the linearity curve, the LOD and LOQ were also calculated by the formula as per ICH Q2 (R1) guideline. The $LOD = 3.3 \times \sigma/S$ and $LOQ = 10 \times \sigma/S$ where σ is standard deviation of intercept from the calibration curve and S is mean slope of the calibration curve.

3.4.2.1.3 Accuracy

The accuracy is the parameter whereby method is challenged to check whether the method is capable of measuring the concentration of alectinib accurately in the range of 50% to 150% of 300 μ g/mL level concentration or not. The accuracy of the method was determined by the standard addition method whereby the 50%, 100% and 150% level concentration was spiked into the pre-quantified sample mixture of alectinib. The spiked solutions were prepared in triplicate sets at each level, injected into the system and the %recovery was calculated at each of the three levels.

3.4.2.1.4 Precision

Method precision is to check for the consistent performance of method in terms of getting response of same concentration solutions injected multiple times in the LC system. It was performed by injecting six replicate sample preparation of sample preparation of 300 μ g/mL concentration. Moreover, it was additionally performed by injecting three different levels of spiked samples at 50%, 100% and 150% levels of 300 μ g/mL in triplicate. The %RSD was calculated from the response observed at each level.

3.4.2.1.5 Robustness:

Robustness was studied by applying small but deliberate changes in flow rate. The flow rate was changed up to +/-0.05mL/min and the effects on the results were monitored. The robustness of the method was estimated in the sample solution of 300 μ g/mL concentration and the retention time, peak shape, theoretical plates and tailing factor were compared.

3.4.2.1.6 Specificity

Specificity was ascertained by performing forced degradation study and identification of elution of the degradation products in the chromatograms. Forced degradation study was performed for acidic, basic, oxidative, thermal and UV light exposure. The separation of any degradation products generated in any of the degradation conditions mentioned is the prime goal of specificity study to prove that the method is capable of estimation of alectinib response in presence of its degradation products.

3.4.2.2 RESULTS AND DISCUSSION

The results obtained for each of the parameters of linearity, sensitivity, accuracy, method precision, robustness and specificity were obtained satisfactorily within the specifications:

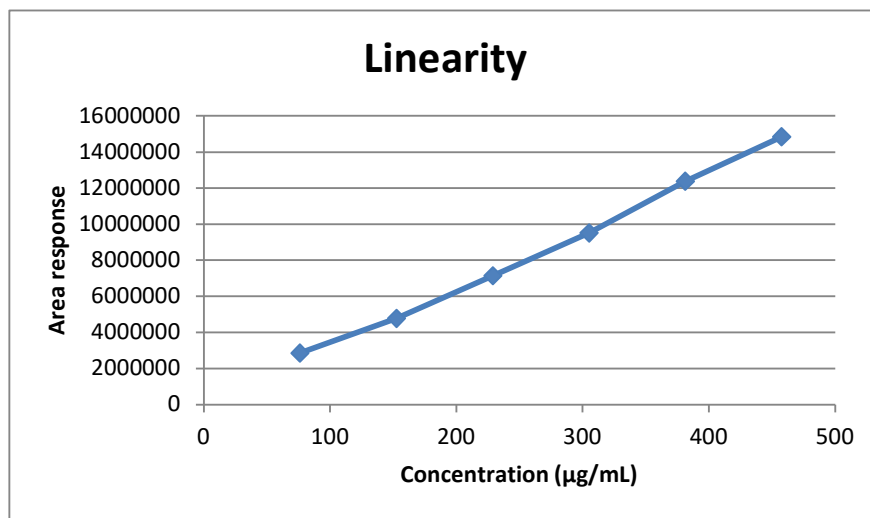
3.4.2.2.1 Linearity

The method was found to be linear in the range of 75µg/mL to 450µg/mL as the correlation coefficient of calibration curve between area response verses concentration was found to be 0.9983. The regression data are mentioned in Table-3.3 and calibration curve in Figure-3.7 demonstrating good linear relationship between specified concentration and response observed.

Table-3.3: Mean area response observed for various linearity levels:

| Linearity level | Concentration (µg/mL) | Mean area response |
|-----------------------------------|-----------------------|--------------------|
| 25% | 75.00 | 2859954 |
| 50% | 150.00 | 4765721 |
| 75% | 225.00 | 7132723 |
| 100% | 300.00 | 9513512 |
| 125% | 375.00 | 12382972 |
| 150% | 450.00 | 14835348 |
| Slope (S) | | 31880.69935 |
| Intercept | | 70753.80000 |
| Correlation Coefficient(r) | | 0.9983 |
| Standard deviation | | 4556877.5075 |
| LOD (µg/mL) | | 4.72 |
| LOQ (µg/mL) | | 14.29 |

Figure-3.7: Linearity curve



3.4.2.2.2 Sensitivity (LOD and- LOQ)

As per ICH guideline, the LOQ level at least below 50% level of target concentration is accepted for the method to be passed for method validation. Based on theoretical formula as per the ICH guideline, LOD was calculated as 4.72% level (1.57µg/mL) and LOQ was calculated as 14.29% level (4.76µg/mL). The results obtained are well within the specifications as per ICH guideline.

The calculated values of LOD and LOQ suggest that the method can be sufficiently sensitive, but considering that the method was applied to study degraded samples, the linearity range was obtained at a higher level.

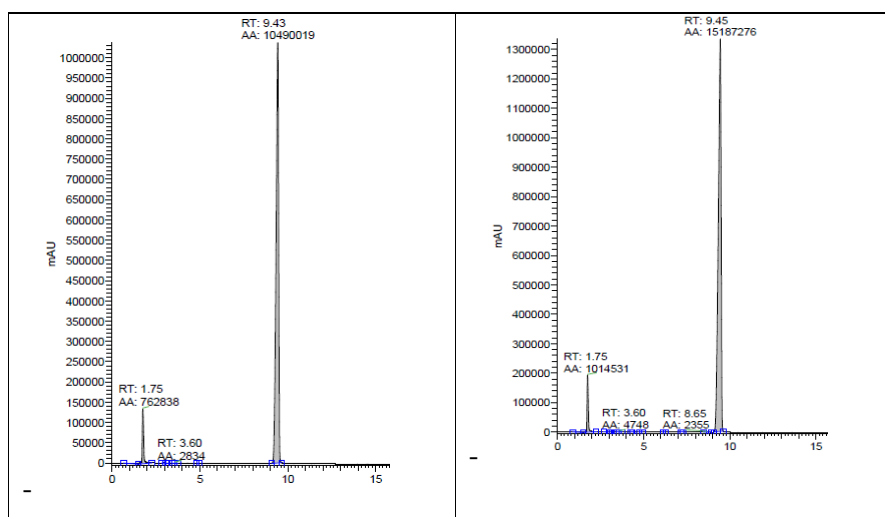
3.4.2.2.3 Accuracy

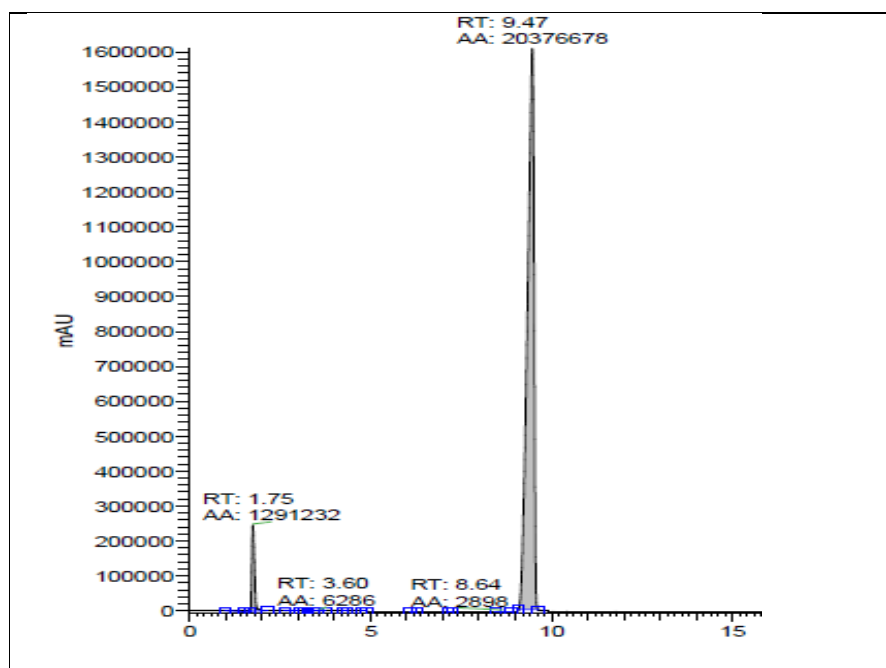
As such there is no any exact specifications of Recovery however; %recovery obtained between 75% to 125% which is considered reasonably acceptable with consideration of analytical errors and other matrix effects. As per the recovery experiment performed, the % recovery at the levels of 50%, 100% and 150% were obtained in the range of 108.49% to 120.34% which proves that the method is capable of estimating the content accurately near to true value as shown in Table-3.4 and Figure-3.8.

Table-3.4: %Recovery results obtained for 50%, 100% and 150% level:

| Accuracy level | Area of as such sample | %Amount spiked in as such sample | Observed area response | Area difference between recovered and as such sample | As such % recovery | % Recovery | Mean of area response | Standard deviation | % RSD |
|----------------|------------------------|----------------------------------|------------------------|------------------------------------------------------|--------------------|---------------|-----------------------|--------------------|-------|
| 50% Set-1 | 4765721 | 50.00 | 10490019 | 5724298 | 60.17 | 120.34 | 5536932.00 | 171749.4 | 3.10 |
| 50% Set-2 | 4765721 | 50.00 | 10265258 | 5499537 | 57.81 | 115.62 | | | |
| 50% Set-3 | 4765721 | 50.00 | 10152682 | 5386961 | 56.62 | 113.25 | | | |
| 100% Set-1 | 4765721 | 100.00 | 15187276 | 10421555 | 109.54 | 109.54 | 10355541.67 | 67237.21 | 0.65 |
| 100% Set-2 | 4765721 | 100.00 | 15052865 | 10287144 | 108.13 | 108.13 | | | |
| 100% Set-3 | 4765721 | 100.00 | 15123647 | 10357926 | 108.88 | 108.88 | | | |
| 150% Set-1 | 4765721 | 150.00 | 20376678 | 15610957 | 164.09 | 109.39 | 15563764.33 | 71825.6 | 0.46 |
| 150% Set-2 | 4765721 | 150.00 | 20364953 | 15599232 | 163.97 | 109.31 | | | |
| 150% Set-3 | 4765721 | 150.00 | 20246825 | 15481104 | 162.73 | 108.49 | | | |

Figure-3.8: Chromatogram of Recovery at 50% level, 100% level and 150% level.





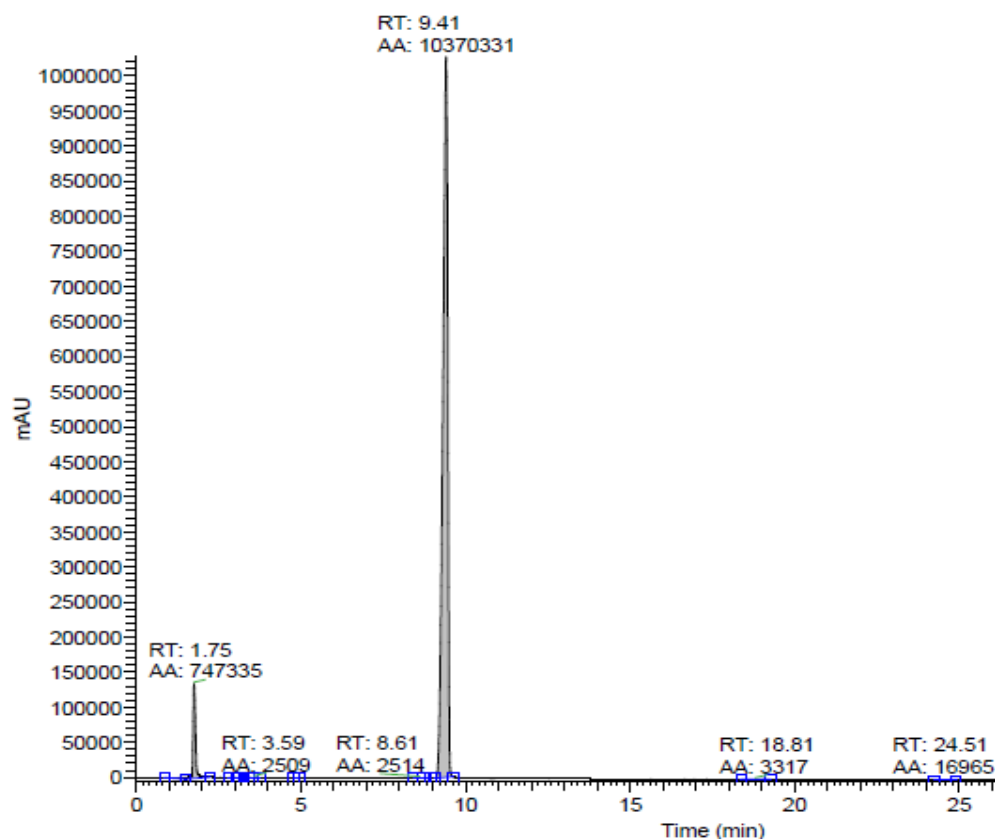
3.4.2.2.4 Precision

The %RSD of response observed for replicate preparation of 300 μ g/mL concentration suggest the variability of the method between the measurements. The % RSD of the six replicate- sample preparation at 100% level solutions was obtained as 0.34% (Table-3.5). The %RSD of the response obtained at 50%, 100% and 150% level concentration was found in the range of 0.46% to 3.10%. Each kind of precision study results proved that the method is capable of giving precise results over entire range of concentrations. (Figure-3.9)

Table-3.5: Method precision results

| Method precision set | Area response observed |
|---------------------------|------------------------|
| Set-1 | 10370331 |
| Set-2 | 10418306 |
| Set-3 | 10435538 |
| Set-4 | 10423901 |
| Set-5 | 10458432 |
| Set-6 | 10473319 |
| Mean | 10429971.17 |
| Standard deviation | 35916.34 |
| %RSD | 0.34 |

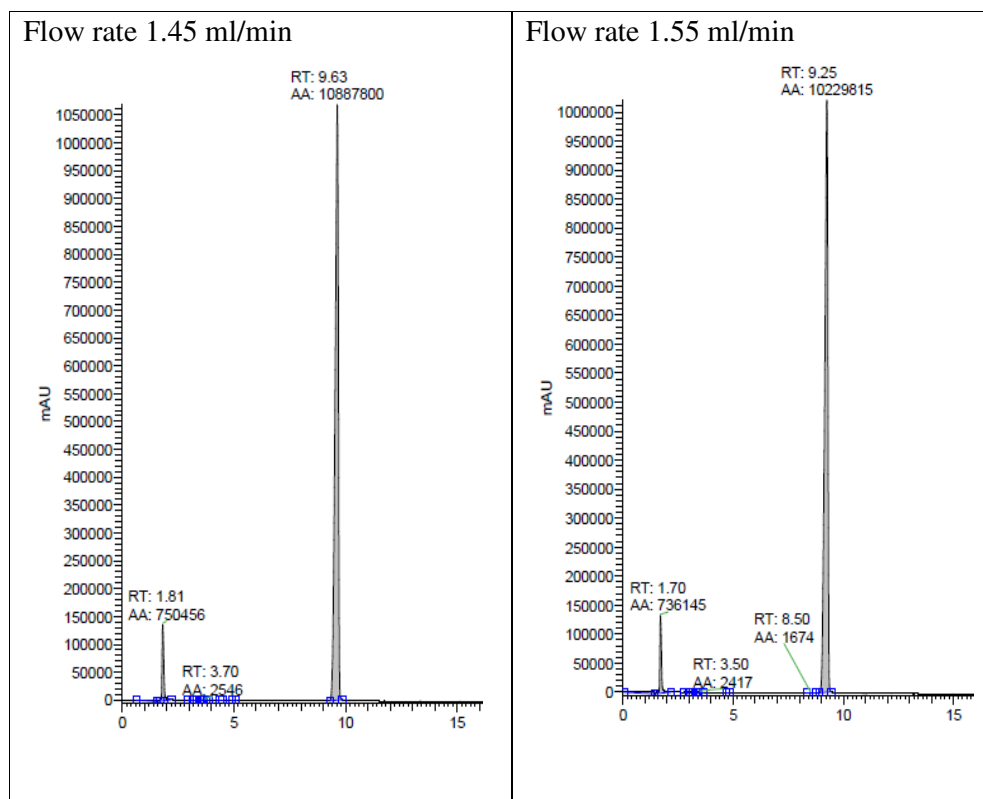
Figure-3.9: Chromatogram of Method precision set-1:



3.4.2.2.5 Robustness

The chromatogram results were observed at flow rate of 1.45 mL/min, 1.55 mL/min (Figure-3.10). The peak shape obtained proper in each of the variations. The theoretical plates, tailing factor and retention times obtained were compared with that of actual method of analysis parameters. These results did not observe to be varied extensively as shown in Figure-3.10. Hence proposed analytical method was proved to be robust.

Figure-3.10: Chromatogram of Robustness flow rate modifications



3.4.3 IDENTIFICATION OF DEGRADATION PRODUCTS BY HRMS

After confirmation of degradation in oxidative condition, oxidative degradation sample was run in LC-MS and HRMS instrument to obtain the exact mass and fragmentation pattern of degradation products.

3.4.3.1 Analytical condition and instrument parameters for HPLC and LC-MS

The liquid chromatography-mass spectroscopy system (LC-MS/MS) of Waters Micro-mass with ZQ-Mass detector and electro-spray ionization mode was used. As MS compatible method was developed as mentioned section 3.4.1, the same analytical conditions and instrument parameters were applied for HPLC and LC-MS instrument analysis.

3.4.3.2 Analytical conditions and instrument parameters for High resolution mass spectrometry

The high-resolution mass spectrometry (HRMS) Orbitrap Q-Exactive plus of

Thermo system was used for identification of fraction masses of impurities observed in degradation studies.

The instrument and method parameters were similar to those mentioned in LC-MS. Other instrument method parameters specifically for HRMS instruments were set as shown in Table-3.6:

Table-3.6: HRMS Instrument method parameters:

| Full MS / dd-MS² (TopN) | |
|-------------------------------------------|-------------------------------|
| General | Full MS |
| Runtime: 0 to 35 min | Microscans 1 |
| Polarity: Positive and Negative | Resolution 70,000 |
| In-source CID: 0.0 eV | AGC target 1e6 |
| Default charge state: 1 | Maximum IT 100 ms |
| Inclusion — NA | Number of scan ranges 1 |
| Exclusion — NA | Scan range 100 to 1000 m/z |
| Tags — NA | Spectrum data type Profile |
| dd-MS² / dd-SIM | dd Settings |
| Microscans 1 | Minimum AGC target 5.00e3 |
| Resolution 17,500 | Intensity threshold 5.0e4 |
| AGC target 5e5 | Apex trigger — |
| Maximum IT 100 ms | Charge exclusion — |
| Loop count 5 | Multiple charge states all |
| MSX count 1 | Peptide match preferred |
| TopN 5 | Exclude isotopes on |
| Isolation window 2.0 m/z | Dynamic exclusion 30.0 s |
| Isolation offset 0.0 m/z | If idle .. do not pick others |
| Scan range 200 to 2000 m/z | |
| Fixed first mass — | |
| (N)CE / stepped (N)CE nce: 30 | |
| Spectrum data type Profile | |
| Tune page parameters | |
| Scan type | Full MS |
| Source | HESI Source |
| Sheath gas flow rate | 60 |
| Aux gas flow rate | 20 |
| Sweep gas flow rate | 0 |
| Spray voltage (kV) | 3.5 |
| Spray current (μA) | 0 |
| Capillary temperature (°C) | 320 |
| S-lens RF level | 55 |
| Aux gas heater temp (°C) | 450 |

Other than the degradation products generated initially in HPLC, there are other many minor degradation products generated in oxidative condition which have been identified and characterized through HRMS studies and are summarized in Table-3.7.

Table-3.7: Degradation products summary of DPs identified through HRMS based study

| Degradation products | RT of Impurity | RRT | Observed molecular ion peak (m/z) |
|----------------------|----------------|------|------------------------------------|
| DP-5 | 2.09 | 0.22 | 515.2649 |
| DP-6 | 2.26 | 0.23 | 503.2647 |
| DP-7 | 2.36 | 0.24 | 533.2755 |
| DP-3 (N-hydroxy) | 2.73 | 0.28 | 499.2698 |
| DP-8 | 3.54 | 0.36 | 517.2803 |
| DP-9 | 3.82 | 0.39 | 499.2699 |
| DP-1 (N-oxide) | 4.13 | 0.42 | 499.2699 |
| DP-10 | 5.23 | 0.54 | 361.1142 (negative) |
| DP-11 | 6.01 | 0.62 | 377.1087(negative) |
| DP-12 | 6.97 | 0.72 | 499.2703 |
| DP-2 (Epoxide) | 8.88 | 0.91 | 499.27 |
| Main peak | 9.72 | 1.00 | 483.275 |
| DP-13 | 10.9 | 1.12 | 487.2700 499.2698 |
| DP-14 | 11.35 | 1.17 | 499.27 |
| DP-15 | 14.24 | 1.47 | 499.2697 |
| DP-16 | 16.26 | 1.67 | 358.1145 (negative) |

The HRMS run was simultaneously injected in positive and negative HESI mode and spectra were evaluated. As per UV chromatogram of HRMS run, total 12 impurities peaks were detected which have been denoted as DP-5 to DP-16 (Figure-3.11). All these peaks except DP-10, DP-11 and DP-16 were observed in positive ion TIC chromatogram having accurate mass values (Table-3.8, 3.9). DP-10, DP-11 and DP-16 peaks were identified from negative ion TIC chromatogram (Table-3.10). Moreover, except DP-6 and DP-7, all the peaks of positive ion TIC chromatogram were observed in negative ion TIC

chromatogram as well confirming the accurate mass values of each peak in both the TIC spectra (Figure-3.12 and 3.13) (Table-3.11, 3.12)

Figure-3.11: UV chromatogram of oxidative degradation sample of alectinib in HRMS:

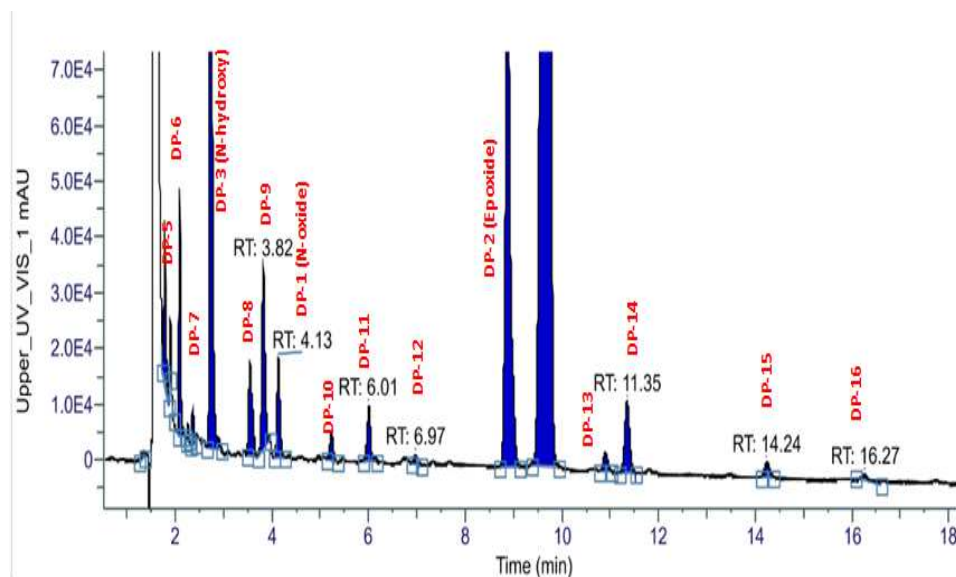


Table-3.8: Peak list UV chromatogram:

| Name | RT (Min) | Peak Area | % Area |
|------|----------|-------------|--------|
| | 1.60 | 17609544.00 | 70.54 |
| | 1.78 | 154697.99 | 0.62 |
| | 1.90 | 112456.61 | 0.45 |
| | 2.09 | 154319.54 | 0.62 |
| | 2.26 | 19828.19 | 0.08 |
| | 2.35 | 34443.16 | 0.14 |
| | 2.73 | 532101.00 | 2.13 |
| | 3.54 | 91088.65 | 0.36 |
| | 3.82 | 178944.23 | 0.72 |
| | 4.13 | 77498.02 | 0.31 |
| | 5.23 | 25648.09 | 0.1 |
| | 6.01 | 48564.50 | 0.19 |
| | 6.97 | 4745.71 | 0.02 |
| | 8.88 | 685090.82 | 2.74 |
| | 9.72 | 5097231.56 | 20.42 |
| | 10.90 | 22878.82 | 0.09 |
| | 11.35 | 90112.32 | 0.36 |
| | 14.24 | 14339.44 | 0.06 |
| | 16.26 | 9726.85 | 0.04 |

Figure-3.12: TIC chromatogram (HESI_Positive)

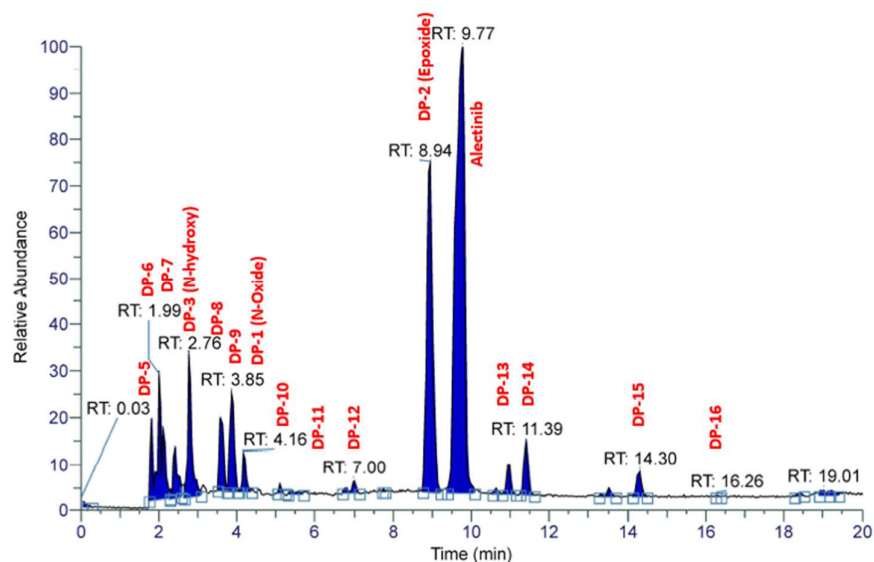


Table-3.9: Peak list TIC chromatogram (HESI positive)

| RT (Min) | Peak Area | % Area | RT (Min) | Peak Area | % Area |
|----------|----------------|--------|----------|-----------------|--------|
| 1.94 | 1119304809.13 | 0.45 | 7.72 | 646275639.05 | 0.26 |
| 2.13 | 2060364882.41 | 0.84 | 7.91 | 207781078.80 | 0.08 |
| 2.40 | 760838184.99 | 0.31 | 8.92 | 7902757252.00 | 3.21 |
| 2.78 | 12259130848.76 | 4.98 | 9.75 | 163219470085.07 | 66.28 |
| 3.60 | 1627669434.25 | 0.66 | 10.71 | 1064492807.38 | 0.43 |
| 3.87 | 5558213808.07 | 2.26 | 10.95 | 2730246455.60 | 1.11 |
| 4.18 | 3996738199.19 | 1.62 | 11.38 | 5015963963.77 | 2.04 |
| 4.61 | 1176524670.51 | 0.48 | 11.96 | 541495163.32 | 0.22 |
| 4.99 | 2271247361.46 | 0.92 | 12.67 | 334753151.93 | 0.14 |
| 5.27 | 1777555332.56 | 0.72 | 12.86 | 126032530.70 | 0.05 |
| 5.50 | 307032722.59 | 0.12 | 13.53 | 1198116272.57 | 0.49 |
| 6.04 | 14595006025.43 | 5.93 | 14.28 | 4276254153.40 | 1.74 |
| 6.78 | 705210862.77 | 0.29 | 14.59 | 334801386.21 | 0.14 |
| | | | 16.28 | 3419831839.26 | 1.39 |
| | | | 17.77 | 1757537028.13 | 0.71 |
| | | | 18.40 | 884058003.77 | 0.36 |

Figure-3.13: TIC chromatogram (HESI Negative)

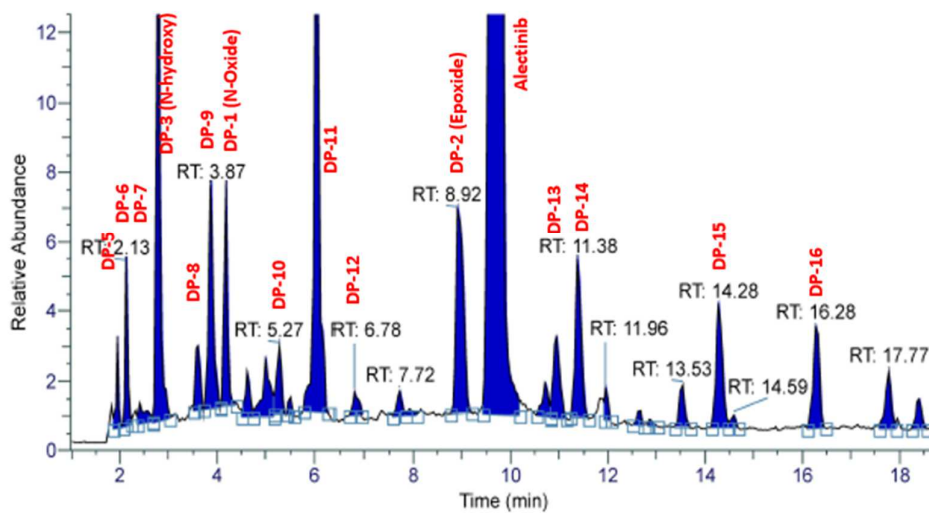


Table-3.10: Peak list of TIC chromatogram (HESI Negative)

| RT (Min) | Peak Area | % Area | RT (Min) | Peak Area | % Area |
|----------|----------------|--------|----------|-----------------|--------|
| 1.94 | 1119304809.13 | 0.45 | 7.72 | 646275639.05 | 0.26 |
| 2.13 | 2060364882.41 | 0.84 | 7.91 | 207781078.80 | 0.08 |
| 2.40 | 760838184.99 | 0.31 | 8.92 | 7902757252.00 | 3.21 |
| 2.78 | 12259130848.76 | 4.98 | 9.75 | 163219470085.07 | 66.28 |
| 3.60 | 1627669434.25 | 0.66 | 10.71 | 1064492807.38 | 0.43 |
| 3.87 | 5558213808.07 | 2.26 | 10.95 | 2730246455.60 | 1.11 |
| 4.18 | 3996738199.19 | 1.62 | 11.38 | 5015963963.77 | 2.04 |
| 4.61 | 1176524670.51 | 0.48 | 11.96 | 541495163.32 | 0.22 |
| 4.99 | 2271247361.46 | 0.92 | 12.67 | 334753151.93 | 0.14 |
| 5.27 | 1777555332.56 | 0.72 | 12.86 | 126032530.70 | 0.05 |
| 5.50 | 307032722.59 | 0.12 | 13.53 | 1198116272.57 | 0.49 |
| 6.04 | 14595006025.43 | 5.93 | 14.28 | 4276254153.40 | 1.74 |
| 6.78 | 705210862.77 | 0.29 | 14.59 | 334801386.21 | 0.14 |
| | | | 16.28 | 3419831839.26 | 1.39 |
| | | | 17.77 | 1757537028.13 | 0.71 |
| | | | 18.40 | 884058003.77 | 0.36 |

Table-3.11: Summary of molecular mass and their fragments' molecular ion peak in TIC chromatogram (HESI positive)

| Degradation products | RT of Impurity | RRT | Observed molecular ion peak (m/z) | Further MS-MS fragmentation molecular ion peaks (m/z) | | | |
|----------------------|----------------|------|------------------------------------|-------------------------------------------------------|-----------------|-----------------|-----------------|
| | | | | | | | |
| DP-5 | 2.09 | 0.22 | 515.2649 | 411.1934 | 412.1976 | | |
| DP-6 | 2.26 | 0.23 | 503.2647 | | | | |
| DP-7 | 2.36 | 0.24 | 533.2755 | 446.207 | | | |
| DP-3 (N-hydroxy) | 2.73 | 0.28 | 499.2698 | 395.1985 | 396.2065 | 397.2095 | |
| DP-8 | 3.54 | 0.36 | 517.2803 | 430.2122 | 413.2049 | 386.2225 | |
| DP-9 | 3.82 | 0.39 | 499.2699 | | | | |
| DP-1 (N-oxide) | 4.13 | 0.42 | 499.2699 | 412.2015 | 396.2062 | | |
| DP-10 | 5.23 | 0.54 | 361.1142 (negative) | 317.0847 | 288.0862 | | |
| DP-11 | 6.01 | 0.62 | 377.1087 (negative) | 377.109 | 305.0525 | | |
| DP-12 | 6.97 | 0.72 | 499.2703 | 412.2014 | 396.2067 | | |
| DP-2 (Epoxide) | 8.88 | 0.91 | 499.27 | 396.2065 | 412.2013 | | |
| Main peak | 9.72 | 1.00 | 483.275 | | | | |
| DP-13 | 10.9 | 1.12 | 487.2700 499.2698 | 400.2185 | 399.2158 | 398.2131 | 397.2102 |
| DP-14 | 11.35 | 1.17 | 499.27 | 412.201 | | | |
| DP-15 | 14.24 | 1.47 | 499.2697 | | | | |
| DP-16 | 16.26 | 1.67 | 358.1145 (negative) | 343.0915 | | | |

Table-3.12: Summary of molecular mass and their fragments 'molecular ion peak in TIC chromatogram (HESI negative)

| Degradation products | RT of Impurity | RRT | Observed molecular ion peak (m/z) | Further MS-MS fragmentation molecular ion peaks (m/z) | | | | |
|----------------------|----------------|------|-----------------------------------|-------------------------------------------------------|----------|----------|----------|----------|
| | | | | | | | | |
| | 1.94 | 0.20 | 513.2434 | 340.1404 | 356.1353 | 394.187 | 410.1816 | |
| DP-5 | 2.13 | 0.22 | 513.2434 | | | | | |
| DP-3 (N-hydroxy) | 2.85 | 0.29 | 497.2487 | 394.1869 | 340.1407 | | | |
| DP-8 | 3.6 | 0.37 | 515.2589 | 471.2701 | 181.0736 | | | |
| DP-9 | 3.87 | 0.40 | 497.2487 | 482.2258 | 394.1871 | 340.1408 | | |
| DP-1 (N-oxide) | 4.18 | 0.43 | 497.2487, 361.1140 | 394.1867 | 340.1405 | 410.1815 | | |
| DP-N1 | 4.61 | 0.47 | 393.1038 | 379.1637 | 279.0735 | | | |
| DP-N2 | 4.95 | 0.51 | 377.1086 | 305.1252 | 167.0316 | 315.1096 | 300.0896 | 123.0421 |
| DP-10 | 5.27 | 0.54 | 361.1142 | 317.0847 | 288.0862 | | | |
| DP-N3 | 5.54 | 0.57 | 513.2437 | 305.1829 | 181.0737 | | | |
| DP-11 | 6.01 | 0.62 | 377.1087 | 305.0525 | 344.0752 | 277.058 | | |
| DP-N4 | 6.2 | 0.64 | 393.1038 | 340.1407 | 379.1638 | | | |
| DP-12 | 6.78 | 0.70 | 361.1143 | 288.0867 | 346.091 | | | |
| DP-N5 | 7.74 | 0.79 | 424.1607 | 409.1377 | 327.1333 | 312.1107 | | |
| DP-2 (Epoxide) | 8.92 | 0.91 | 497.2486 | 394.1871 | 340.1408 | | | |
| Main peak | 9.75 | 1.00 | 481.2537 | | | | | |
| DP-N6 | 10.71 | 1.10 | 362.1016 | 481.0539 | 595.2459 | 265.144 | | |
| DP-13 | 10.95 | 1.12 | 497.2486 | 482.2255 | | | | |
| DP-14 | 11.38 | 1.17 | 497.2486 | 482.2255 | | | | |
| DP-N7 | 12.67 | 1.30 | 435.1765 | No fragments observed | | | | |
| DP-N8 | 13.53 | 1.39 | 505.2307 | 469.2544 | 454.2316 | | | |
| DP-15 | 14.28 | 1.46 | 497.2486 | 482.226 | | | | |
| DP-N9 | 14.59 | 1.50 | 345.1193 | 330.0962 | 315.073 | | | |
| DP-16 | 16.28 | 1.67 | 358.1145 | 343.0915 | 326.0889 | | | |
| DP-N10 | 17.77 | 1.82 | 342.1197 | 324.1099 | 311.115 | 299.1023 | 284.0793 | |
| DP-N11 | 18.4 | 1.89 | 513.2434 | 498.2205 | | | | |

3.5 SECTION-B: DEGRADATION KINETIC STUDY:

3.5.1 EXPERIMENTAL

The degradation kinetics study for alectinib was performed in oxidative medium only as the drug was found to be stable under all other stress conditions.

3.5.1.1 Chemicals, reagents and Materials

Refer Section 3.4.2.1.1

3.5.1.2 Instrumentation and analytical conditions

Same as Section-3.4.2.1.2

3.5.1.3 Preparation of solutions:

The degradation kinetics study was performed in oxidative degradation condition where 300ppm solutions of alectinib were exposed to varied concentration of 30% H₂O₂ solutions (1mL, 2mL, and 3 mL) at 70°C temperature for varied time duration exposure (30 minutes, 60 minutes, 90 minutes, and 120 minutes) and samples were analyzed using developed HPLC method. During initial forced degradation study, it was noted that the temperature of 50°C to 80°C have similar degradation profile, hence in degradation kinetics study temperature of 70°C was kept constant with difference of concentration of H₂O₂ and time duration of exposure.

Table-3.13: Solution preparation for degradation kinetic study:

| Time | Volume of H ₂ O ₂ added | | |
|-------------|-----------------------------------------------|-----|-----|
| | 1 mL | 2mL | 3mL |
| 30 minutes | 1 mL | 2mL | 3mL |
| 60minutes | 1 mL | 2mL | 3mL |
| 90 minutes | 1 mL | 2mL | 3mL |
| 120 minutes | 1 mL | 2mL | 3mL |

3.5.2 RESULTS AND DISCUSSION:

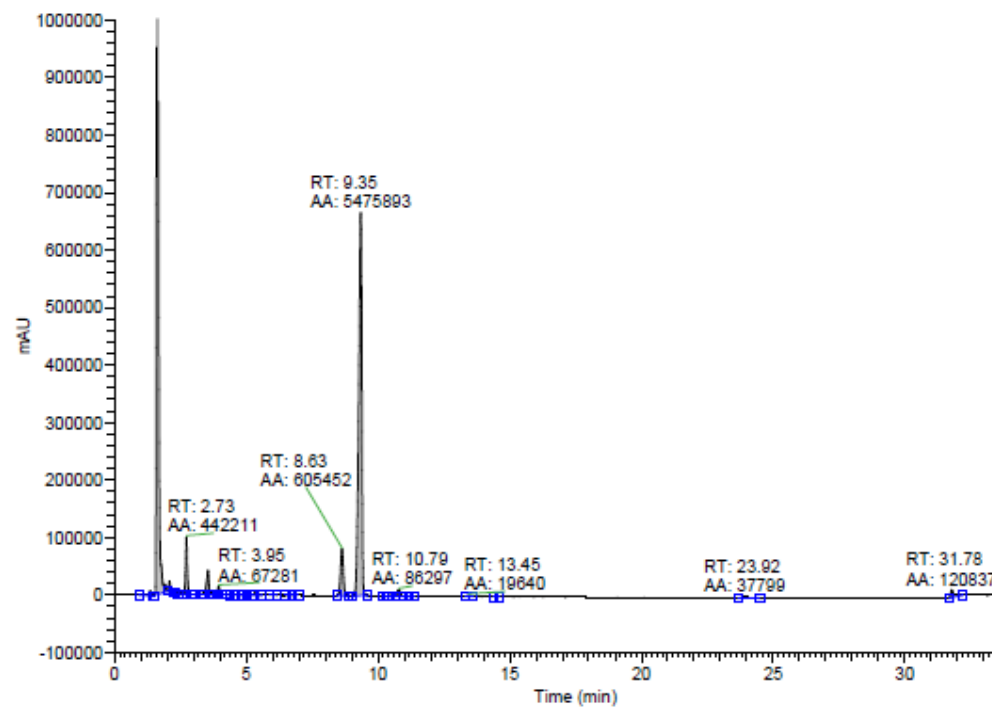
Initially with the increase in reagent (H₂O₂) concentration and time of reaction, the degradation was observed to be increased but as the time is increased to 90 minutes and 120 minutes, the volume of H₂O₂ does not have any major effect on degradation kinetics because the percentage degradation at the levels of 90 minutes and at 120minutes with varied concentration of H₂O₂ were found to be fluctuating and not in increasing mode with increment of concentration.

Moreover, maximum degradation in oxidative degradation condition was observed within initial 60 to 90 minutes. After that it remains constant at the level of 65-75% degradation.

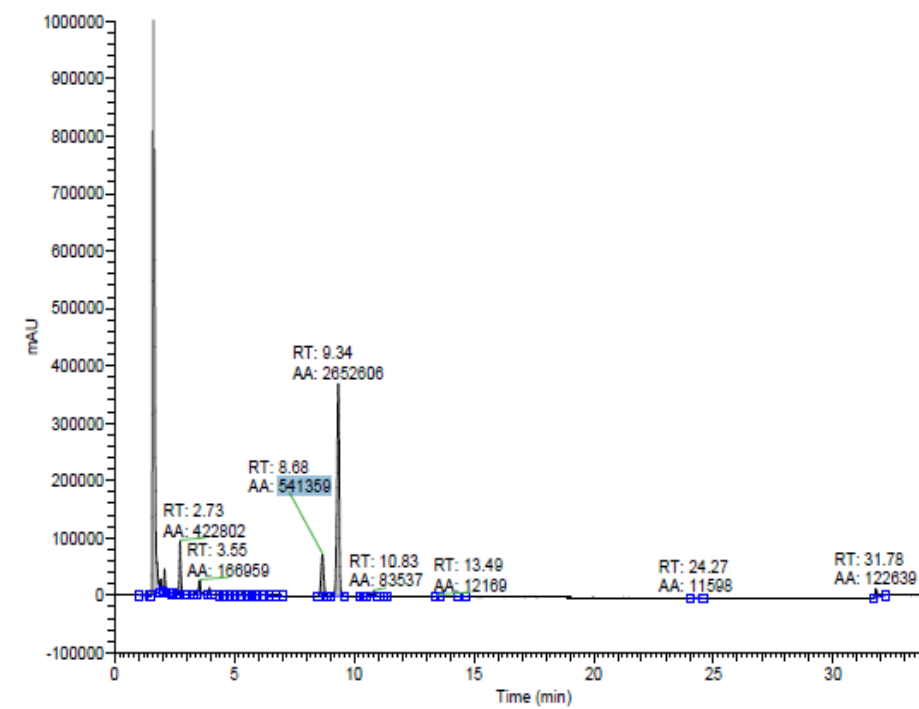
The two major degradation impurities peaks that were generated from alectinib after oxidative degradation condition are enhanced almost linearly with time duration and are observed at RRT 0.29 (RT 2.73 min) and RRT 0.93 (RT 8.63 min) (Figure-3.14-A to 3.14-D). When the degradation kinetics of formation of these two impurities were monitored, it was found that at each time point level, the area response of both the impurities were increased as the concentration of 30% H_2O_2 increases. The amount of both the impurities remained fluctuating between the time points of 0-90 minutes but finally the maximum amount of this impurity was observed at 120 minutes time point and that too found increasing with the volume of 30% H_2O_2 solution. Based on the standard correlation values observed, both of them follow first order kinetics both with time as well as with concentration of H_2O_2 solution. (Table-3.14, Figure-3.15-A, 3.15-B, 3.15-C). Based on rate of reaction, rate constant, activation energy and half-life has been calculated and show in Table-3.14.

Figure-3.14: Chromatogram of degradation solution alectinib

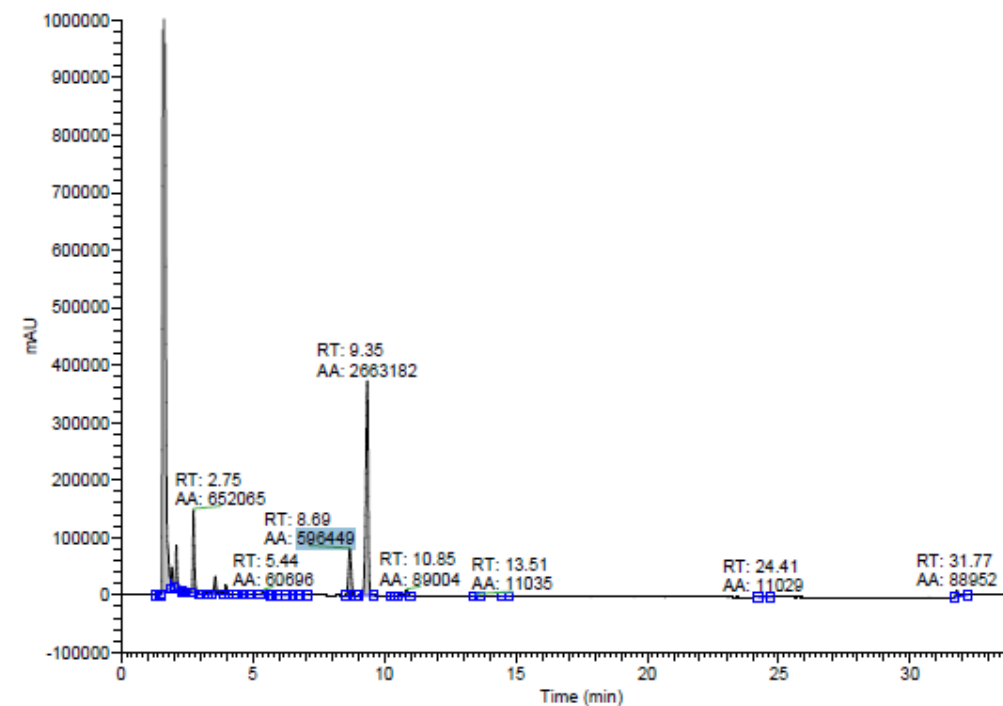
A. Condition: 1mL H_2O_2 at 70°C for 30min



B. Condition: 2mL H₂O₂ at 70°C for 60min



C. Condition: 3mL H₂O₂ at 70°C for 90min



D. Condition: 3mL H₂O₂ at 70°C for 120min

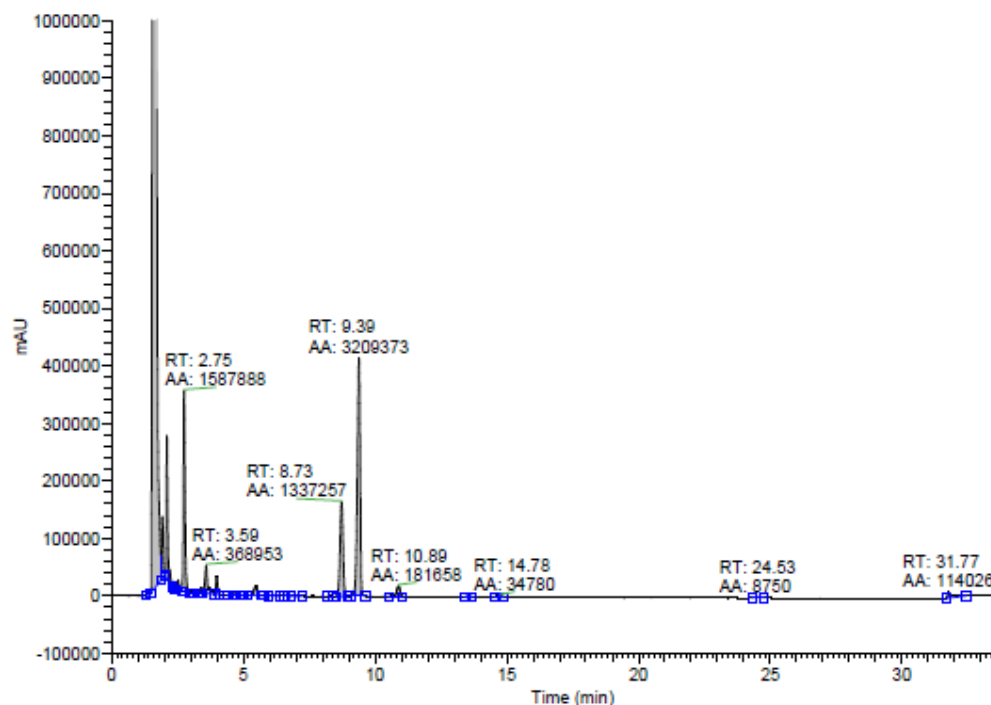


Table-3.14 : Degradation of alectinib under varied concentration of H₂O₂ and varied time duration

| | Time duration (Minutes) | Volume of 30% H ₂ O ₂ solution added | Area response of alectinib | Percentage of Main peak with respect to as such sample | % Degradation | Mean | Log (% Degradation) | 1/Log (% Degradation) |
|-------|-------------------------|------------------------------------------------------------|----------------------------|--------------------------------------------------------|---------------|-------|---------------------|-----------------------|
| Set-1 | 30 minutes | 1 mL | 5475893 | 57.56 | 42.44 | 41.68 | 1.6199 | 0.6173 |
| Set-2 | 30 minutes | 2 mL | 5110311 | 53.72 | 46.28 | | | |
| Set-3 | 30 minutes | 3 mL | 6058833 | 63.69 | 36.31 | | | |
| Set-4 | 60 minutes | 1 mL | 4785121 | 50.30 | 49.70 | 65.41 | 1.8156 | 0.5508 |
| Set-5 | 60 minutes | 2 mL | 2652606 | 27.88 | 72.12 | | | |
| Set-6 | 60 minutes | 3 mL | 2435534 | 25.60 | 74.40 | | | |
| Set-7 | 90 minutes | 1 mL | 1923303 | 20.22 | 79.78 | 72.97 | 1.8632 | 0.5367 |
| Set-8 | 90 minutes | 2 mL | 3126622 | 32.87 | 67.13 | | | |
| Set-9 | 90 minutes | 3 mL | 2663182 | 27.99 | 72.01 | | | |

| | | | | | | | | |
|-------------------------------------------------|-------------|------|---------|-------|-------|----------|----------|----------|
| Set-10 | 120 minutes | 1 mL | 2580449 | 27.12 | 72.88 | 70.86 | 1.8504 | 0.5404 |
| Set-11 | 120 minutes | 2 mL | 2525949 | 26.55 | 73.45 | | | |
| Set-12 | 120 minutes | 3 mL | 3209373 | 33.73 | 66.27 | | | |
| Slope (S) | | | | | | 0.31700 | 0.00709 | -0.33665 |
| Intercept | | | | | | 38.95500 | 1.33086 | 1.16252 |
| Correlation Coefficient (r) | | | | | | 0.8532 | 0.9718 | -0.9998 |
| Standard deviation | | | | | | 14.3903 | 0.1049 | 0.0353 |
| Rate constant (K) (minute⁻¹) | | | | | | -0.31700 | -0.01633 | 0.33665 |
| Activation energy (E_a) | | | | | | -2.636 | -0.0589 | 2.799 |
| Half-life (minutes) = ln 2/K = 0.693 / K | | | | | | NA | 42.44 | NA |

Figure-3.15-A: Plot between %Degradation vs time duration (minutes)

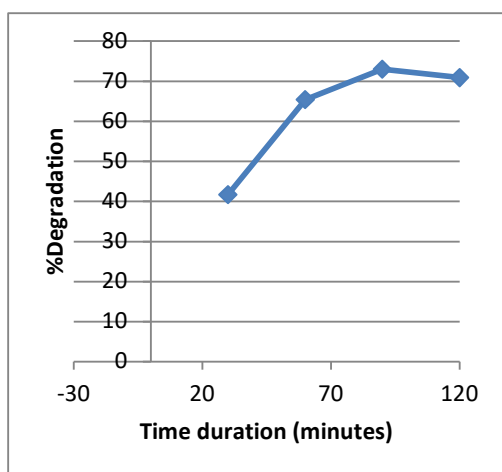


Figure-3.15-B: Plot between Log %Degradation vs time duration (minutes)

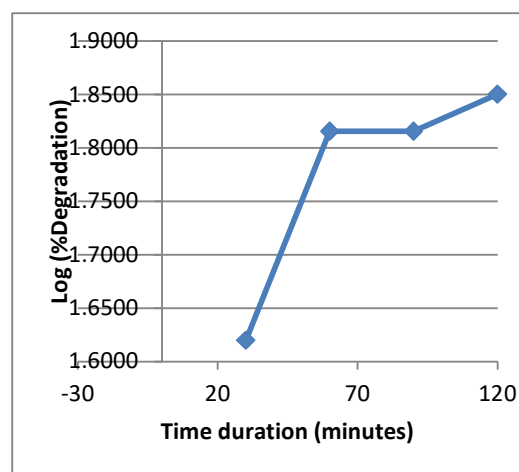
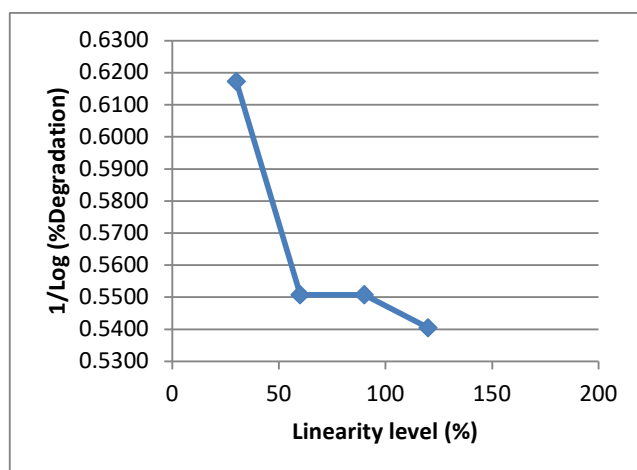


Figure-3.15-C: Plot between 1/Log %Degradation vs time duration (minutes)



3.6 SECTION-C: ISOLATION AND CHARACTERIZATION OF MAJOR DEGRADATION PRODUCTS OF ALECTINIB

3.6.1 ISOLATION OF DEGRADATION PRODUCTS

3.6.1.1 Experimental

3.6.1.1.1 Chemicals, reagents and materials

Refer Section-3.4.2.1.1

3.6.1.1.2 Instruments

Preparative HPLC (Shimadzu LC-20AP) with the PDA detector and LC-solution software was used for isolation of major degradants. The column used was Phenomenex C18 (250X25) mm, 5 μ .

3.6.1.1.3 Sample preparation for Isolation of Impurities by Preparative-HPLC

A series of sample solutions (8 mg/mL), prepared in the diluent mixture of dimethyl sulfoxide and H₂O₂ (30%) in the ratio of 20:80 were degraded for isolation of degradation products through preparative-HPLC. An approximately 40 mg of alectinib was transferred into a 5 mL volumetric flask and diluted up to the mark with the diluent mixture. The solution was further heated at 80 °C for 75 minutes to maximize the generation of oxidative degradation products.

3.6.1.1.4 Analytical condition for Preparative high performance liquid chromatography method

The column used was Phenomenex C18 (250X25) mm, 5 μ . The mobile phase used was similar to that was used in analytical studies. The chromatographic separation was achieved with an injection volume of 5 ml and a flow rate of 25 mL/min for 35 minutes run time. The detection wavelength and gradient were similar to that used in the analytical method.

3.6.1.2 Results and discussion:

As shown in Figure-3.16, the degradation sample of alectinib shows maximum generation of degradation impurities which were isolated in preparative test tubes. The collected fractions were confirmed in analytical HPLC method for elution at the same retention time. After confirmation, the collected fractions were evaporated on rota-vapor to remove the organic portions and then freeze dried the

aqueous medium contained desired degradation products to get in solid form. The isolated products were again injected in analytical method to confirm their purity. All the four degradation products' purity were obtained as shown in Table-3.15 and Figure 3.17-A, B, C and D.

Table-3.15: Purity results of isolated degradation products

| Degradation product | Purity |
|---------------------|--------|
| DP-1 | 97.81% |
| DP-2 | 86.91% |
| DP-3 | 56.12% |
| DP-4 | 94.64% |

Figure-3.16 Chromatogram of degradation of alectinib for isolation of degradation products from preparative LC

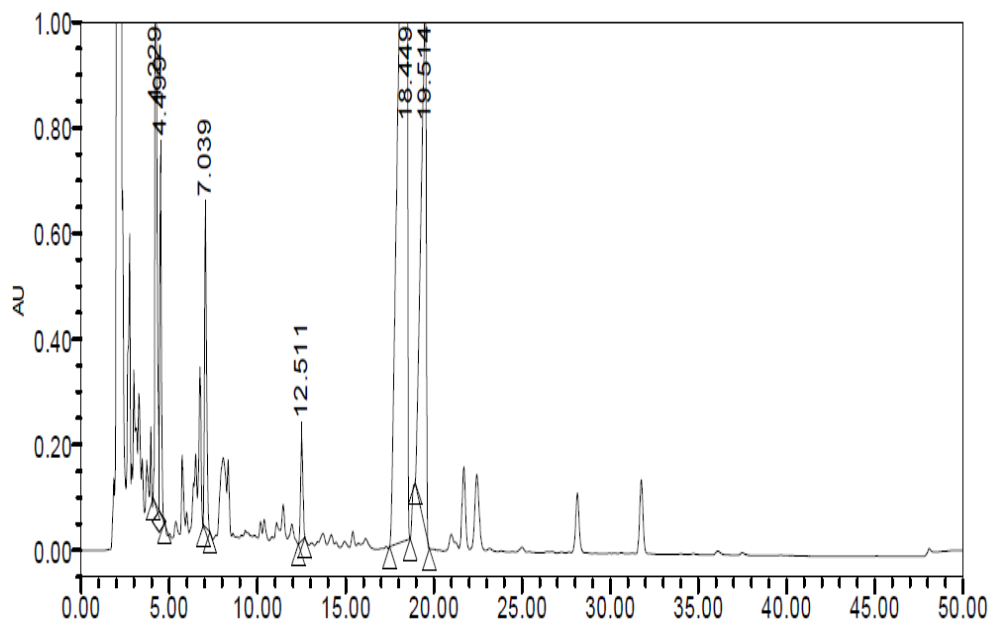


Figure-3.17-A: Chromatogram of isolated DP-1

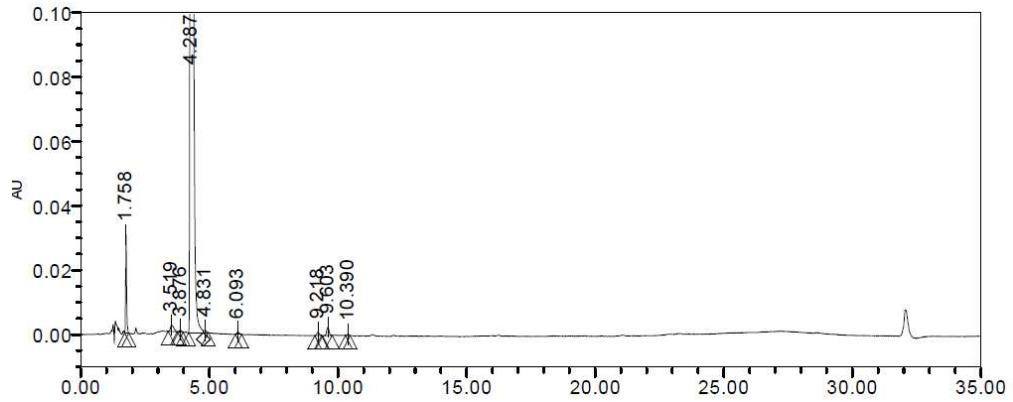


Figure-3.17-B: Chromatogram of isolated DP-2

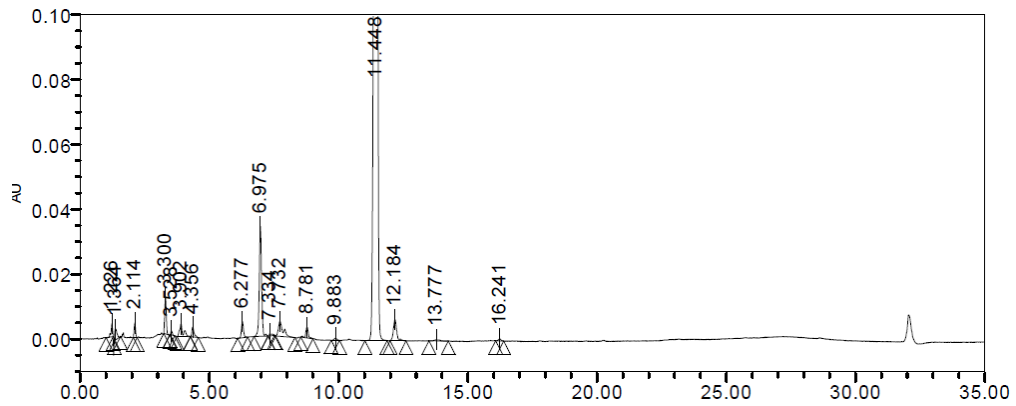


Figure-3.17-C: Chromatogram of Isolated DP-3

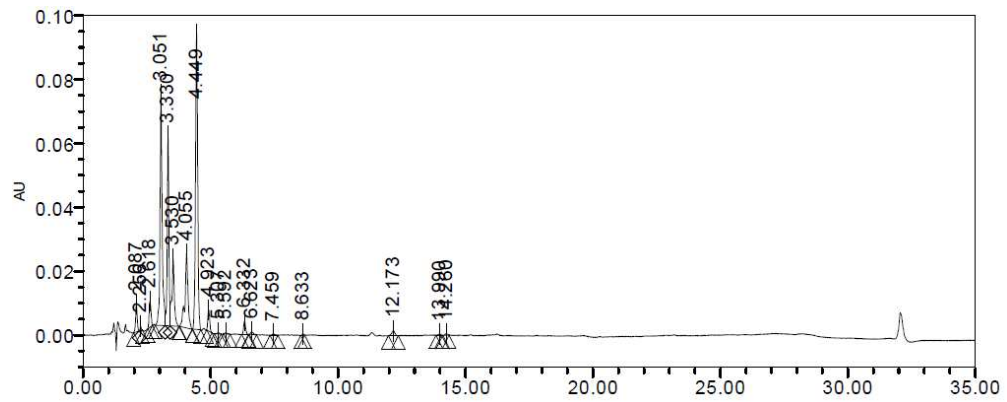
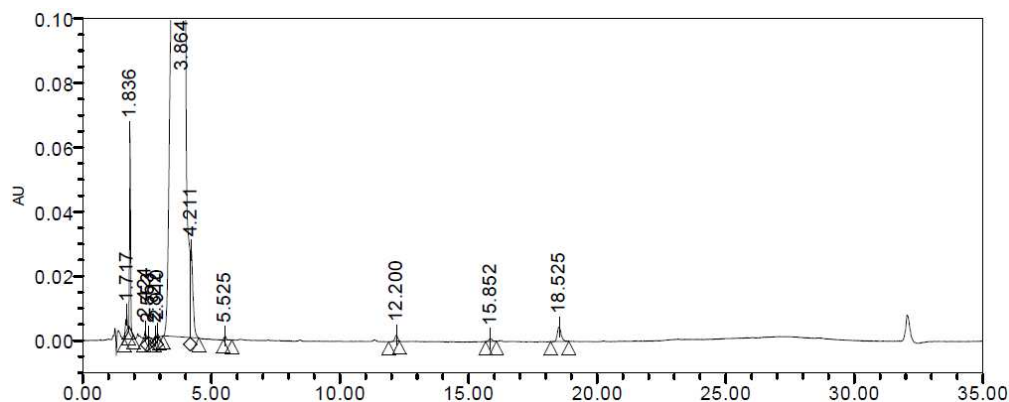


Figure-3.17-D: Chromatogram of Isolated DP-4



3.6.2 CHARACTERIZATION OF MAJOR DEGRADATION PRODUCTS OF ALECTINIB

3.6.2.1 Experimental

3.6.2.1.1 Chemicals, reagents and materials

Refer Section-3.4.2.1.1

3.6.2.1.2 Instruments

3.6.2.1.2.1 Liquid chromatography mass spectrometry

Refer section 3.4.2.1.2 Instrument used for forced degradation study.

3.6.2.1.2.2 High resolution mass spectrometry

Refer section 3.4.2.1.3 Instrument used for forced degradation study.

3.6.2.1.2.3 Nuclear magnetic resonance spectrometry

The NMR experiments for alectinib and its degradation products were performed on Bruker AVANCE 400 MHz NMR instrument equipped with Broadband Observe (BBO) probe.

3.6.2.1.3 Sample solution preparation:

Refer Section 3.4.1.1.2.3 Oxidation condition sample solution preparation under

forced degradation study. As the degradation products were generated majorly in oxidative stress condition, this conditions samples were run in LC-MS and HRMS for structure elucidation study.

3.6.2.1.4 Analytical condition and instrument parameters for HPLC and LC-MS

The conditions were set same as mentioned in Section 3.4.1.1.3.

3.6.2.1.5 Analytical conditions and instrument parameters for High resolution mass spectrometry

The conditions were set same as mentioned in Section 3.4.1.1.4.

3.6.2.1.6 Analytical conditions and instrument parameters for Nuclear magnetic resonance spectrometry

The probe temperature was set as 298K throughout experiment cycle. The chemical shifts of ^1H and ^{13}C spectra were recorded on a delta scale in ppm with reference to tetra methyl silane (TMS). The axis of the scale was calibrated as 2.56 ppm for dimethyl sulphoxide (DMSO-d6) peak in ^1H spectra and at 39.5 ppm for DMSO-d6 peak in ^{13}C NMR spectra.

3.6.2.2 Results and discussion:

3.6.2.2.1 Spectroscopic aspects of alectinib

When the LC-MS data was obtained from LC-MS/MS (Waters Micro-mass, ZQ-Mass detector) with electron spray ionization (positive) mode, alectinib was identified as parent ion $(\text{C}_{30}\text{H}_{34}\text{N}_4\text{O}_2)^+$ at m/z 483.32 $(\text{M}+1)^+$ corresponding to the molecular mass of it as 482.62(M) Da. In the mass spectra of the degraded solution of alectinib under oxidative condition, the degradation products' ion peaks were observed as 499.15, 499.26, 499.19, and 501.27 for DP-1, DP-2, DP-3, and DP-4 respectively (Figure-3.19). Proton ^1H NMR, ^{13}C broadband decoupled (BBD), distortion-less enhancement by polarization transfer-90 (DEPT-90), and DEPT-135 data was obtained for alectinib on NMR spectrometer in a diluent of DMSO-d6. The proton and carbon skeleton as identified is mentioned in Table-3.16 and Table-3.17 and is shown in Figure-3.20, 3.21 and 3.22 [22]. The FTIR spectrum was generated for alectinib for the identification of characteristic functional groups present in structure (Table-3.17, Figure-3.18) [23, 24].

Table-3.16 Proton identification of Alectinib, DP-1 and DP-4 through ¹H spectra

| Chemical shift of Alectinib (ppm) | Chemical shift of DP-1 (ppm) | Chemical shift of DP-4 (ppm) | Multiplicity | No. of Protons | Assignment in structure (Figure-18) |
|-----------------------------------|------------------------------|------------------------------|--------------|----------------|-------------------------------------|
| 1.34 | 1.33 | 1.34 | Triplet | 3 | 8 |
| 1.82 | 1.83 | 1.81 | Singlet | 6 | 10, 11 |
| 1.90-4.20 | 2.14-4.29 | 2.10-4.25 | Multiplet | 19 | 7, 22 to 28, 29, 30 |
| 7.35-8.45 | 7.55-8.38 | 7.80-8.28 | Multiplet | 5 | 1, 4, 15, 16, 18 |
| 10.79 | Absent | Absent | Singlet | 1 | HCl |
| 12.88 | 13.62 | 12.43 | Singlet | 1 | -NH |
| Absent | Absent | 7.33-7.44 | Singlet | 1 | -CONH ₂ |
| Total | | 35 | | - | |

Figure-3.18 Structures of alectinib and its degradation products

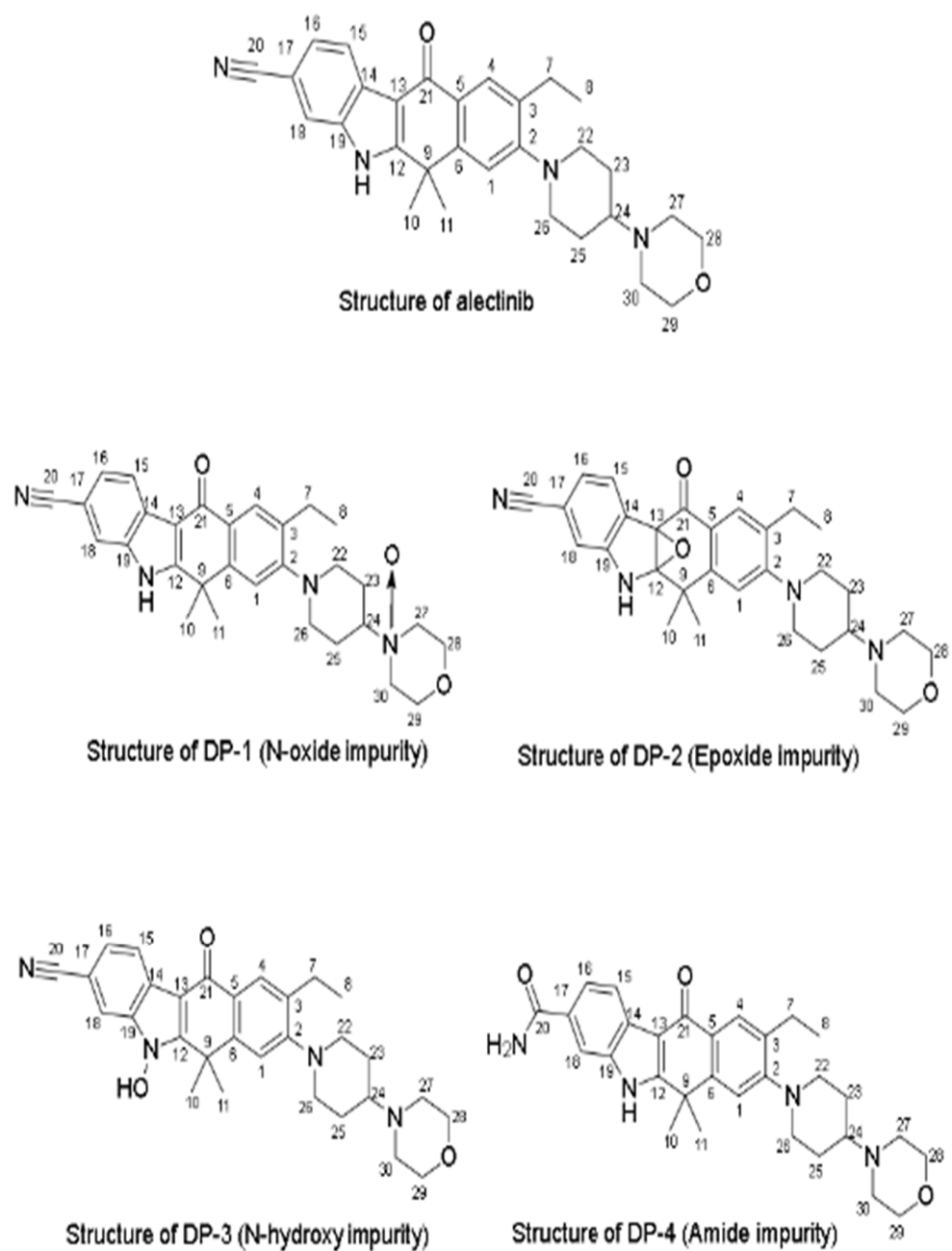


Table-3.17 Carbon identification of Alectinib, DP-1 and DP-4 through ¹³C-BBD, DEPT-90 and DEPT-135 spectra

| Chemical shift of Alectinib (ppm) | Chemical shift of DP-1 (ppm) | Chemical shift of DP-4 (ppm) | No. of Carbons | Assignment in structure |
|------------------------------------------------------------------------------------------------|------------------------------------------------------------------------------------------------|------------------------------------------------------------------------------------------------|----------------|-----------------------------------------|
| 14.30, 30.03 | 14.54, 30.21 | 15.60, 30.79 | 3 | 8, 10, 11 |
| 22.53, 26.31, 48.29, 50.58, 63.36 | 22.76, 24.87, 51.11, 59.10, 60.77 | 23.78, 24.70, 49.70, 54.67, 64.20 | 9 | 7, 22, 23, 25, 26, 27, 28, 29, 30 |
| 36.47 | 36.79 | 37.93 | 1 | 9 |
| 62.44, 116.38, 116.76, 121.58, 124.76, 125.86 | 74.75, 117.51, 117.71, 121.81, 124.97, 126.25 | 60.38, 113.08, 120.55, 121.41, 122.56, 128.36 | 6 | 1, 4, 15, 16, 18, 24 |
| 104.53, 109.28, 120.07, 126.43, 127.65, 135.68, 136.24, 146.78, 154.55 | 104.69, 109.34, 120.27, 127.39, 127.74, 135.78, 136.47, 147.12, 153.08 | 109.88, 127.53, 129.47, 132.37, 136.68, 137.18, 144.86, 148.66, 160.88 | 9 | 2, 3, 5, 6, 12, 13, 14, 17, 19 |
| 160.05, 179.09 | 160.27, 179.20 | 170.52, 179.21 | 2 | 20, 21 |
| | | Total no. of Carbons | 30 | - |

Figure-3.19. LC-MS chromatogram of alectinib and its degradation products with their molecular ion peaks

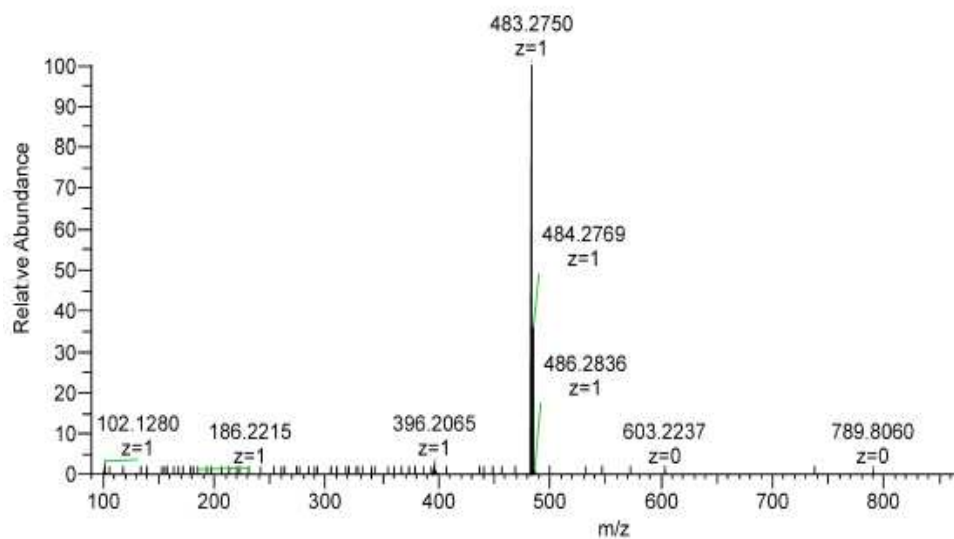
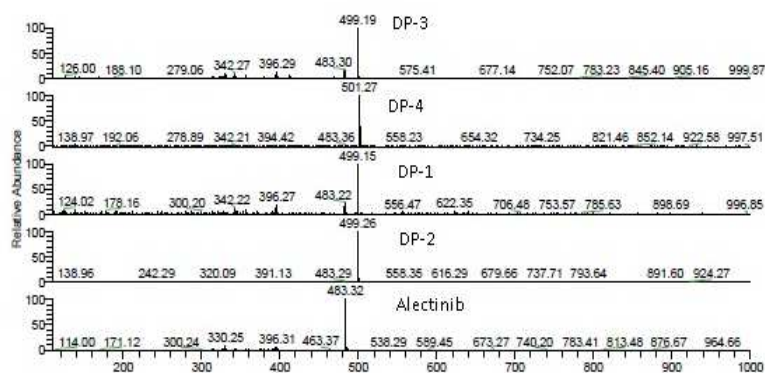
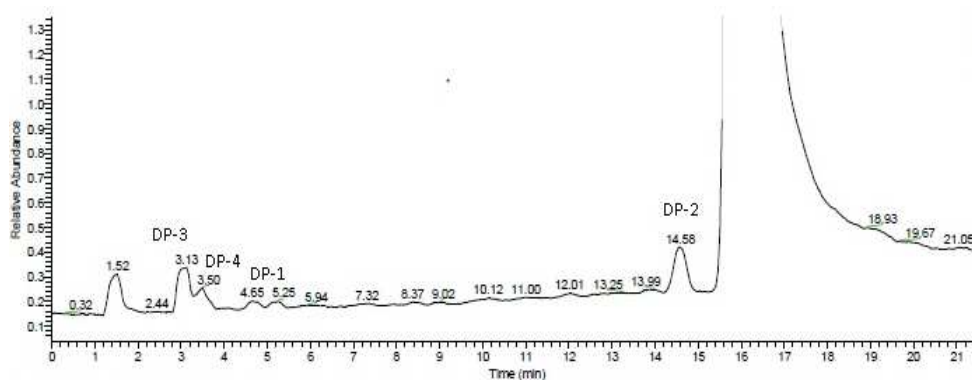


Figure-3.20. Proton (^1H) spectra of alectinib

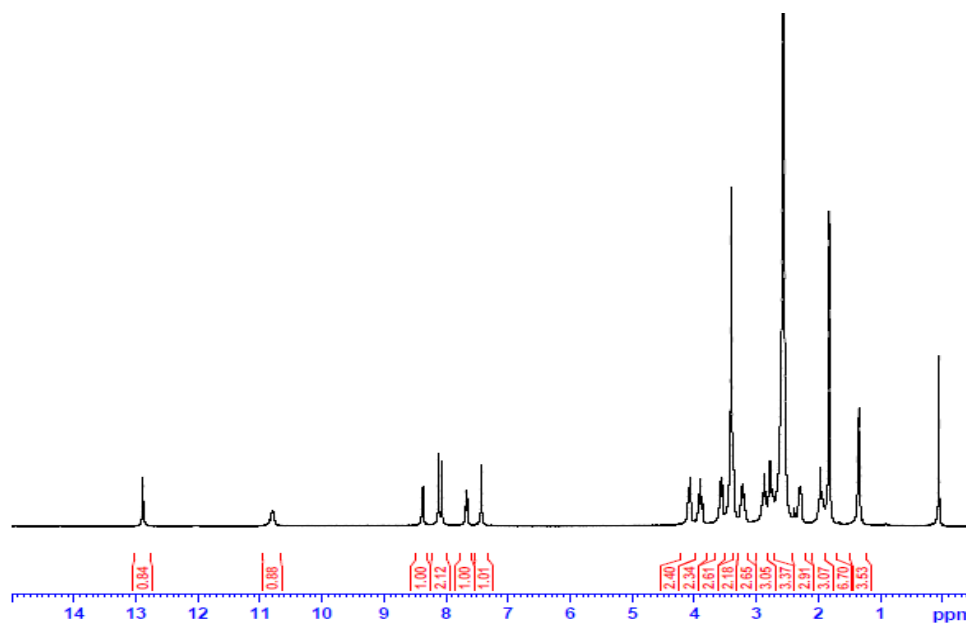


Figure-3.21: Carbon (^{13}C)_BBD_ spectra of alectinib

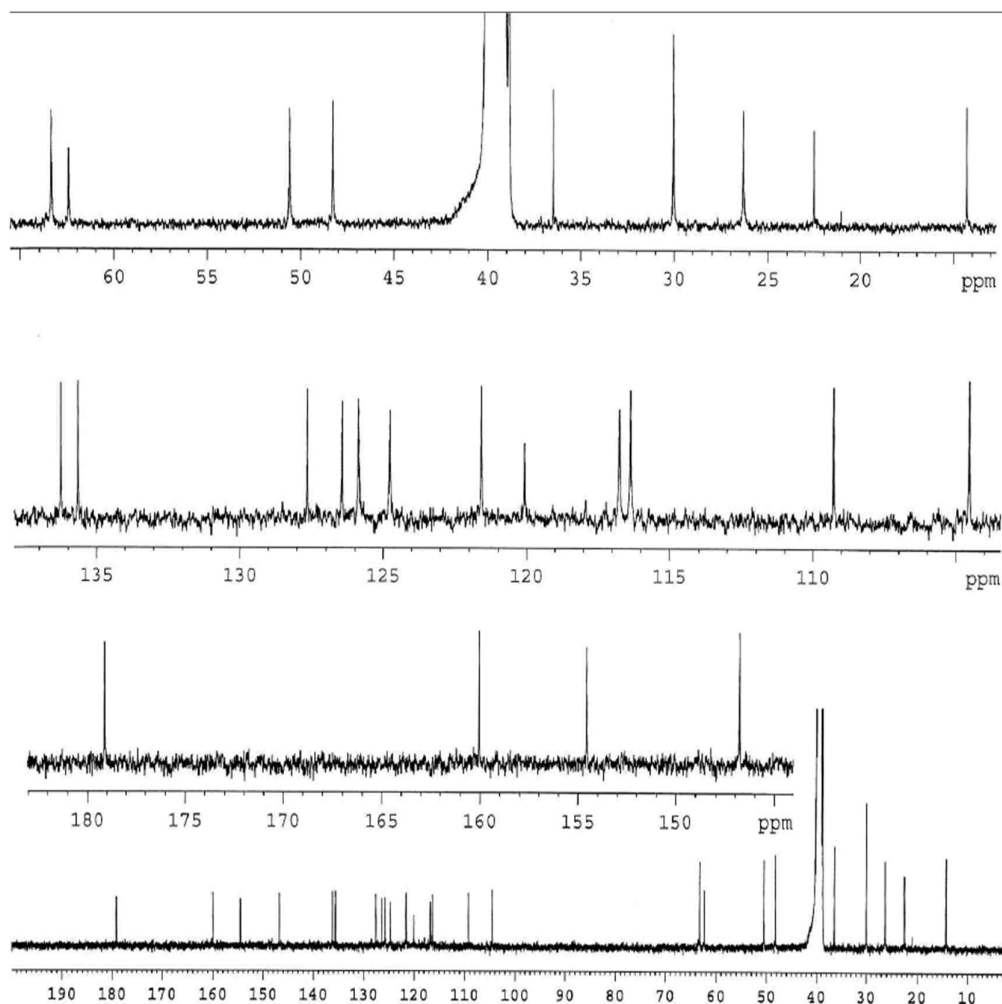
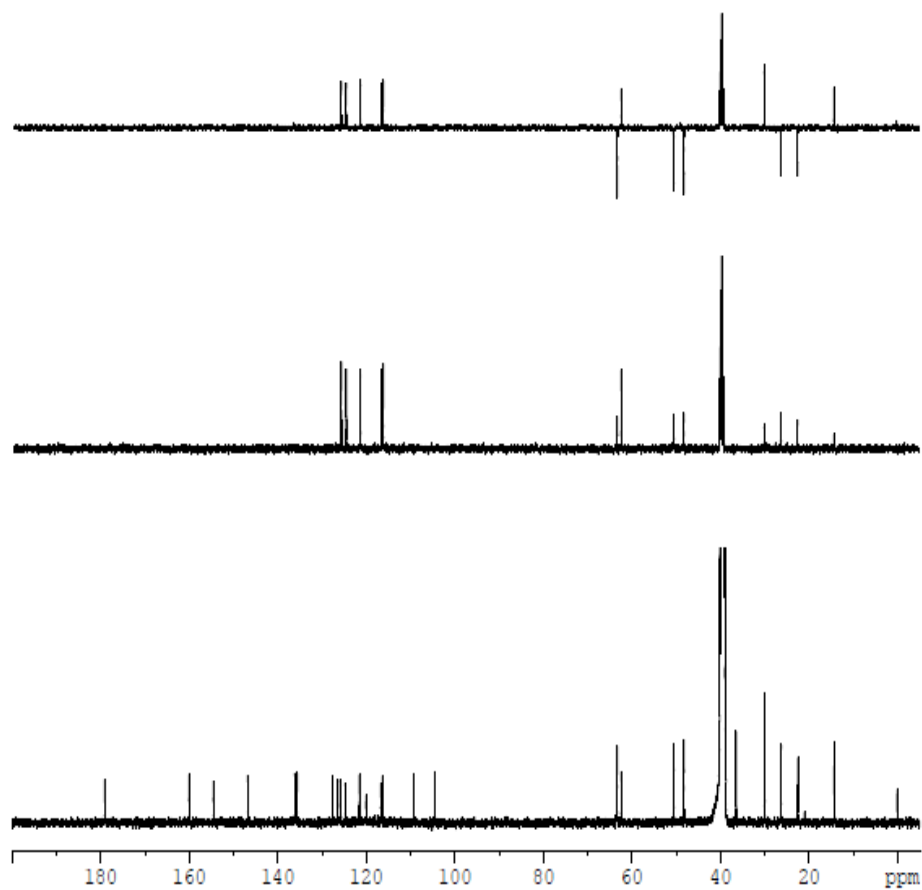


Figure-3.22: Carbon (^{13}C) spectra of BBD, DEPT-90 and DEPT-135 experiment of alectinib

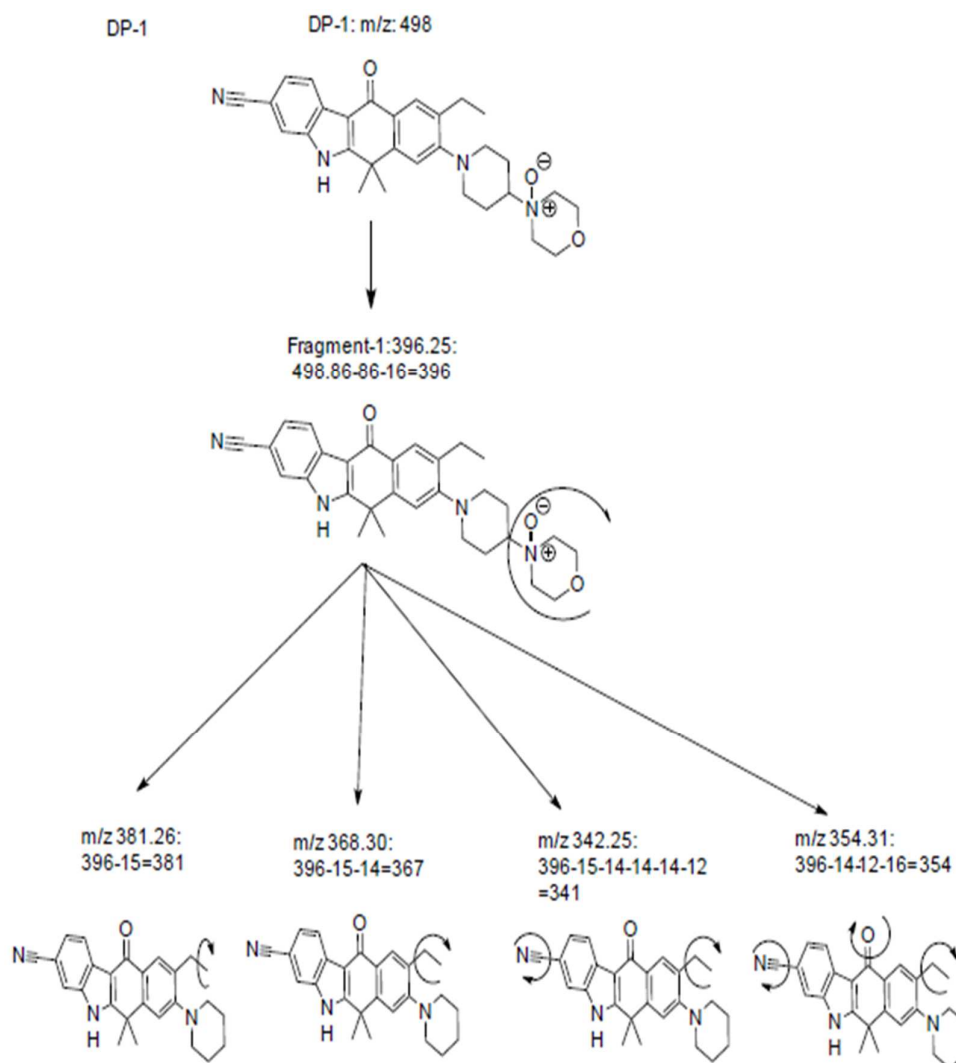


3.6.2.2.2 Structure elucidation of degradation product-1 (N-oxide impurity)

The LC-MS spectral analysis of each oxidative degradation product revealed that three of them have the same molecular mass i.e., 499.15, 499.26, and 499.19. However, the degradation products were shown to be different by HPLC chromatogram as they were eluted at different retention time. This was later confirmed by their NMR, IR spectra and LC-MS/MS fragmentation patterns. The MS daughter ion spectra of DP1 showed the major fragment ion peak at m/z 396.26 which may be formed by loss of morpholine ring with oxygen molecule attached to it. When the major peak at m/z 396.26 was further fragmented, it raised characteristic fragment ions at m/z 381.25 due to removal of a methyl group from ethyl side chain at position 3 of the structure. The fragment ion appearing at m/z 368.32 is because of removal of entire ethyl side chain at position 3 of the structure. Furthermore, when cyano functional group at position 20 along with ethyl side chain was eliminated, it produced fragment ion of m/z 342.25. Similarly, when oxygen of ketone functional group along with the ethyl side chain was eliminated, it raised the fragment ion at m/z 354.29. All of these fragment ions were depicted in Figure-3.24-A to C. Direct mass spectra of DP-1 also suggest the major peak at m/z 499.15. Apart from this, from some literature, it was revealed that the N-oxide impurities may undergo characteristic de-oxygenation under atmospheric pressure chemical ionization (APCI) [25-28]. Considering this, when DP-1 was introduced directly into the LC-MS/MS system with APCI probe, two characteristic fragment ions were observed at m/z 499.12 and 483.22. The fragment ion at m/z 483.22 arises from de-oxygenation of DP-1 under thermal energy activation at APCI source (Figure-3.23 and Figure-3.24-C). As this degradation product does not add any proton to the structure, the total number of protons in ^1H NMR spectra of DP-1 remains the same as compared with alectinib except for the removal of a proton of the hydrochloride salt. It was also noted that the proton numbered between 22 and 30 have resonated at the chemical shift values between 2.14 to 4.25 ppm which is slightly different from 1.90 to 4.20 of alectinib. The reason behind this change in chemical shift is the change in the neighboring environment because of the addition of nitrogen atom between 27 and 30 numbered CH_2 of the structure in DP-1. Also, in ^{13}C spectra, the chemical shift values of peaks due to carbon in the region between 22 and 30 have been slightly changed (Table-3.16, Table-3.17, and Figure-3.25, 3.26, 3.27).

The plausible mechanism of formation of N-oxide impurity is displayed in Figure-3.28 [29]. The probable structure of DP-1 is proposed with the IUPAC name as N-oxide Impurity: 4-(1-(3-cyano-9-ethyl-6, 6-dimethyl-11-oxo-6, 11-dihydro -5H-benzo[b] carbazol-8-yl) piperidin-4-yl) morpholine 4-oxide.

Figure-3.23 LCMS fragmentation pattern of DP-1 (N-oxide impurity)



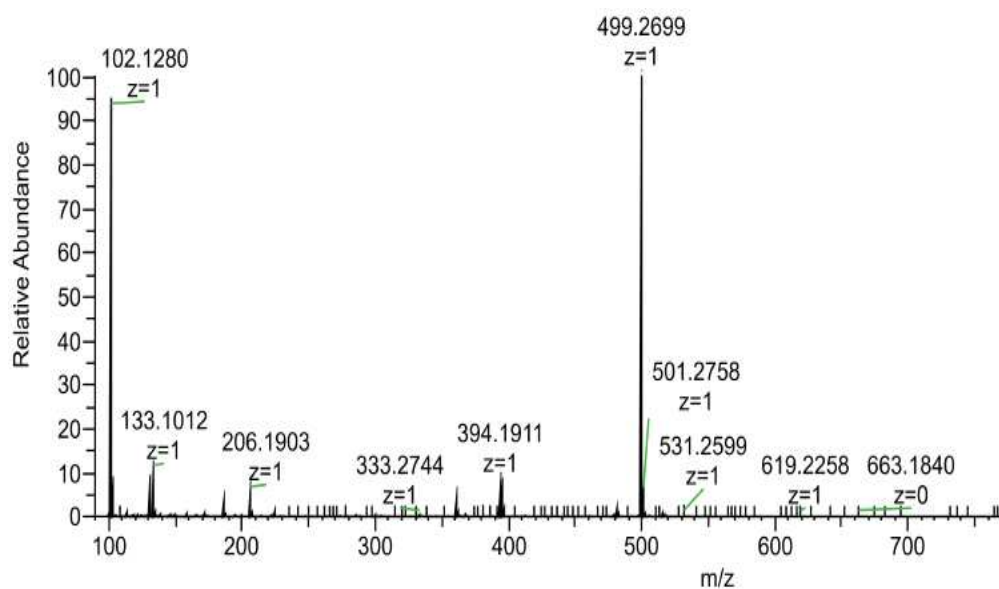
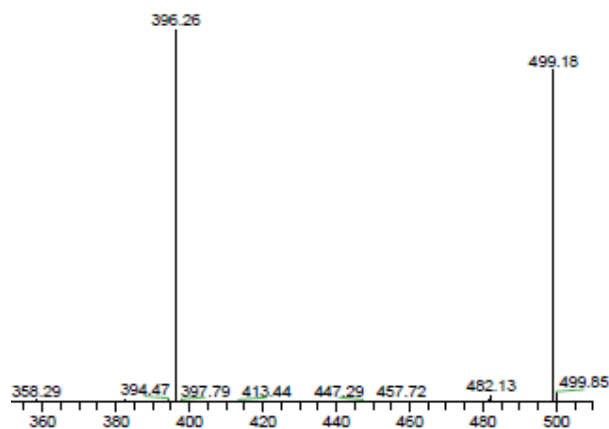
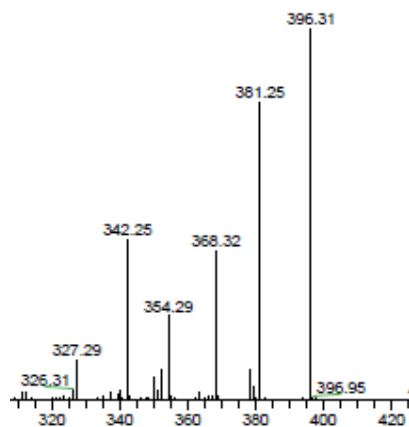


Figure-3.24 LC-MS/MS fragmentation spectra of DP-1 (N-oxide impurity)

A. Fragmentation spectrum-1



B. Fragmentation spectrum-2



C. Characteristic fragment ions of DP-1 in APCI probe in LC-MS/MS

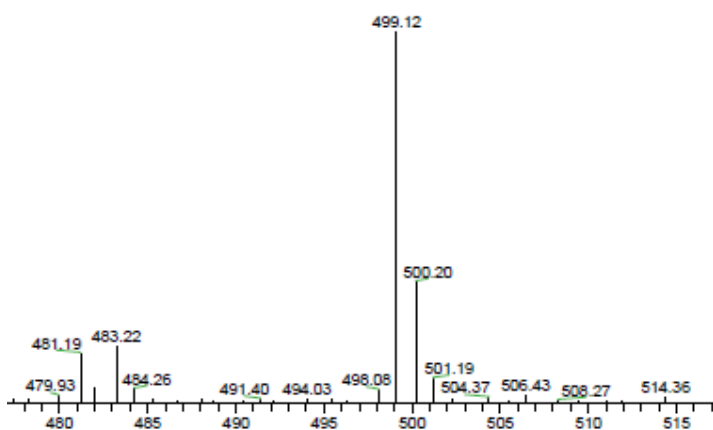


Figure-3.25 Proton (¹H) spectra of DP-1 (N-oxide impurity)

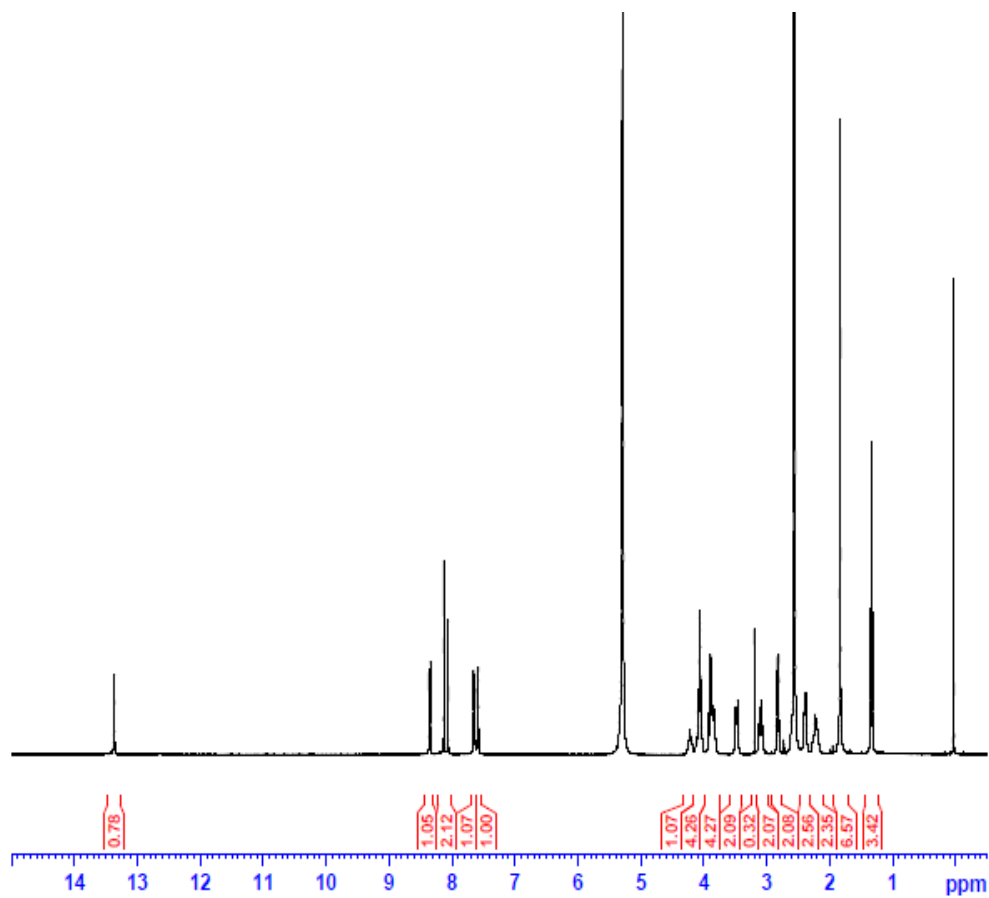


Figure-3.26: Carbon (¹³C) BBD spectra of DP-1

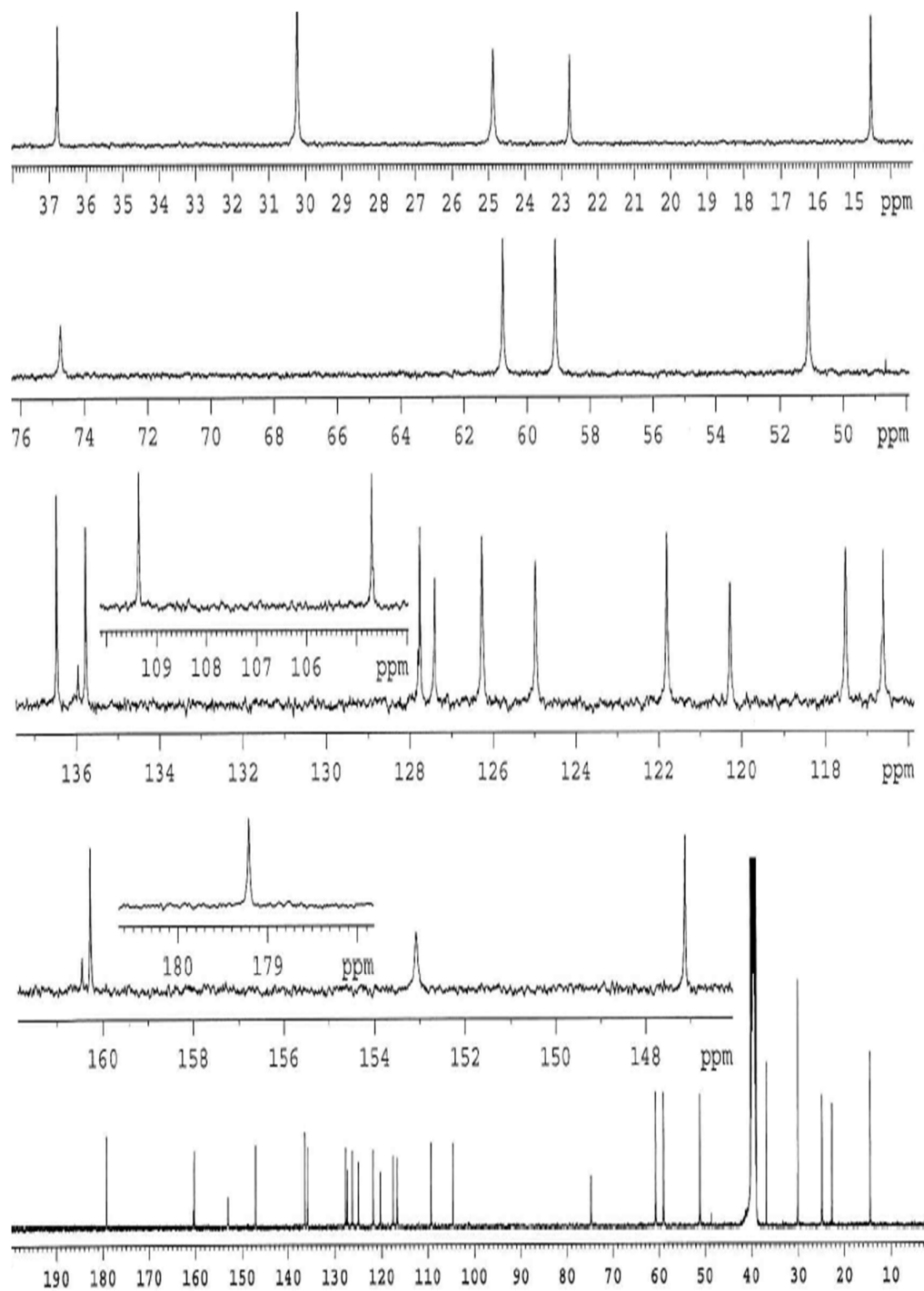
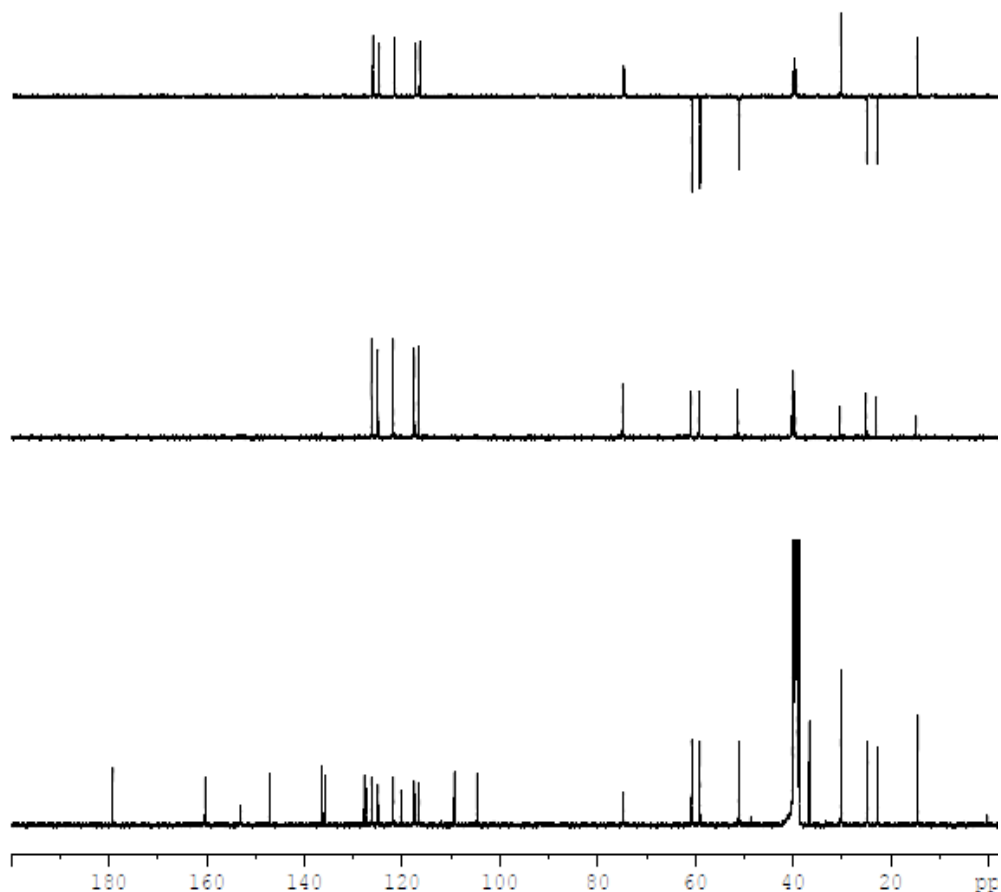


Figure-3.27: Carbon (^{13}C) spectra of BBD, DEPT-90 and DEPT-135 experiment of DP-1 (N-oxide impurity)



3.6.2.2.3 Structure elucidation of degradation product-2 (epoxide Impurity)

The mass spectrum shows the major ion peak at m/z 499.26 suggesting that oxygen molecule may have been incorporated in the structure of alectinib. The same molecular mass of DP-1, DP-2, and DP-3 indicates the possibility of the addition of one oxygen atom in each of these structures. For this, there are six possibilities; firstly, inclusion of oxygen atom at nitrogen atom between position 27 and 30 in molecular structure as in case of DP-1, Secondly at the nitrogen atom between position 22 and 26, thirdly at the nitrogen atom between position 12 and 19,

fourthly at the nitrogen atom of cyanide (CN) group at position 20, fifthly epoxide formation between position 12 and 13 and sixthly N-hydroxy formation at nitrogen between 12 and 19 positions. However, the fourth possibility was eliminated as the significant CN peak was detected at 2217 cm^{-1} in the FTIR spectra of DP-2 (Figure-3.30).

Based on the first LC-MS daughter ion spectra of DP-1 showing the major peak at m/z 412.28, the loss of morpholine ring was indicated which is having a mass value of 86 (Figure-3.31, 3.32-A, 3.32-B). This was the main difference between DP-1 and DP-2. In DP-1 the oxygen atom was attached to nitrogen of morpholine ring so the first fragment was formed by loss of morpholine ring plus attached oxygen atom, i.e., $498-86-16=396$.

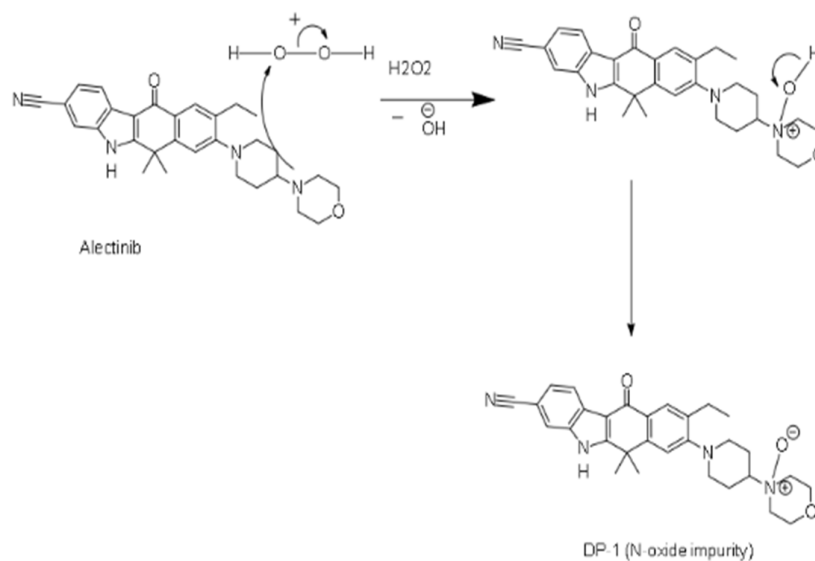
For DP-2, further fragmentation of 412.28 peak of LC-MS spectrum shows the presence of peaks at m/z 384.33 because of loss of ethyl group at position 3 of the structure. Also, removal of cyano and ketone functional group along with the ethyl side chain resulted in fragment ions at m/z 368.25 and m/z 358.28 respectively. The pathway for the generation of all these fragments is shown in Figure-3.33 and Figure-3.32-A, 3.32-B).

Here also, the total number of carbon and proton does not change which is reflected in Proton NMR, ^{13}C -BBD NMR spectra; however, some changes in chemical shift values were noted especially in the region of 5, 6, 9, 10, 11, 12 and 13 due to alteration of neighboring environment because of formation of epoxide ring. One significant change in chemical shift values of DP-2 was noted in the region of 1.0 to 2.0. In the ^1H NMR spectrum of alectinib spectrum, singlet peak due to 6 protons of two methyl groups designated as 10 and 11 in alectinib structure was resonated clearly as a separate peak from the singlet peak due to 3 proton of methyl group designated as 8 in alectinib structure. However, in the ^1H spectra of DP-1, these two singlet peaks were observed to be slightly merged. This is because of the change in the shielding impact of methylene groups due to the formation of the epoxide ring (Figure-3.33). The plausible mechanism of generation of epoxide impurity is mentioned in Figure-3.32 [30]. Hence, the structure of DP-2 (epoxide Impurity) can be confirmed with IUPAC name as 9-ethyl-6, 6-dimethyl-8-(4-morpholinopiperidin-1-yl)-11-oxo-6, 11-dihydro-5H-5a, 11a-poxybenzo

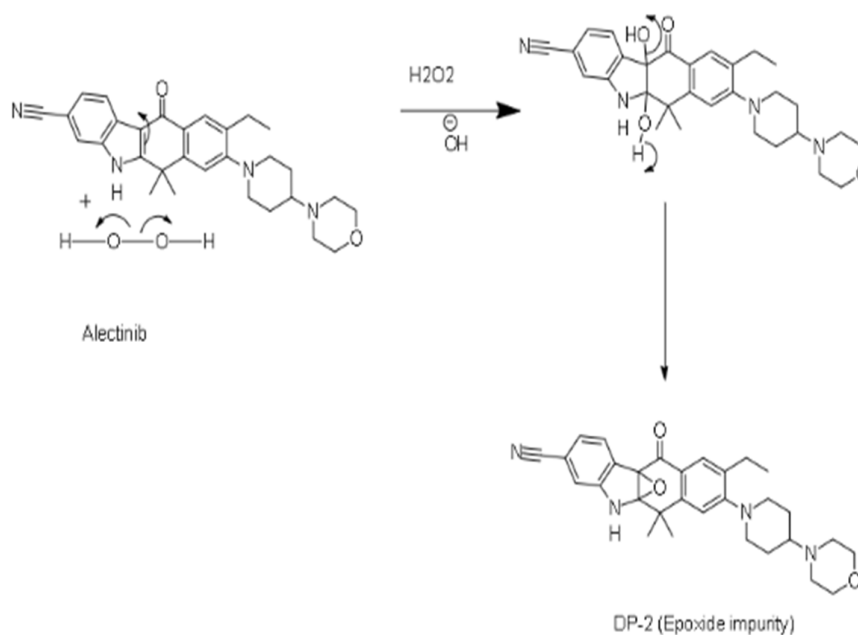
[b]carbazole-3-carbonitrile.

Figure-3.28: Plausible mechanism of formation of degradation products of alectinib

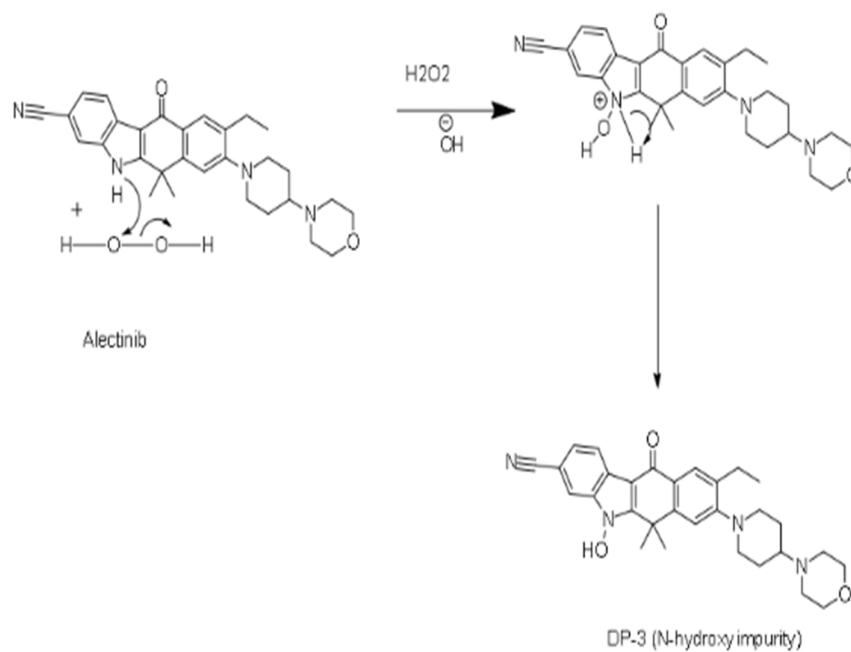
Plausible mechanism of formation of DP-1 (N-oxide impurity)



Plausible mechanism of formation of DP-2 (epoxide impurity)



Plausible mechanism of formation of DP-3 (N-hydroxy impurity)



Plausible mechanism of formation of DP-4 (amide impurity)

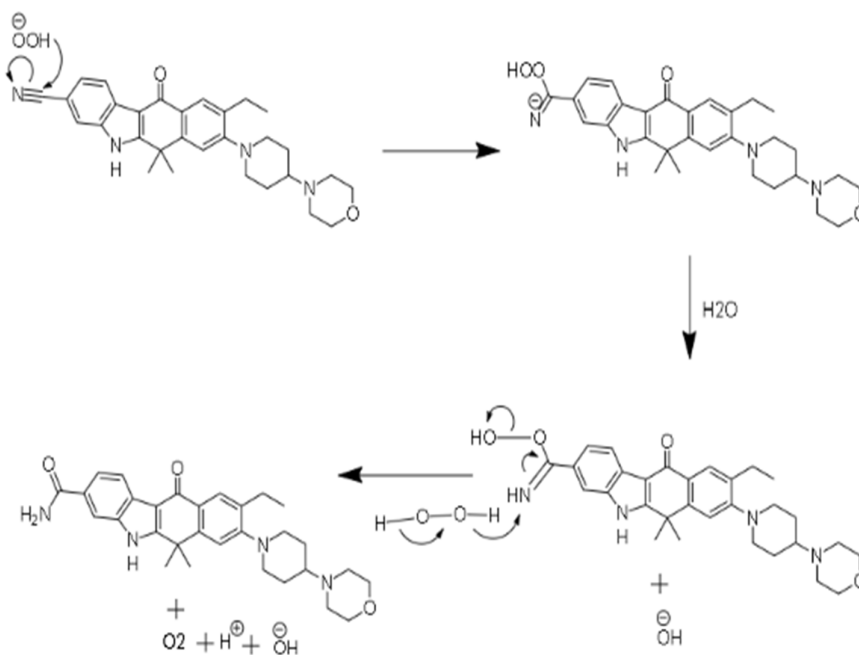


Figure-3.29: LCMS fragmentation pattern of DP-2 (Epoxide impurity)

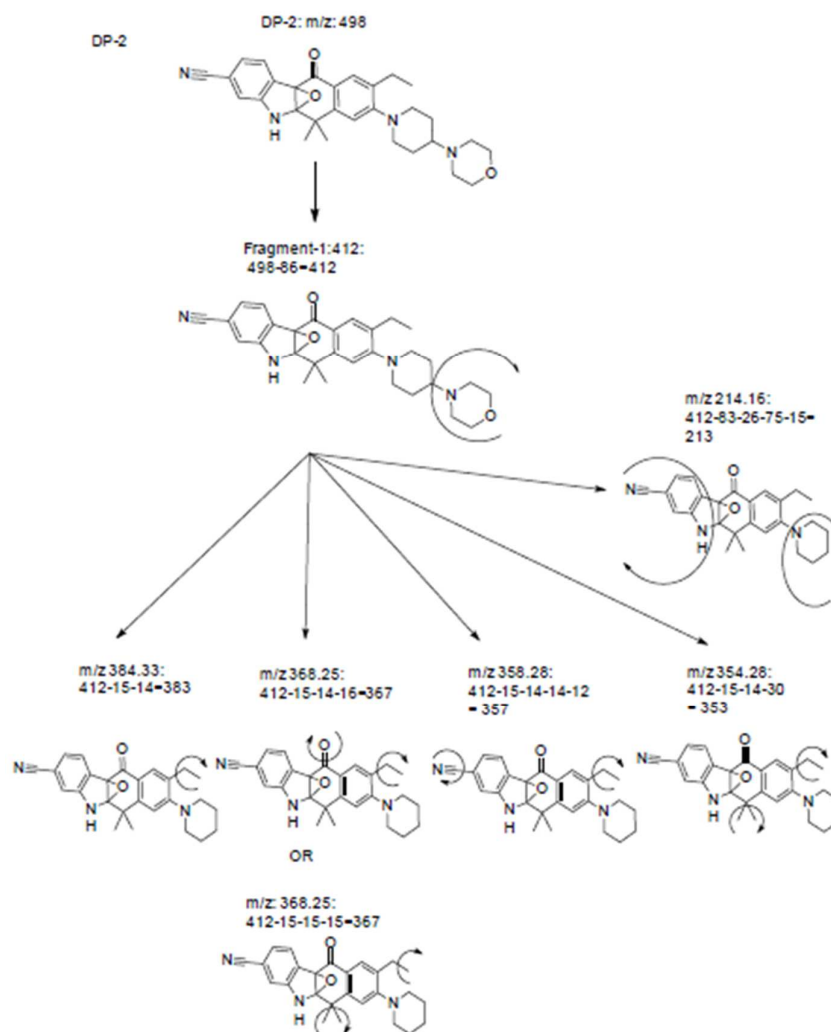


Figure-3.30: FTIR spectra of DP-2 (epoxide impurity)

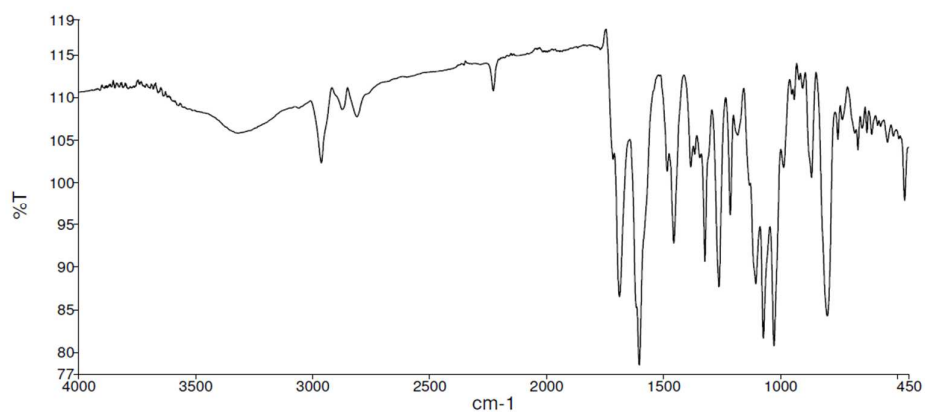


Figure-3.31: HRMS spectra of DP-2 (epoxide impurity)

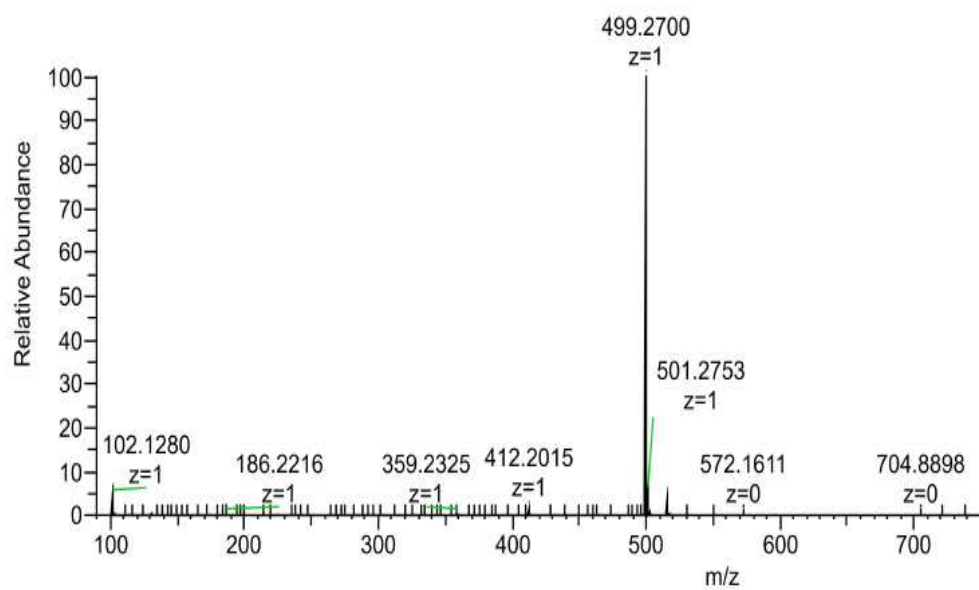
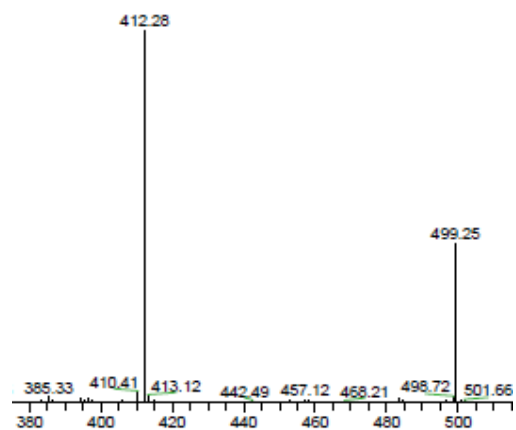


Figure-3.32: LC-MS/MS fragmentation spectra of DP-2 (epoxide impurity)

A. Fragment spectrum-1



B. Fragment spectrum-2

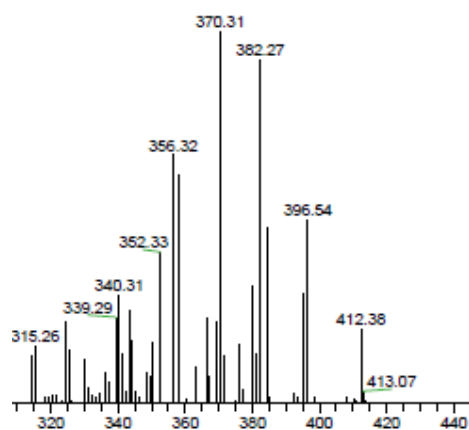
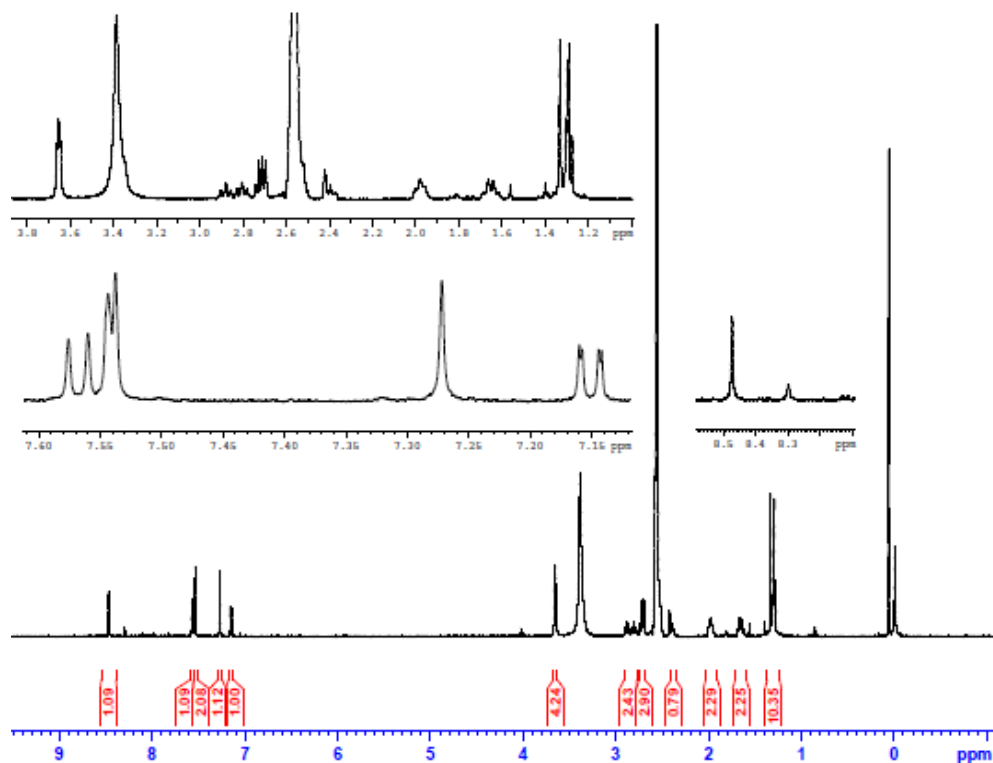


Figure-3.33: Proton (¹H) spectra of DP-2 (epoxide impurity)



3.6.2.2.4 Structure elucidation of degradation product-3 (N-hydroxy impurity)

Out of six possibilities for inclusion of oxygen atom mass in the alectinib structure, the sixth possibility i.e., formation of N-hydroxy at nitrogen between 12 and 19 positions was confirmed in DP-3 MS fragmentation. This is due to the presence of mass fragment at m/z 481.99 (i.e., $498-17=481$) which can only be observed by the removal of a hydroxy functional group from DP-3 structure. The presence of major m/z peak in first LC-MS fragmentation of DP-3 obtained at m/z 395.25 which is in agreement with the removal of this hydroxy group in addition to morpholine ring (i.e., $498-86-16-1=395$) (Figure-3.35-A, 35-B, 35-C). This is in contrast from DP-1 first fragmentation pattern where it generates a molecular ion peak at m/z 396.26 ($498-86-16=396$) instead of 395. The further fragmentation of 395.25 peak of LC-MS spectrum shows peaks at m/z 380.27 which corresponds to the elimination of methyl group at the position of 3 in the structure. All these fragments' structures are presented in Figure-3.34. The plausible mechanism of formation of DP-3 could be as displayed in Figure-3.28 [31]. Hence the structure of DP-3 (N-hydroxy impurity) can be stated with IUPAC name as N-hydroxy Impurity: 9-ethyl-5-hydroxy-6, 6-dimethyl-8-(4-morpholine piperidin-1-yl)-11-oxo-6, 11-dihydro-5H-benzo [b]carbazole-3-carbonitrile.

Figure-3.34: LCMS fragmentation pattern of DP-3 (N-hydroxy impurity)

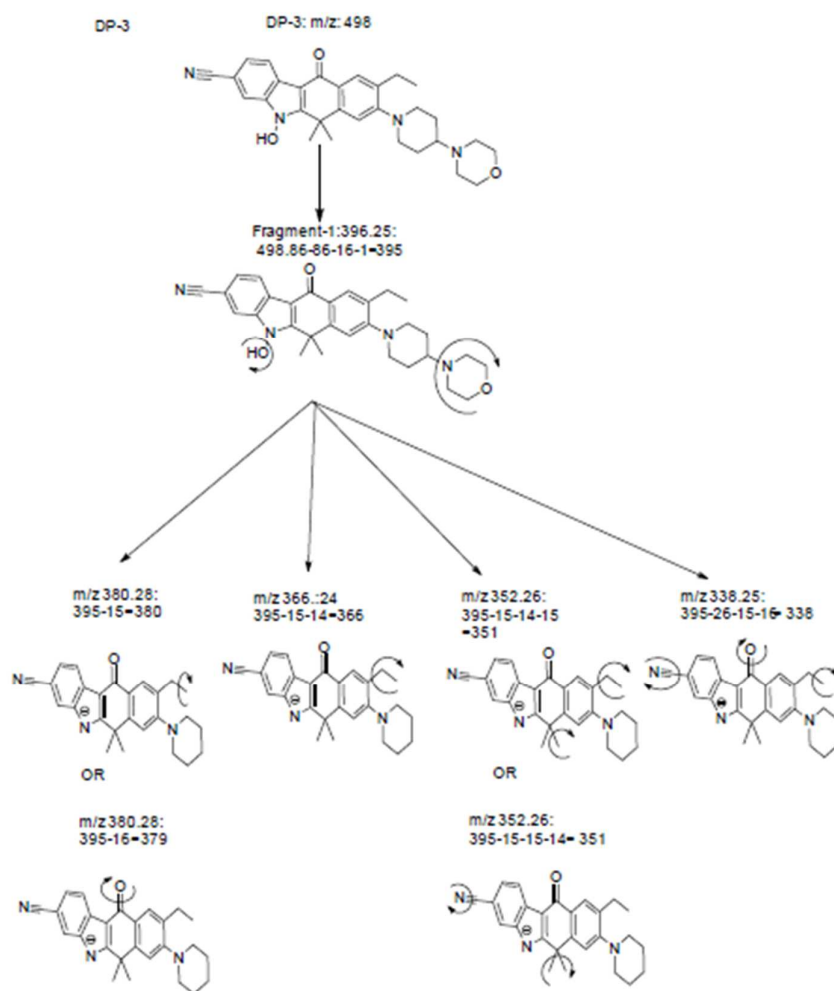
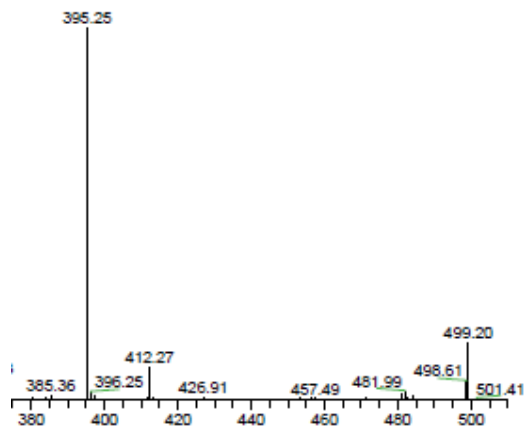
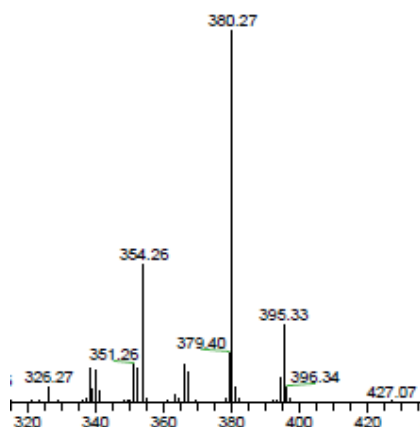


Figure-3.35: LC-MS/MS fragmentation spectra of DP-3 (N-hydroxy impurity)

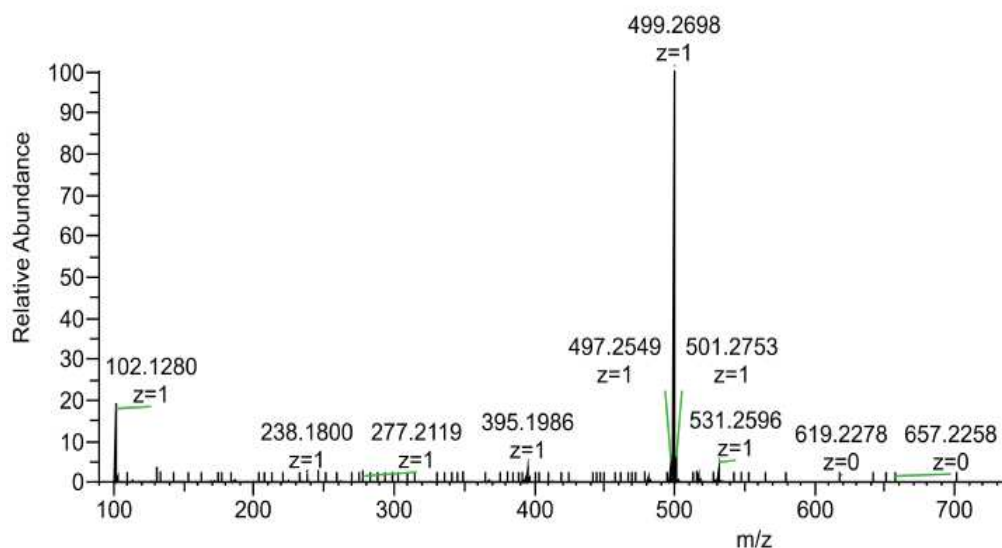
A. Fragment spectrum-1



B. Fragment spectrum-2



C. HRMS spectrum of DP-3 (N-hydroxy impurity)

**3.6.2.2.5 Structure elucidation of degradation product-4 (amide impurity)**

The proton ^1H NMR spectrum suggests the presence of a peak at 7.30 of two protons due to the CONH_2 group in the structure and at the position of the nitrogen molecule of the cyanide group. This characteristic peak is not present in all other degradation products as well as in alectinib ^1H NMR spectrum (Figure-3.36). The FTIR spectrum does not contain the characteristic CN peak at around 2200 due to the formation of the CONH_2 group (Figure-3.37 and Table-3.18). This peak is present in the FTIR spectra of alectinib as well as in other degradation products where the CN group is intact. Apart from this, direct mass LC-MS spectra suggest

the molecular ion peak at m/z 501.27 which agrees with structural molecular mass (Figure-3.38). The plausible mechanism of formation of this degradation product is displayed in Figure-3.28 [32]. Hence the structure of DP-4 (epoxide impurity) can be confirmed with IUPAC name as 9-ethyl-6, 6-dimethyl-8-(4-morpholino piperidin-1-yl)-11-oxo-6,11-dihydro-5H-benzo [b]carbazole-3-carboxamide.

Table-3.18 FTIR spectra interpretation of Alectinib, DP-1 and DP-4

| IR Absorption Band in Alectinib (vcm-1) | IR Absorption Band in DP-1 (vcm-1) | IR Absorption Band in DP-4 (vcm-1) | Peak assignment |
|-----------------------------------------|------------------------------------|------------------------------------|-----------------|
| 3432 | 3418 | 3427 | N-H Stretching |
| 3081, 3051, 2967 | 3037, 2973, 2933 | 2968, 2932 | C-H Stretching |
| 2219 | 2217 | Absent | CN Stretching |
| 1631 | 1625 | 1667, 1630 | C=O Stretching |
| 1132 | 1126 | 1116 | C-O-C Stretch |

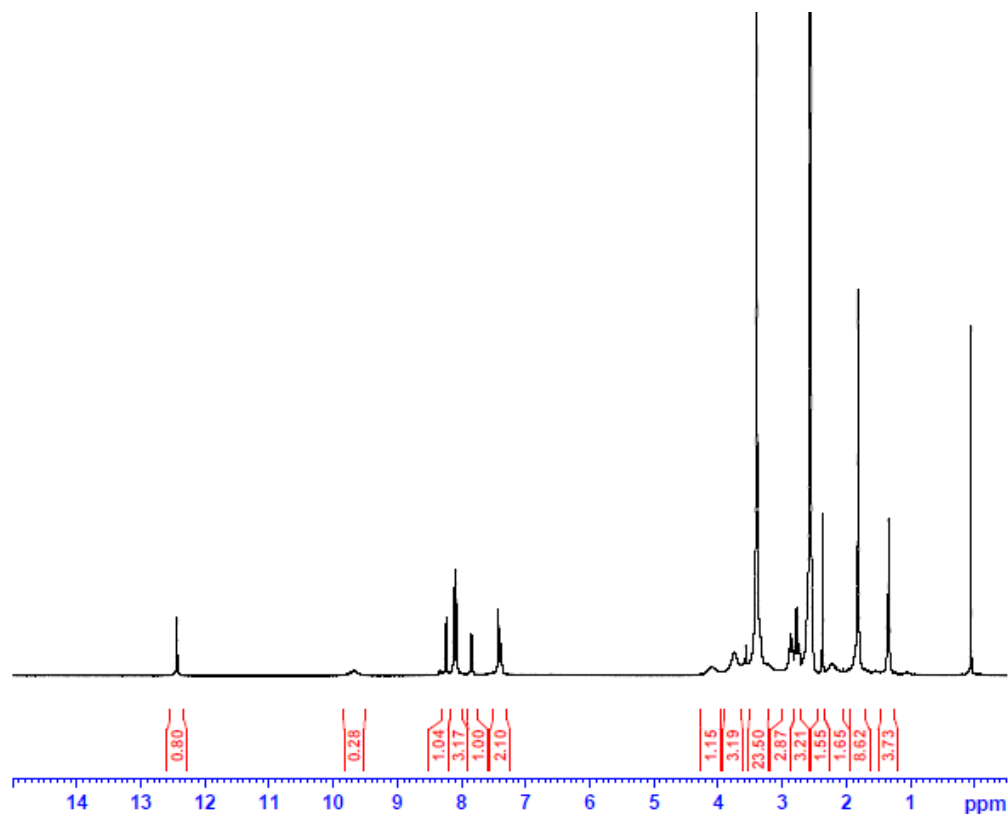
Figure-3.36: Proton (^1H) spectra of DP-4 (amide impurity)

Figure-3.37: FTIR spectra of DP-4 (amide impurity) overlay with alectinib

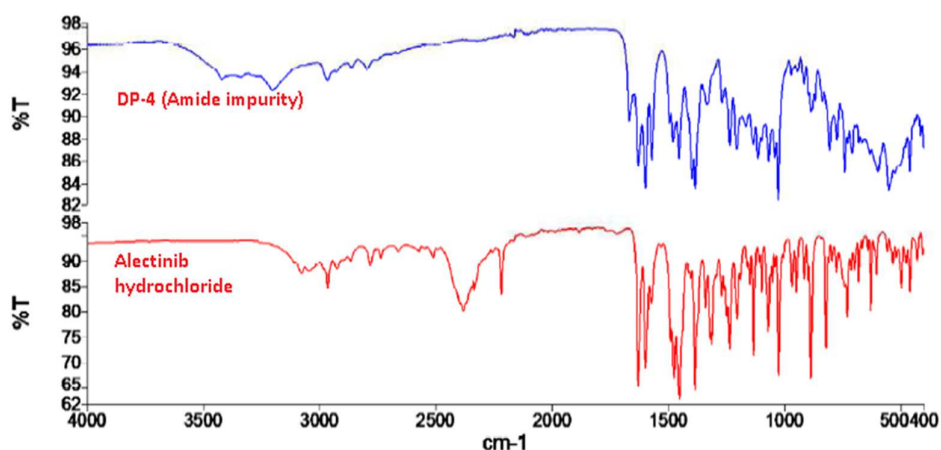
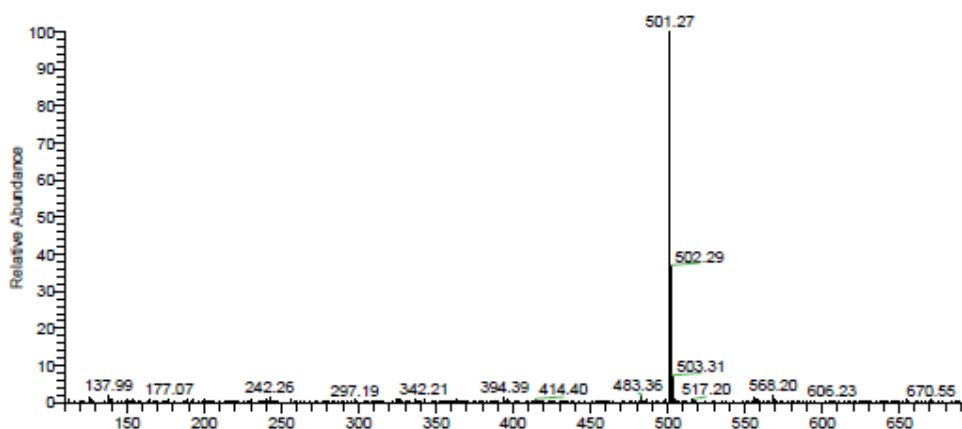


Figure-3.38: LCMS parent ion spectrum of DP-4 (amide impurity)



3.6.2.2.6 Degradation product-5:

Based on molecular ion peak observed as 515.2649 m/z it seems this impurity is generated with addition of two oxygen molecules in the structure of alectinib i.e., $482+16+16=514.62$. This is only possible when the n-oxidation happened at any two position of nitrogen atom in alectinib structure. Because of MS-MS fragments 411.1934 and 412.1976 observed in first MS-MS fragmentation spectra of this impurity, it is clear that one n-oxygen must be there with morpholine ring system so that removal of morpholine moiety along with oxygen molecule attached would produce molecular ion peak near to 411 and 412 ($515-86-16-2=411$) (Figure-3.39 and Figure-3.40). This same fragmentation pattern was observed in other

impurities as well as in alectinib where 396 molecular fragment has been clearly observed ($499-86-16-1=396$). For second n-oxidation, the most prominent and obvious position is the nitrogen atom of piperidine ring next to morpholine moiety. Hence, the probable chemical name of this degradation product is 4-(1-(3-cyano-9-ethyl-6,6-dimethyl-11-oxo-6,11-dihydro-5H-benzo[b]carbazol-8-yl)-1-oxidopiperidin-4-yl)morpholine 4-oxide with exact mass as 514.6260000036 and molecular structure as per Figure-3.38.

Figure-3.38: Molecular structure of Degradation product-5

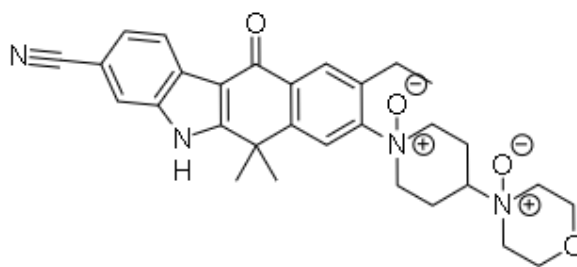


Figure-3.39: HRMS Spectra of DP-5

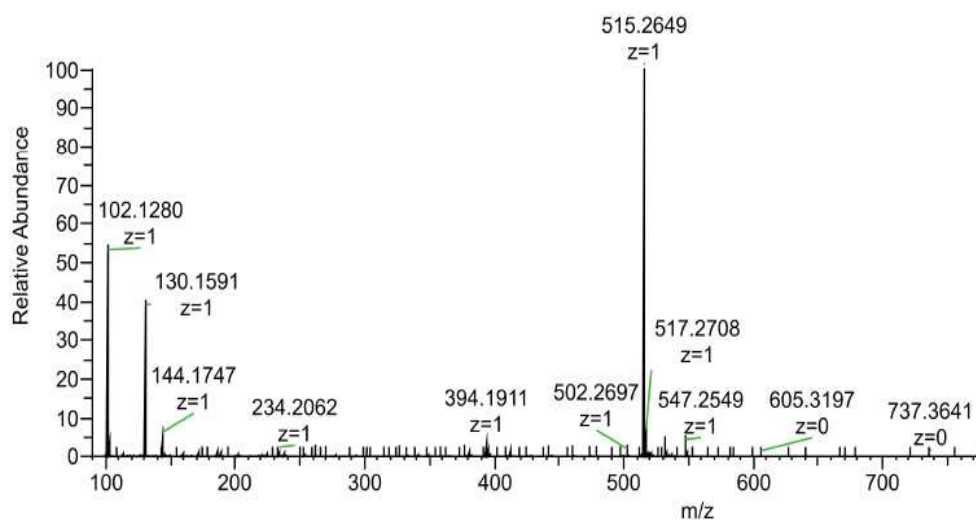
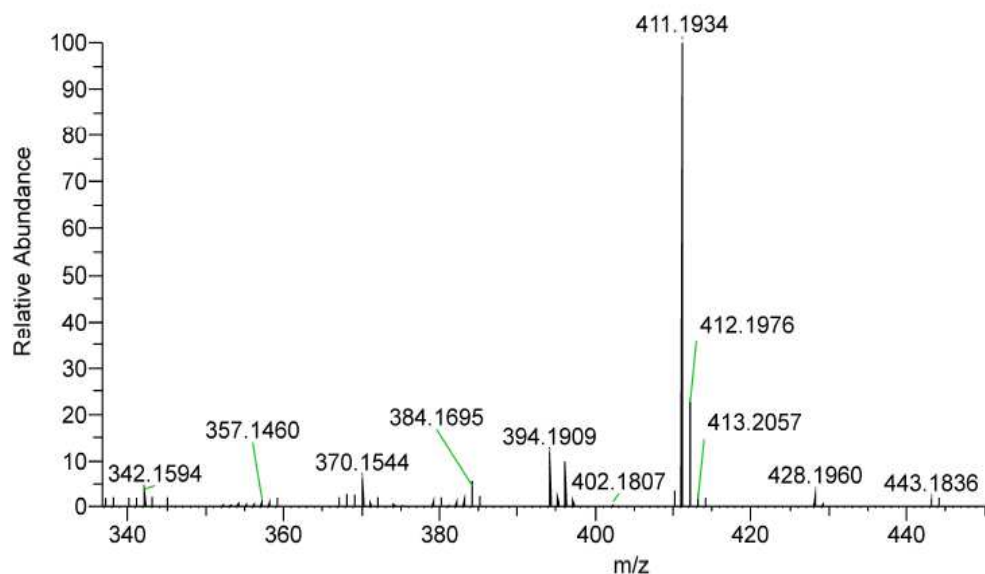


Figure-3.40: HRMS-MS (MS2) Spectra of DP-5



3.6.2.2.7 Degradation product-6:

The molecular ion peak observed for this degradation product is 503.2647 m/z as shown in Figure-3.42 which indicates the mass increment difference of 20 to alectinib ($482+20=502$). This would be possible if one oxygen molecule is incorporated with 4 hydrogen atoms. Out of all the possibilities in the structure for this incorporation, this is only possible when carboxamide formation happens in cyanide functional group of alectinib plus formation of hydroxy group from ketone group of the structure. Formation of carboxamide from cyano functional group adds one oxygen plus two hydrogen mass whereas formation of hydroxy group from ketone group again adds two hydrogen atom mass in the structure. This would lead to the chemical name of this degradation product as 9-ethyl-11-hydroxy-6,6-dimethyl-8-(4-morpholinopiperidin-1-yl)-6,11-dihydro-5H-benzo[*b*]carbazole-3-carboxamide with exact molecular mass as 502.65900000375. The chemical structure of this degradation product shall be as per Figure-3.41.

Figure-3.41: Molecular structure of Degradation product-6

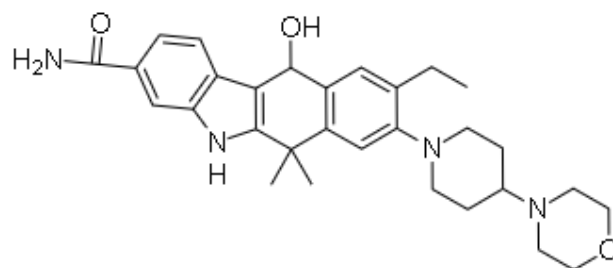
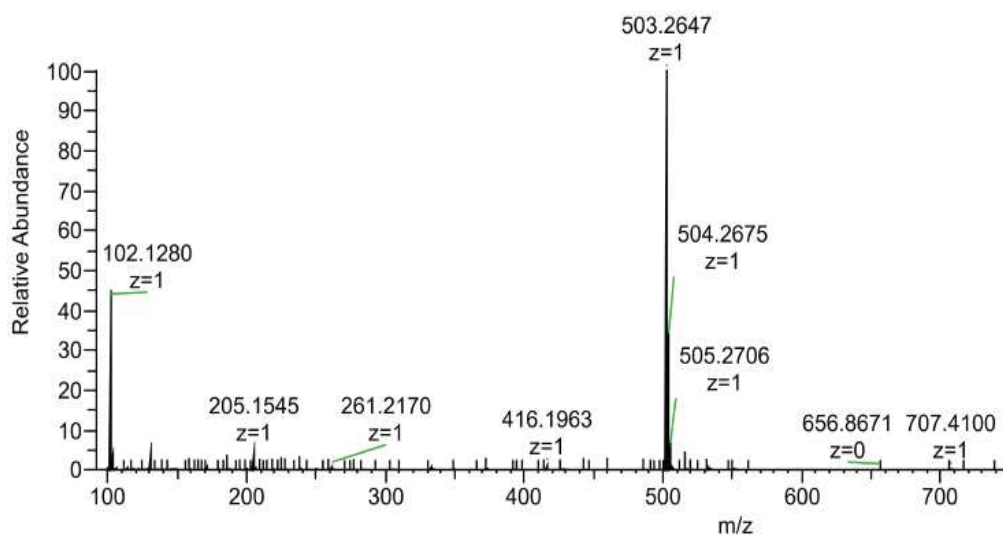


Figure-3.42: HRMS Spectra of DP-6



3.6.2.2.8 Degradation product-7:

This degradation product elutes at RRT 0.24 (RT 2.36min) and produces the molecular ion peak at 533.2755 (Figure-3.44) which suggests that there is addition of three oxygen atoms plus two hydrogen atoms in the structure of alectinib. First probability (Figure-3.46) that was thought of was again formation of n-oxide in morpholine ring system and in next piperidine ring system in addition to carboxamide formation from cyano group which not only adds oxygen atom but also two hydrogen atoms generating final structure with exact molecular mass as 532.64100000375. But when further fragmentation pattern was reviewed it was

found that the prominent molecular ion peak observed in MS-MS spectrum of this degradation product is 446.2070 (Figure-3.45) which is only possible when the morpholine ring system of the alectinib structure remains intact so that it can be removed from the structure with lesser mass of oxygen mass of 16. Based on this fact, first possibility was nullified as this would generate the MS-MS mass at 431.5360000305 and not near to 446.2070. It is obvious therefore that instead of n-oxidation in the morpholine ring system, the oxygen atom needs to be incorporated somewhere else in the structure. Now, the second possibility (Figure-3.47) in the structure for this incorporation is in the N-H group of pyrol 5 membered ring system. Conversion of this N-H group with N-OH group is very much possible generating the molecular mass as 532.64100000375. Moreover, further fragmentation peak of 446.2070 would also feasible when only morpholine ring system without any oxygen atom is removed from this structure ($533-86 = 447$). However, here carboxamide functional group is not possible as the further fragmentation would generate 447 instead of 445. Therefore, formation of N-hydroxy function group from cyano group is possible generating N-oxide formation generating 445 in the MS-MS spectrum. Hence the third and final probability (Figure-3.48) of this degradation product would be formation of n-hydroxy in cyano group and in N-H group of pyrol 5 membered ring system as well as formation of n-oxide in piperidine ring system keeping morpholine ring system as intact. Hence the chemical name of this degradation product would be 1-(9-ethyl-5-hydroxy-3-((hydroxyimino)methyl)-6,6-dimethyl-11-oxo-6,11-dihydro-5H-benzo[b]carbazol-8-yl)-4-morpholinopiperidine 1-oxide with exact mass as 532.64100000375 and chemical structure as per Figure-3.43.

Figure-47_3.43: Molecular structure of Degradation product-7

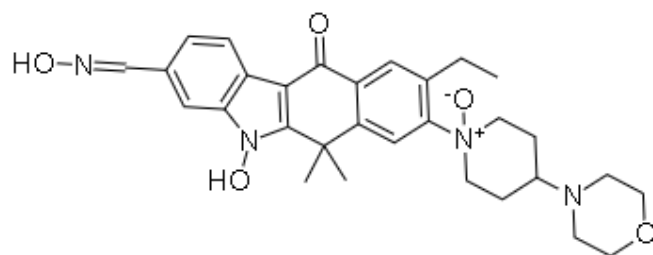


Figure-3.44: HRMS Spectra of DP-7

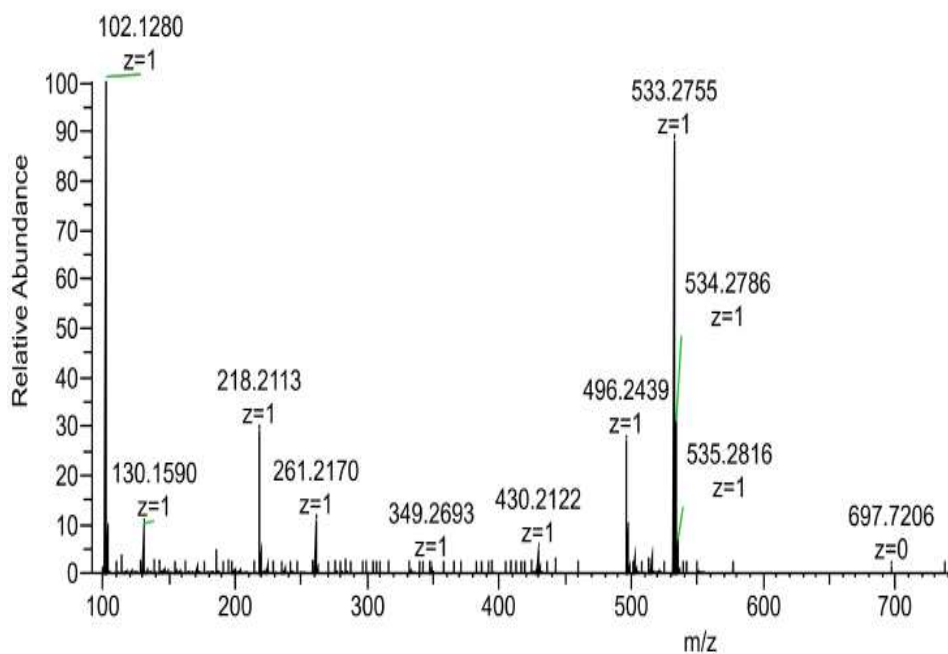


Figure-3.45: HRMS-MS (MS2) Spectra of DP-7

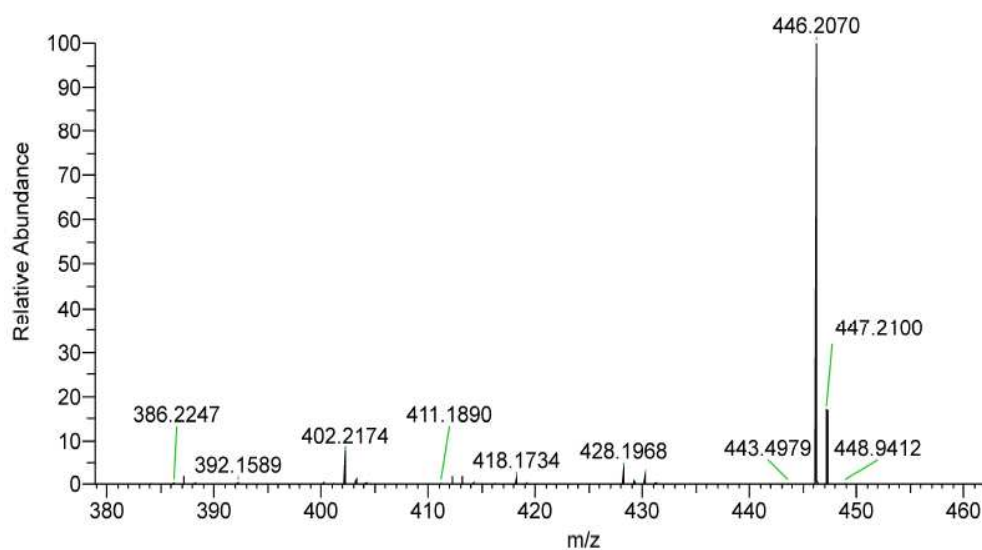
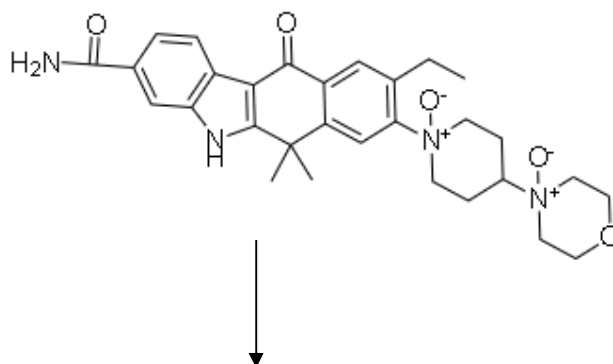


Figure-3.46: Fragmentation pattern of first possibility for molecular mass 532.64100000375:

A. 532.64100000375



Further fragments after removing end ring

431.53600000305

1-(3-carbamoyl-9-ethyl-6,6-dimethyl-11-oxo-6,11-dihydro-5*H*-benzo[*b*]carbazol-8-yl)piperidine 1-oxide

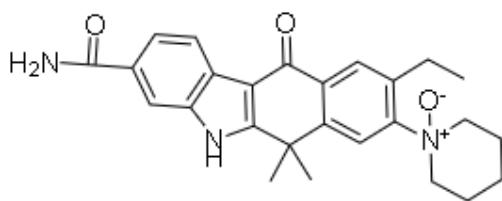
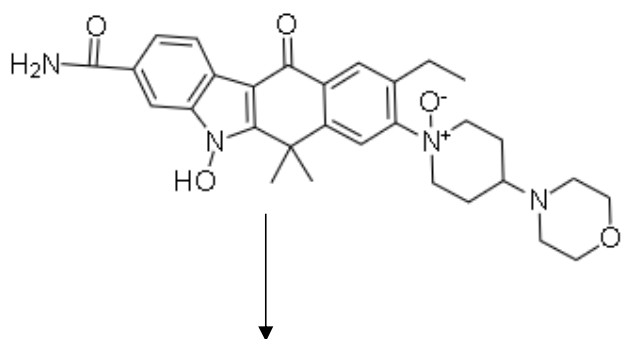


Figure-3.47: Fragmentation pattern of second possibility for molecular mass 532.64100000375:

B.

532.64100000375

1-(3-carbamoyl-9-ethyl-5-hydroxy-6,6-dimethyl-11-oxo-6,11-dihydro-5*H*-benzo[*b*]carbazol-8-yl)-4-morpholinopiperidine 1-oxide



Further fragments after removing end ring

447.5350000031

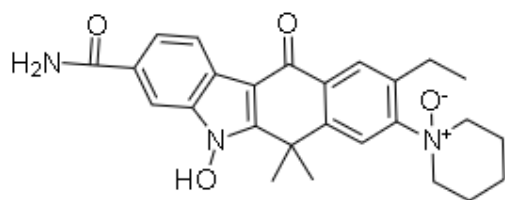
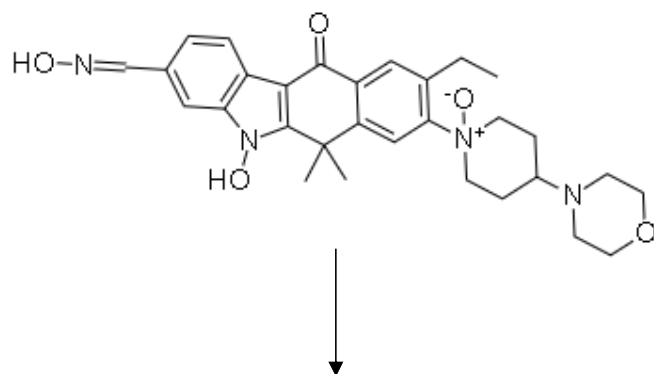


Figure-3.48: Fragmentation pattern of third possibility for molecular mass

532.64100000375:

C. 532.64100000375

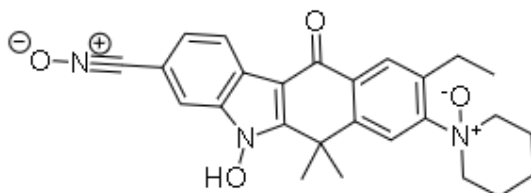
1-(9-ethyl-5-hydroxy-3-((hydroxyimino)methyl)-6,6-dimethyl-11-oxo-6,11-dihydro-5H-benzo[b]carbazol-8-yl)-4-morpholinopiperidine 1-oxide



Further fragments after removing end ring

445.519000003

1-(3-(((1¹-oxidaneyl)-1⁴-azaneylidyne)methyl)-9-ethyl-5-hydroxy-6,6-dimethyl-11-oxo-6,11-dihydro-5*H*-benzo[*b*]carbazol-8-yl)piperidine 1-oxide



3.6.2.2.9 Degradation product-8:

The molecular ion peak observed for this degradation product is 517.2803 (Figure-3.50) which seem that incorporation of 18 molecular mass would be there after n-oxidation of any one ring that is piperidine or morpholine ring system. Again, the MS-MS fragmentation spectrum suggest the presence of molecular ion peak at 430.2122 m/z (Figure-3.51) which indicates the intactness of morpholine ring system confirmation the n-oxidation at piperidine ring system. Apart from this, increment of 18 molecular mass strongly suggest that there would not be any further n-oxidation or n-hydroxy formation which add 16 or 17 molecular mass and not 18. Addition of 18 molecular mass would only be possible in some double bond in the structure so that two more hydrogen atoms can be incorporated in the structure in addition to oxygen atoms. This is again only possible at cyano group of the alectinib structure converting it into n-hydroxy functional group. This would create again the structure same as degradation product-7 but the only difference is the absence of n-hydroxy group in N-H position of pyrol 5 membered ring system. Further fragmentation masses observed in MS-MS spectrum are 430.2122, 413.2049, and 386.2225 which clearly correlates as shown in the Figure-3.51 and with exact mass of 429.5200000295, 413.5210000029,

and 385.467000026 respectively (Figure-3.52). Therefore, the chemical name of this degradation product would be 1-(9-ethyl-3-((hydroxyimino)methyl)-6,6-dimethyl-11-oxo-6,11-dihydro-5H-benzo[*b*]carbazol-8-yl)-4-morpholinopiperidine 1-oxide with exact mass of 516.642000037 and the chemical structure can be depicted as shown in Figure-3.49.

Figure-3.49: Molecular structure of Degradation product-8

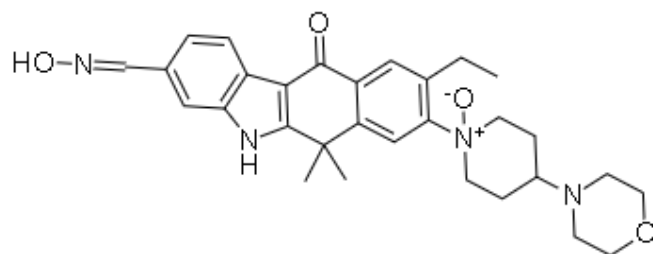


Figure-3.50: HRMS Spectra of DP-8

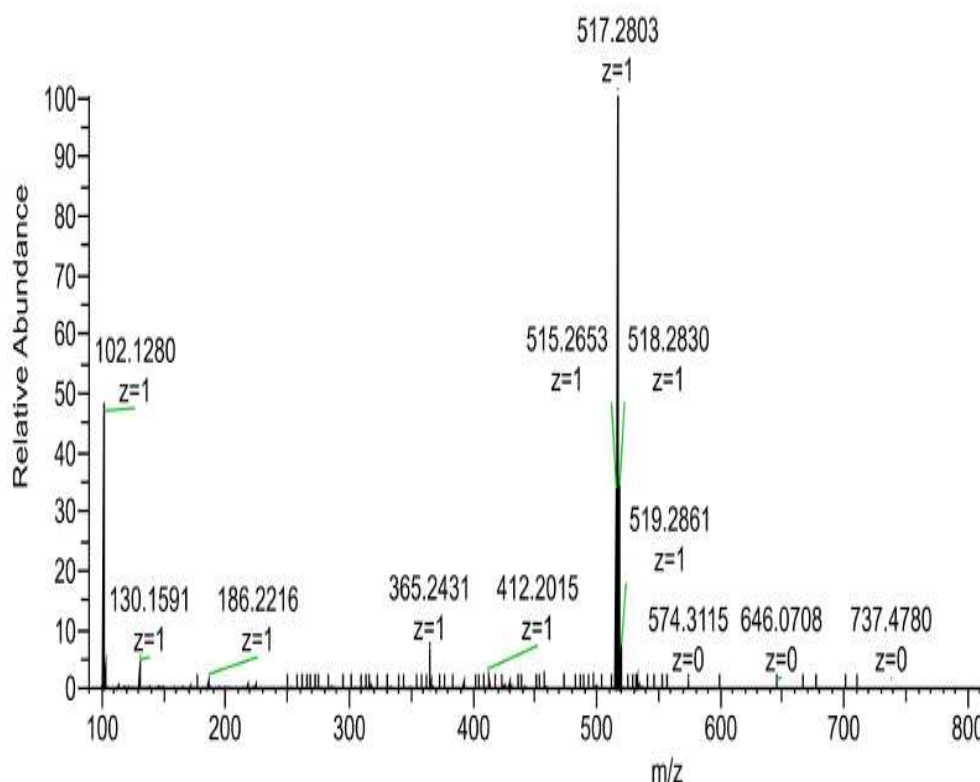


Figure-3.51: HRMS-MS (MS2) Spectra of DP-8

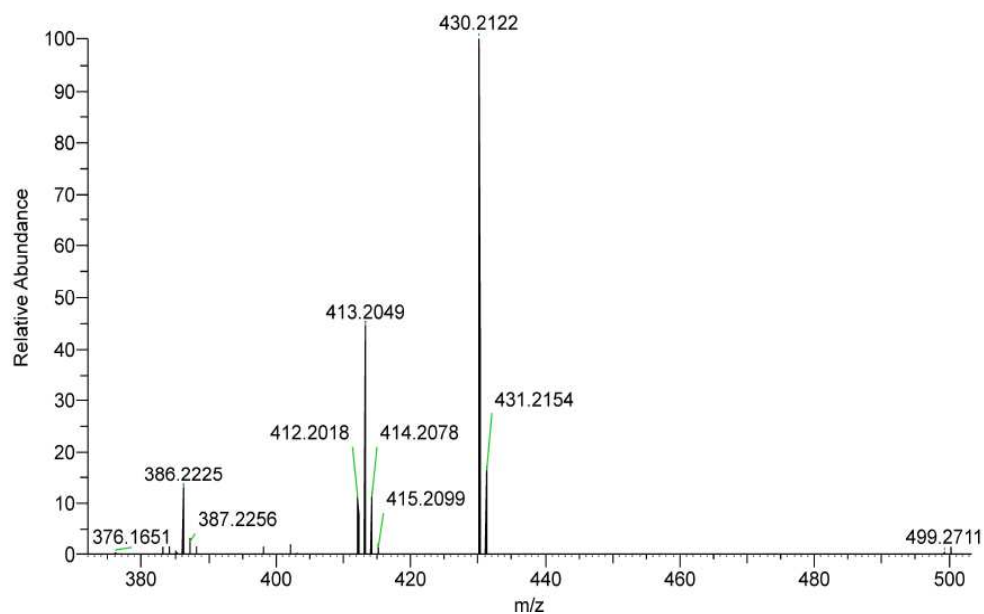
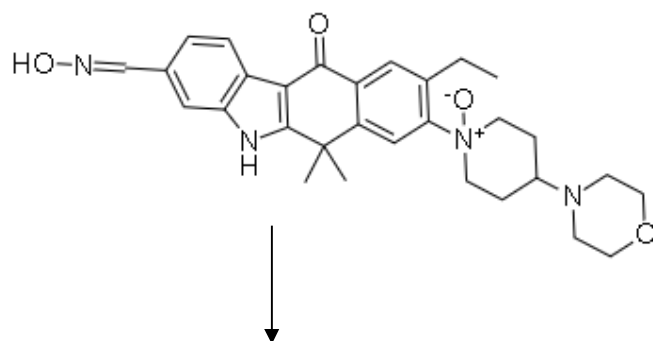


Figure-3.52: Fragmentation pattern of molecular mass 516.6420000037

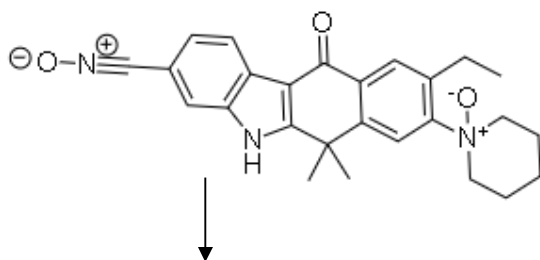
516.6420000037

1-(9-ethyl-3-((hydroxyimino)methyl)-6,6-dimethyl-11-oxo-6,11-dihydro-5H-benzo[b]carbazol-8-yl)-4-morpholinopiperidine 1-oxide



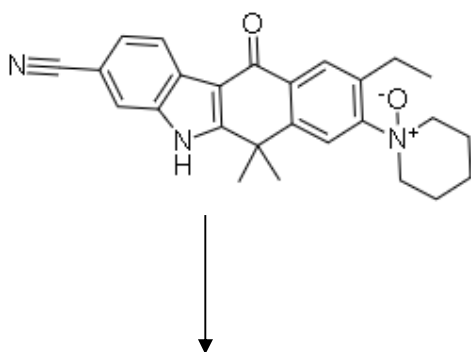
429.52000000295

1-(3-(((1¹-oxidaneyl)-1⁴-azaneylidyne)methyl)-9-ethyl-6,6-dimethyl-11-oxo-6,11-dihydro-5H-benzo[b]carbazol-8-yl)piperidine 1-oxide



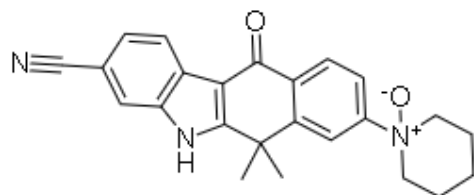
413.5210000029

1-(3-cyano-9-ethyl-6,6-dimethyl-11-oxo-6,11-dihydro-5*H*-benzo[*b*]carbazol-8-yl)piperidine 1-oxide



385.4670000026

1-(3-cyano-6,6-dimethyl-11-oxo-6,11-dihydro-5*H*-benzo[*b*]carbazol-8-yl)piperidine 1-oxide



3.6.2.2.10 Degradation product-9:

It seems from the extensive oxidative degradation of alectinib that this drug is highly sensitive to oxidative degradation condition and generates many isomeric structures with 498 molecular mass giving rises to 499 m/z molecular ion peak in the MS spectra. However, all the isomers are different to one another because their elution in chromatography is different and in some the further fragmentation pattern also differs. When the mass of 499 was extracted from TIC chromatogram of HRMS spectra (Figure-3.54), it gave rise to clear XIC peaks at 8 positions i.e., at 2.76, 3.85, 4.16, 7.00, 8.94, 10.90, 11.35, and at 14.30 minutes which indicates that the degradation products with the same molecular mass of 499 is present at these 8 positions. Out of these, three degradation products i.e., at 2.76 minutes, 4.16 minutes and 8.94 minutes were extensively characterized initially as DP-3, DP-1 and DP-2 respectively. Remaining five degradation products are i.e., 3.85, 7.00, 10.90, 11.35 and 14.30 which are designated as DP-9, DP-12, DP-13, DP-14, and DP-15 respectively (Figure-3.54).

If the possibilities of incorporation of one oxygen molecule in the structure of alectinib are thought of then there are multiple positions, out of which morpholine ring n-oxidation, pyrrol ring N-hydroxy group formation and epoxide formation have been confirmed in DP-1, DP-3 and DP-2 respectively. Two remaining obvious positions in the structure are piperidine ring N-oxide and cyano group N-oxide. Again, these structural modifications have also been observed in DP-5, DP-6, DP-7 and in DP-8 in one or more combination with each other. But if individually taken, these would generate two separate degradation products which has been designated as DP-9 and DP-12 respectively for piperidine ring N-oxide and cyano group N-oxide.

Out of these, if DP-9 is to be considered, it is possible when n-oxidation forms in the piperidine ring next to morpholine ring. Hence the chemical name of DP-9 can be stated as 1-(3-cyano-9-ethyl-6,6-dimethyl-11-oxo-6,11-dihydro-5H-benzo[b]carbazol-8-yl)-4-morpholinopiperidine 1-oxide and the structure shall be as shown in Figure-3.53

Figure-3.53: Molecular structure of Degradation product-9

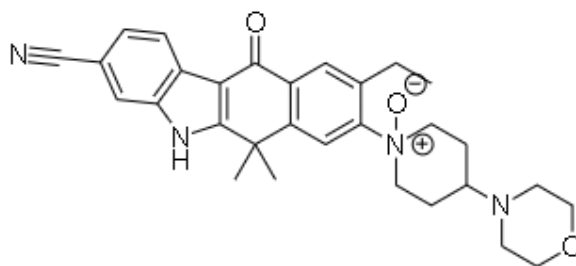


Figure-3.54: HRMS-XIC spectra of molecular mass of 499.2699

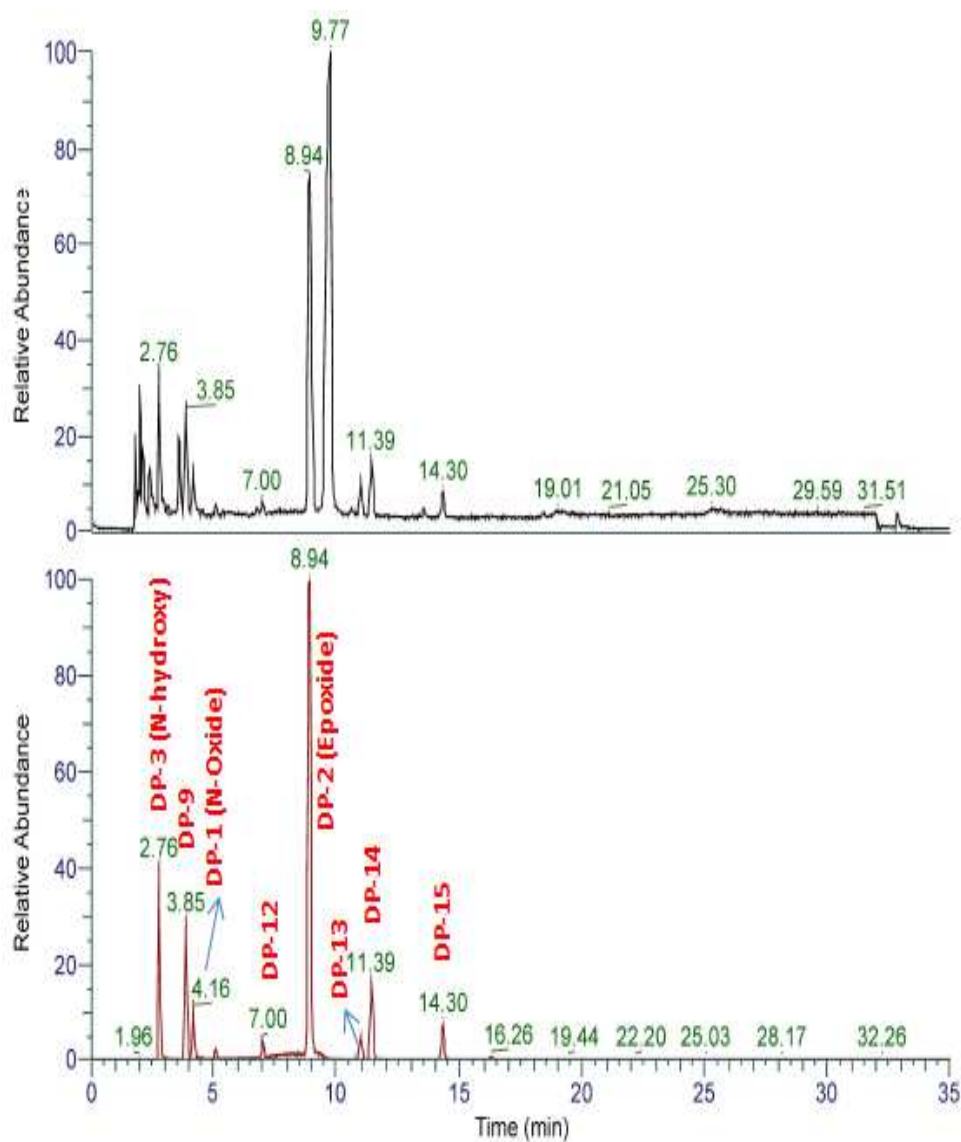


Figure-3.55: HRMS Spectra of DP-9

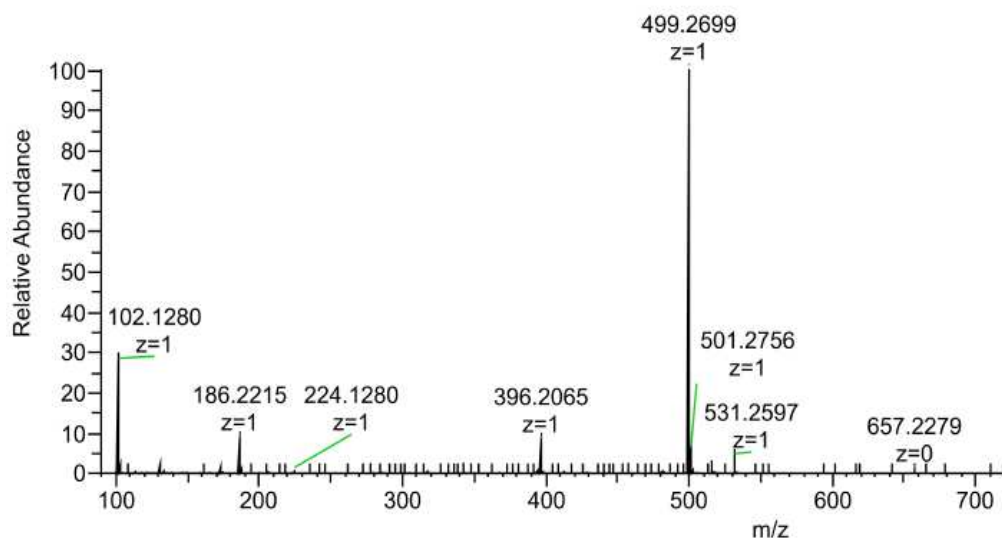
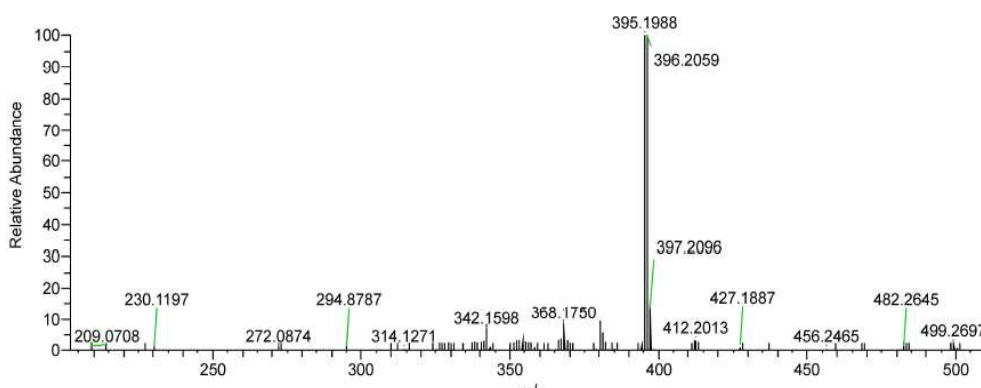


Figure-3.56: HRMS-MS (MS2) Spectra of DP-9



3.6.2.2.11 Degradation product-10:

The molecular ion peaks of degradation product-10, 11 and 16 have not been detected in positive ESI mode of HRMS instrument but same were detected in negative ESI mode of instrument (Figure-3.58). In each of these three degradation products, the end morpholine ring is highly probable to be removed from the structure as all of these degradation products have mass in the range of 358 to 377 which is only possible with that hypothesis. After removal of the morpholine ring in the alectinib structure, the moiety with 397 molecular mass is generated which get further modification by oxidation and generate other degradation products with

molecular masses in the range of 358 to 377. Out of these possibilities, degradation product-10 is thought to be produced when dimethyl group is removed from 397 moiety in addition to double bond generation at three positions i.e., one bond in ethyl side chain and two bonds in piperidine ring moiety. This product would have the theoretical molecular mass of 363.42000000225 for which the molecular ion peak of 362.1170 m/z has been observed in the HRMS spectra which has isotopic molecular ion peak of 361.1142 m/z (Figure-3.59). Based on this the chemical name of DP-10 can be stated as 11-oxo-8-(pyridin-1(4*H*)-yl)-9-vinyl-6,11-dihydro-5*H*-benzo[*b*]carbazole-3-carbonitrile and the molecular structure can be depicted as shown in Figure-3.57.

Figure-3.57: Molecular structure of Degradation product-10

363.42000000225

11-oxo-8-(pyridin-1(4*H*)-yl)-9-vinyl-6,11-dihydro-5*H*-benzo[*b*]carbazole-3-carbonitrile

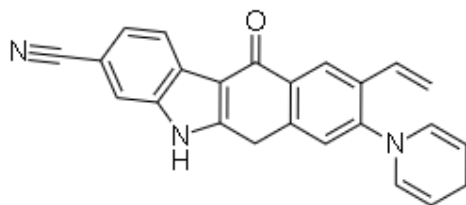


Figure-3.58: HRMS Spectra of DP-10

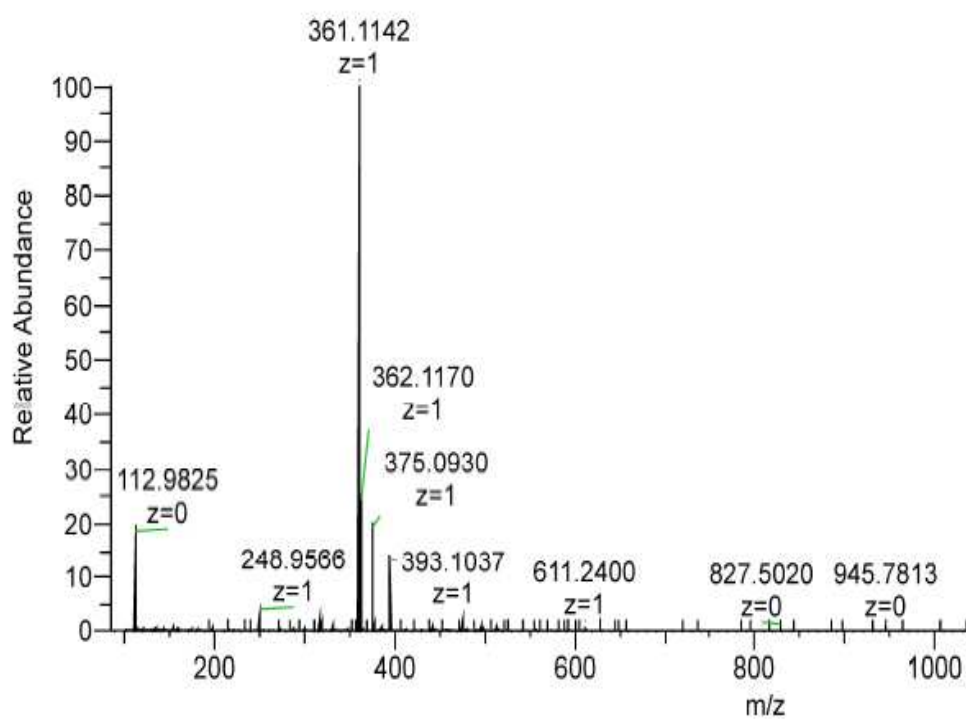
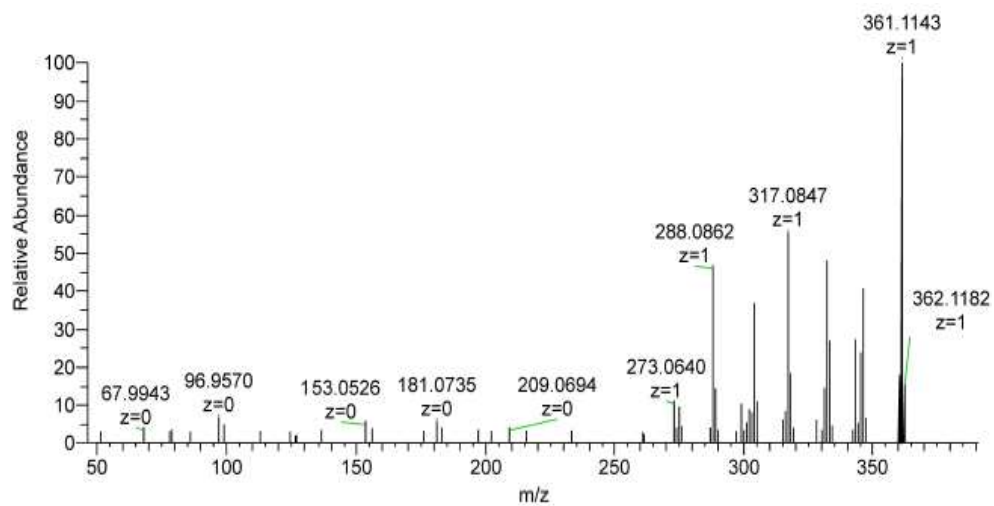


Figure-3.59: HRMS-MS (MS2) Spectra of DP-10



3.6.2.2.12 Degradation product-11:

Further to the results and discussion for degradation product-10, if same three double bonds are produced in the same positions except removal of dimethyl group in the alectinib structure. In addition, if oxygen molecule of the alectinib group is removed, the structure with molecular mass 377.4910000026 would be produced which correlates with the molecular ion peak of 377.1087 m/z observed in HRMS HESI negative mode (Figure-3.61). Hence based on this, the chemical name of the DP-11 can be stated as 6,6-dimethyl-8-(pyridin-1(4*H*)-yl)-9-vinyl-6,11-dihydro-5*H*-benzo[*b*]carbazole-3-carbonitrile and the molecular structure can be depicted as shown in Figure-3.60.

Figure-3.60: Molecular structure of Degradation product-11

377.4910000026

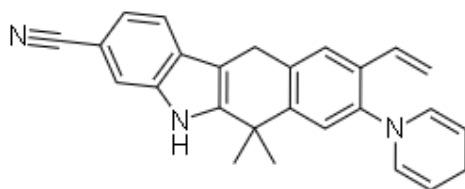
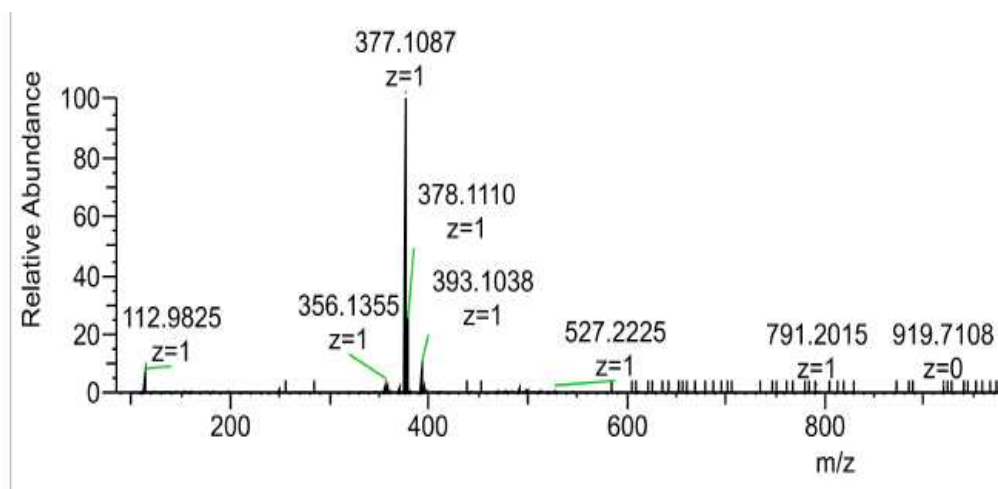
6,6-dimethyl-8-(pyridin-1(4*H*)-yl)-9-vinyl-6,11-dihydro-5*H*-benzo[*b*]carbazole-3-carbonitrile

Figure-3.61: HRMS Spectra of DP-11



3.6.2.2.13 Degradation product-12:

Out of the two remaining positions for N-oxidation discussed in the section of degradation product-9, the second probability suits with this fragmentation pattern where cyano group of alectinib gets oxidized and converted to cyanon-oxide as depicted in Figure-3.62 with molecular mass 499.2703.

Figure-3.62: Molecular structure of Degradation product-12

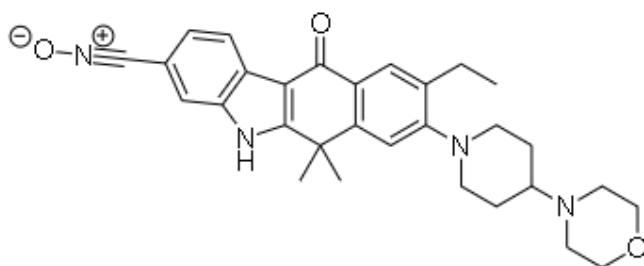


Figure-3.63: HRMS Spectra of DP-12

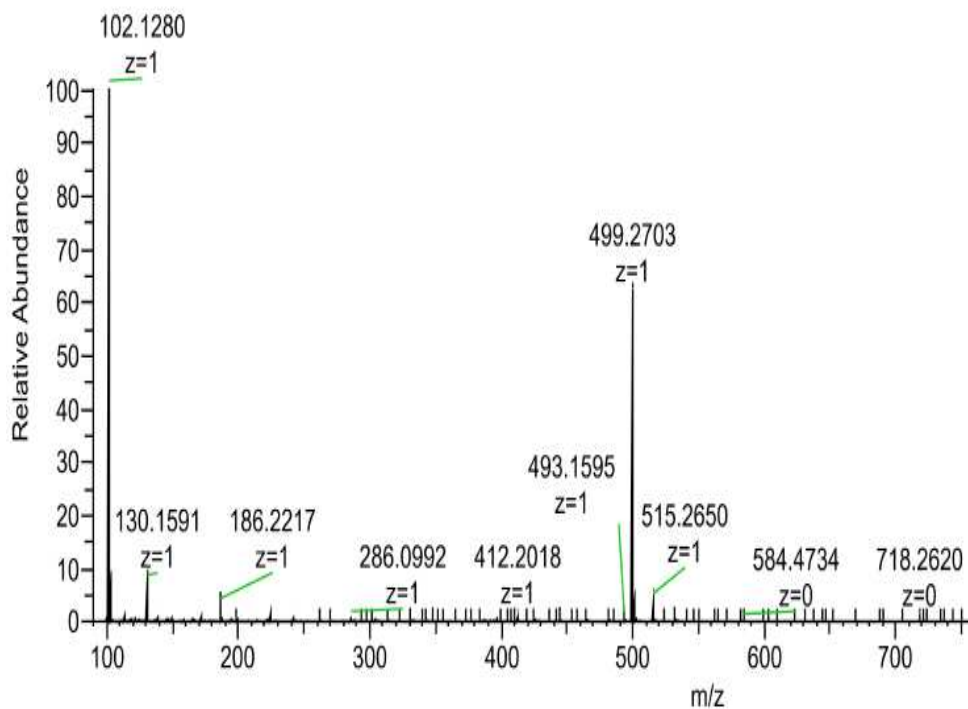
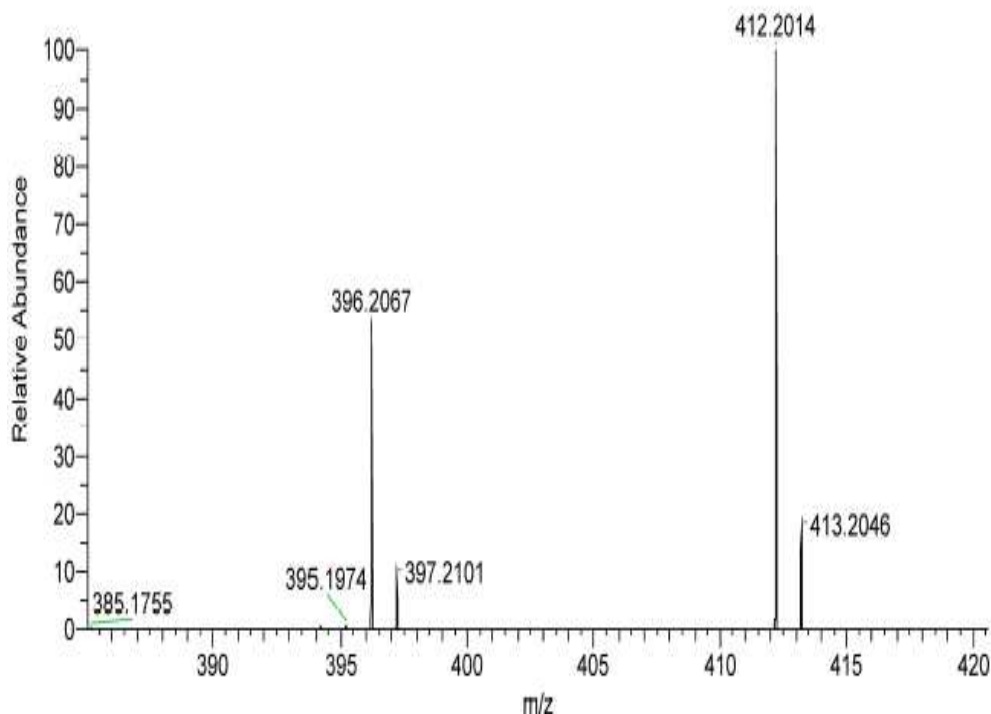


Figure-3.64: HRMS-MS (MS2) Spectra of DP-12



3.6.2.2.14 Degradation product-13

All the oxidation isomeric peaks eluted before alectinib peak are thought to have high polarity compared to the same isomeric peaks eluted after alectinib peak. Hence all the peaks eluted before alectinib peak i.e., DP-1, DP-2, DP-3, DP-9, and DP-12 are characterized as N-oxide or N-hydroxy group formation in the structure. However, there are three more peaks with molecular mass 499 after alectinib main peak which may have some common factor of getting oxidized with modification in side chain containing CH₂-CH₃ group. Out of these two adjacent peaks of DP-13 and DP-14 are probable when -CH₂-CH₃ group gets converted to either -CH₂-C=O-CH₃ (ketone) or -CH₂-CHO (aldehyde) with formation of C-OH from C=O at position 21 of alectinib structure. These two modifications would have same molecular mass of 498.62700000355. Out of these two, ketone modification is thought to have formed in DP-13. Moreover, the MS-MS fragmentation pattern of DP-13 (Figure-3.67) is unique out of all the eight isomeric degradation products

which give 487.4868 m/z and 400.2182 m/z molecular ion peaks which are not observed in any of the other degradation products. These two fragments molecular masses have also been found correlated. When ketone functional group again gets reversed with formation of $-\text{CH}-\text{CH}_3$, structure with 486.660000037 gets formed which is responsible for generation of molecular ion peak at 487.4868 m/z as shown in Figure 3.68. From this structure, if characteristic morpholine ring is removed, it produces fragment with molecular mass 400.545451423. This fragment is having isotopic molecular ion peaks of 401.2216, 400.2186, 399.2158, 396.2131, and 397.2102 (Figure-3.67 and 3.68).

The chemical name can be stated as 9-acetyl-11-hydroxy-6,6-dimethyl-8-(4-morpholinopiperidin-1-yl)-6,11-dihydro-5*H*-benzo[*b*]carbazole-3-carbonitrile and the structure can be depicted as shown in Figure-3.65.

Figure-3.65: Molecular structure of Degradation product-13

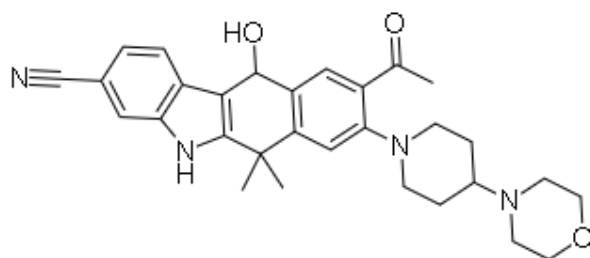


Figure-3.66: HRMS Spectra of DP-13

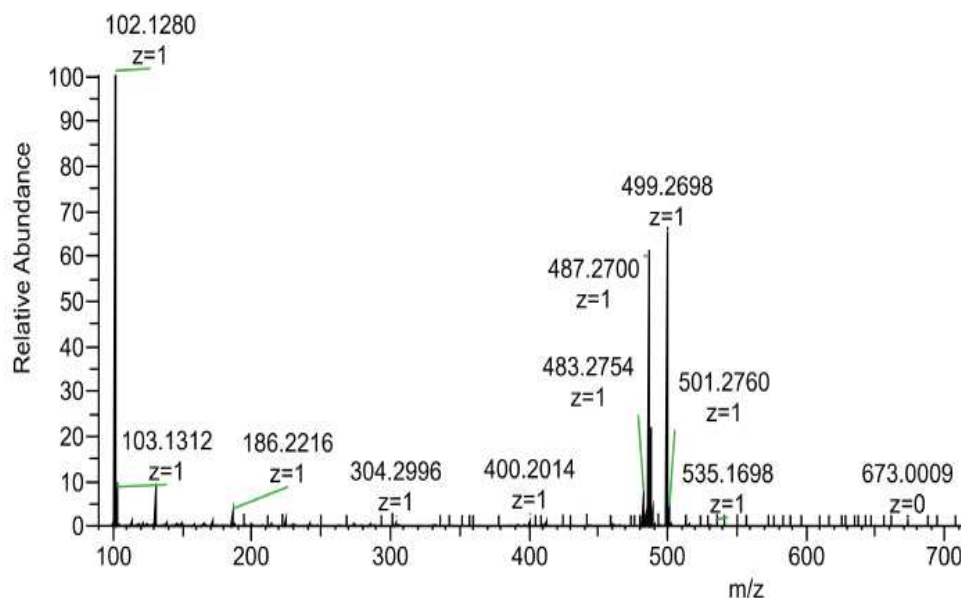


Figure-3.67: HRMS-MS (MS2) Spectra of DP-13

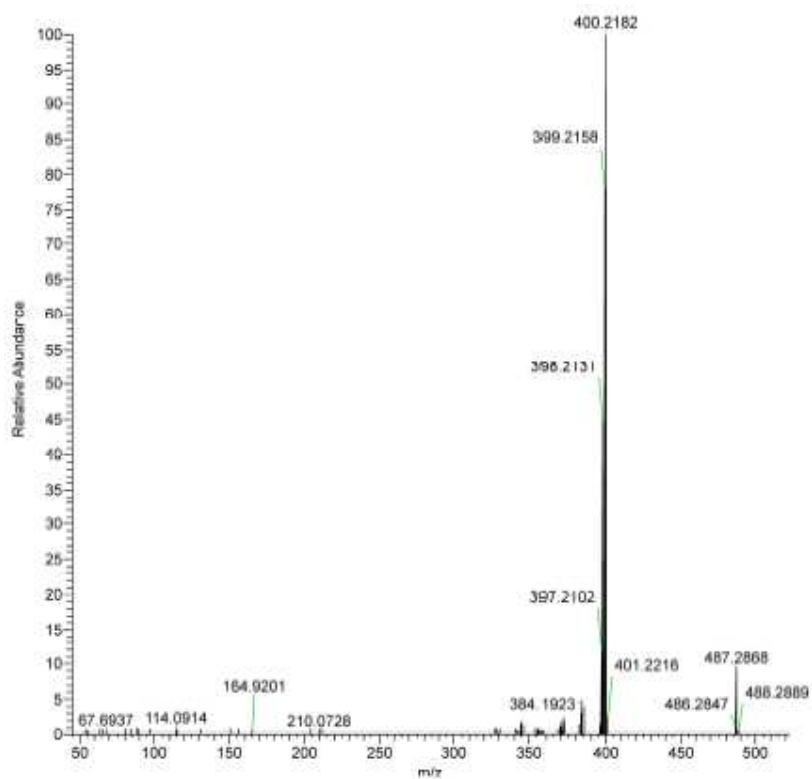
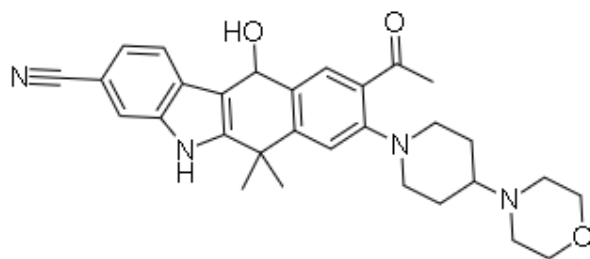


Figure-3.68: Fragmentation pattern of molecular mass 498.62700000355:

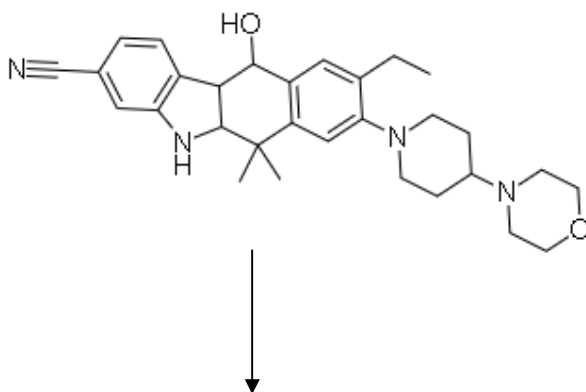
498.62700000355

9-acetyl-11-hydroxy-6,6-dimethyl-8-(4-morpholinopiperidin-1-yl)-6,11-dihydro-5H-benzo[b]carbazole-3-carbonitrile



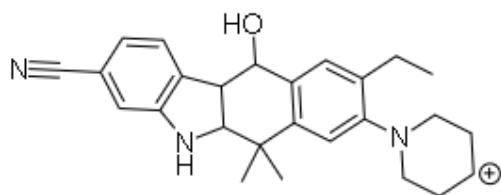
486.660000037

9-ethyl-11-hydroxy-6,6-dimethyl-8-(4-morpholinopiperidin-1-yl)-5a,6,11,11a-tetrahydro-5H-benzo[b]carbazole-3-carbonitrile



400.545451423

1-(3-cyano-9-ethyl-11-hydroxy-6,6-dimethyl-5a,6,11,11a-tetrahydro-5H-benzo[b]carbazol-8-yl)piperidin-4-ylum



3.6.2.2.15 Degradation product-14:

Out of the two possibilities of modification of -CH₂-CH₃ group discussed under section DP-13, if aldehyde functional group (-CH₂-CHO) forms from -CH₂-CH₃, it is probable to form in DP-14. This modification would also generate same molecular mass 498.6270000355 giving molecular ion peak at 499.2700 m/z (Figure-3.70). The chemical name of the structure can be stated as 11-hydroxy-6,6-dimethyl-8-(4-morpholinopiperidin-1-yl)-9-(2-oxoethyl)-6,11-dihydro-5H-benzo[b]carbazole-3-carbonitrile and the structure

has been shown in Figure-3.69.

Figure-3.69: Molecular structure of Degradation product-14:

498.6270000355

11-hydroxy-6,6-dimethyl-8-(4-morpholinopiperidin-1-yl)-9-(2-oxoethyl)-6,11-dihydro-5H-benzo[*b*]carbazole-3-carbonitrile

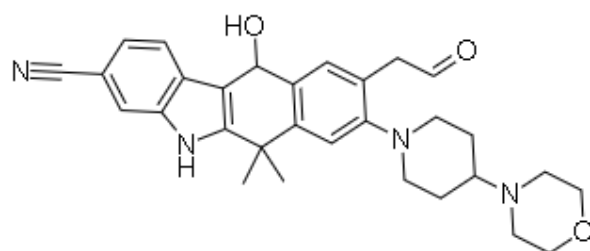


Figure-3.70: HRMS Spectra of DP-14

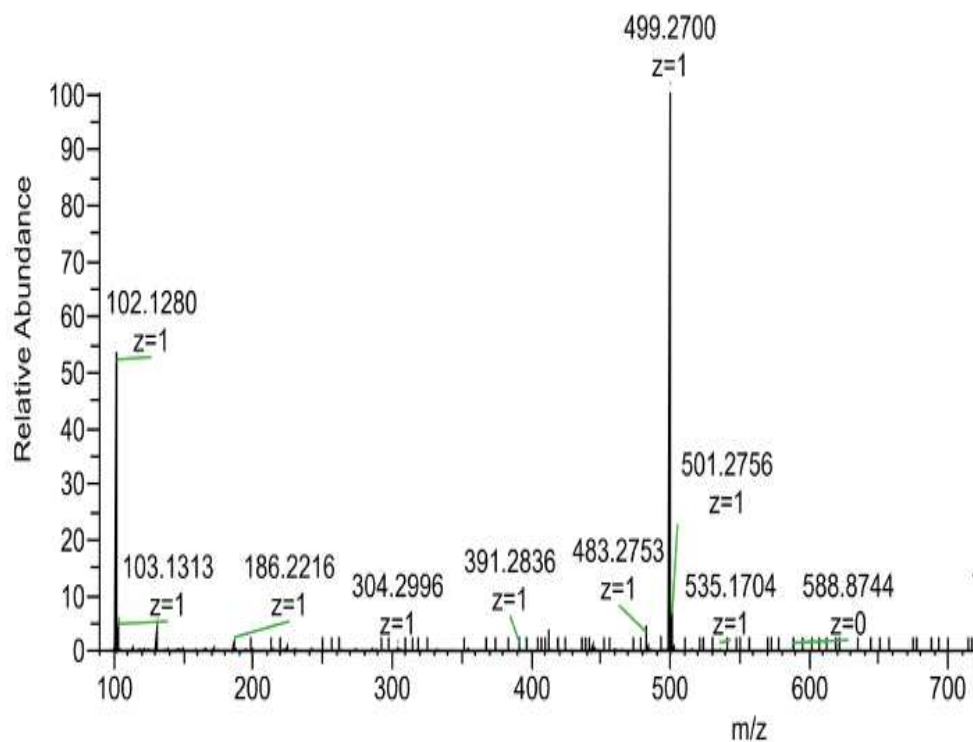
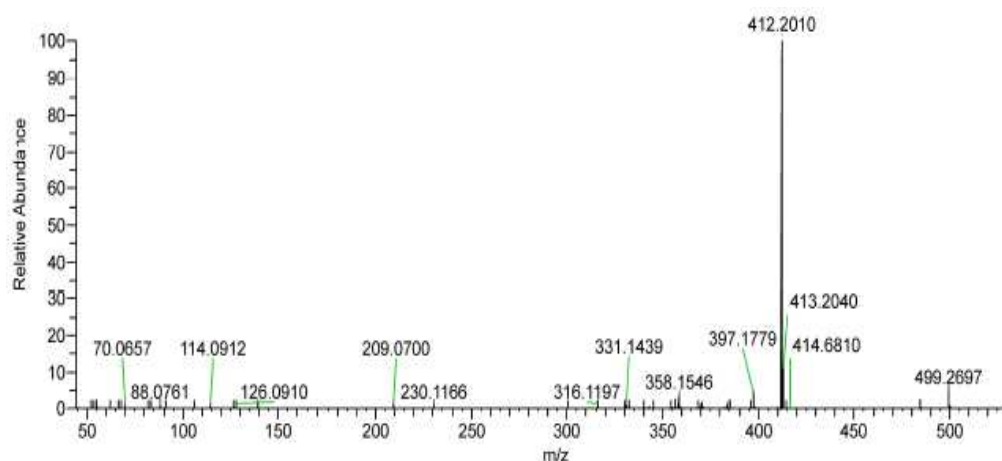


Figure-3.71: HRMS-MS (MS2) Spectra of DP-14



3.6.2.2.16 Degradation product-15:

Apart from the modifications of $-\text{CH}_2\text{-CH}_3$ group discussed in DP-13 and DP-14; the only possibility remains is alcohol ($-\text{CH}_2\text{-CH}_2\text{-OH}$) formation from $-\text{CH}_2\text{-CH}_3$. This again would have same molecular mass as 498.62700000355 with chemical name as 9-(2-hydroxyethyl)-6,6-dimethyl-8-(4-morpholinopiperidin-1-yl)-11-oxo-6,11-dihydro-5H-benzo[b]carbazole-3-carbonitrile. The structure is shown in Figure-3.72.

Figure-3.72: Molecular structure of Degradation product-15

498.62700000355

9-(2-hydroxyethyl)-6,6-dimethyl-8-(4-morpholinopiperidin-1-yl)-11-oxo-6,11-dihydro-5H-benzo[b]carbazole-3-carbonitrile

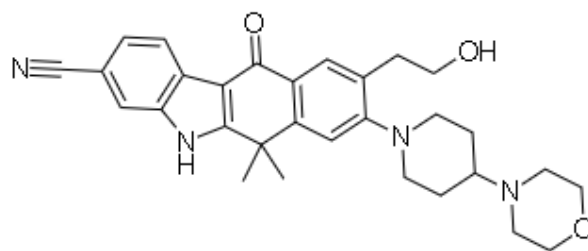
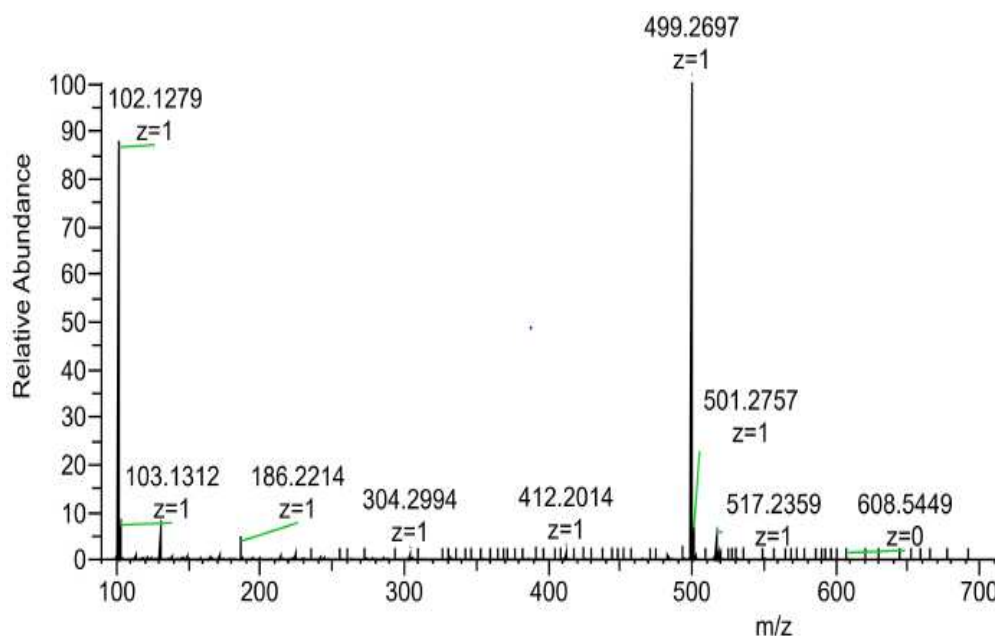


Figure-3.73: HRMS Spectra of DP-15



3.6.2.2.17 Degradation product-16:

This degradation product's molecular ion peak was observed at 358.1145 m/z (Figure-3.75). As per discussion in DP-10 and DP-11, this DP-16 would also have molecular structure where morpholine ring moiety is removed and some other modifications in probable functional groups are happened. Out of all the possibilities of oxygen group, diethyl group, dimethyl group and cyano group, the only possibility that can be correlated with the molecular ion peak observed at 358.1145 m/z (Figure 3.76) and the MS2 fragment ion molecular ion peak at 343.0915 m/z is removal of dimethyl group along with conversion of cyano group to methyl group. This would produce the molecular structure as per Figure-3.74 which has theoretical molecular mass as 358.48500000265 generating 358.1145 m/z molecular ion peak in HRMS negative mode. Moreover, if methyl group is again removed from DP-16 structure, it would generate molecular mass of 344.4580000025 which is also correlated with the MS2 fragment molecular ion peak at 343.0915 m/z (Figure-3.76 and Figure-3.77).

Figure-3.74: Molecular structure of Degradation product-16

358.48500000265

9-ethyl-3-methyl-8-(piperidin-1-yl)-5,6-dihydro-11H-benzo[*b*]carbazol-11-one

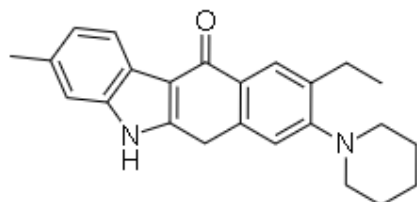


Figure-3.75: HRMS Spectra of DP-16

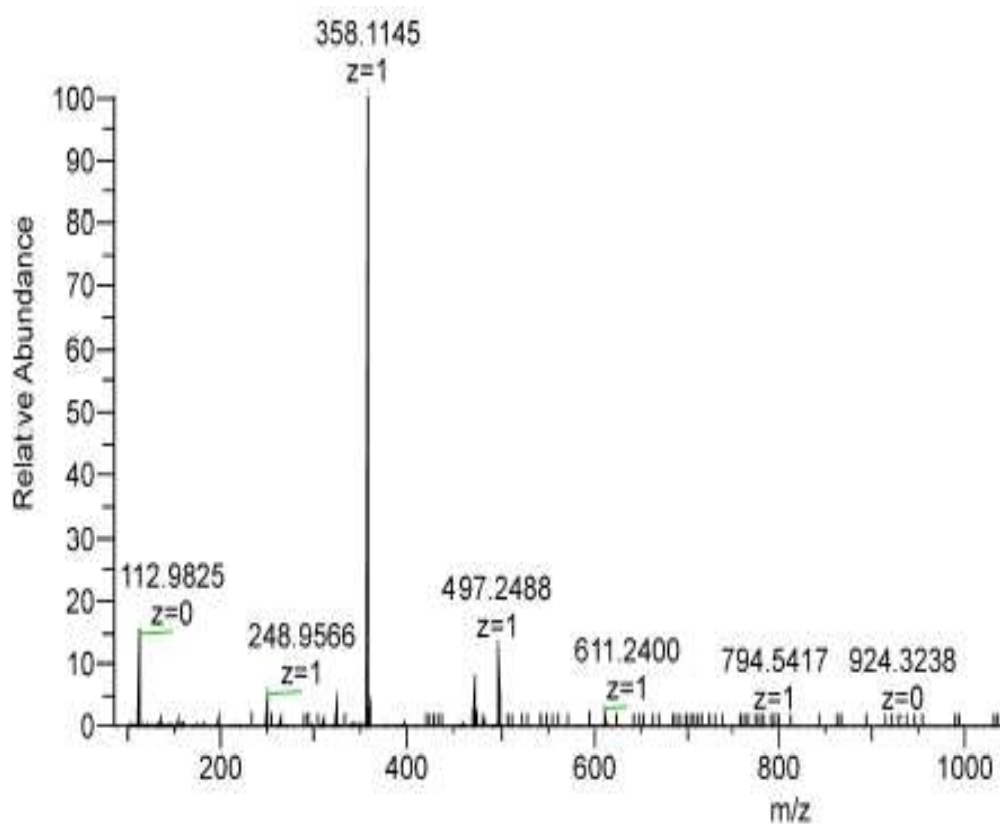


Figure-3.76: HRMS-MS (MS2) Spectra of DP-16

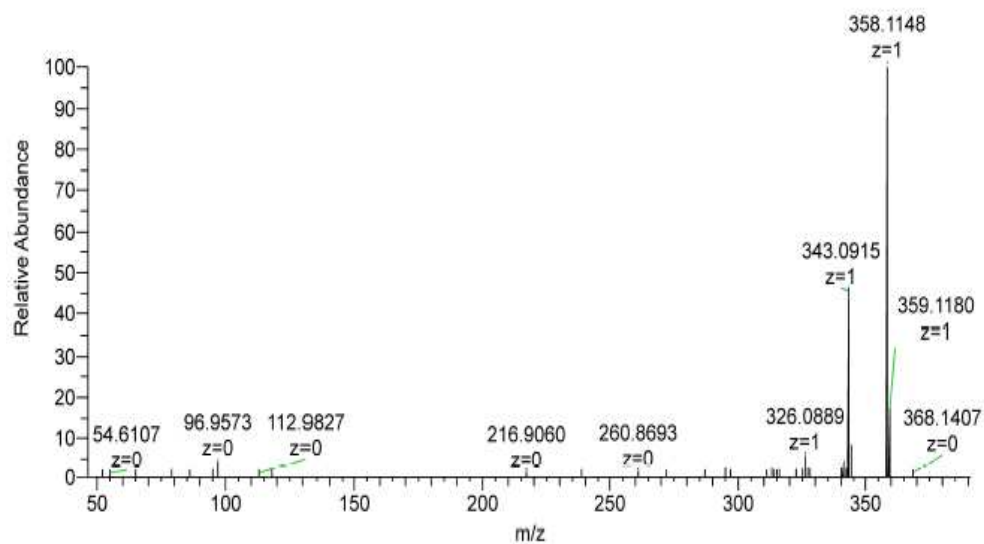
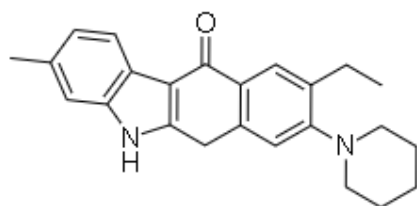


Figure-3.77: Fragmentation pattern of molecular mass 358.48500000265

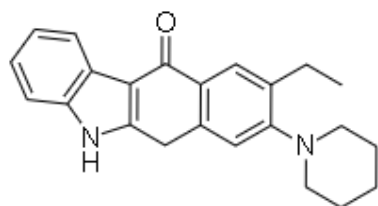
358.48500000265

9-ethyl-3-methyl-8-(piperidin-1-yl)-5,6-dihydro-11H-benzo[*b*]carbazol-11-one



344.4580000025

9-ethyl-8-(piperidin-1-yl)-5,6-dihydro-11H-benzo[*b*]carbazol-11-one



3.7 CONCLUSION

Stability indicating method for estimation of alectinib in presence of all the possible degradation products was developed and validation satisfactorily. It was all within the acceptance criteria. Forced degradation study was conducted extensively to identify the degradation products and possible degradants were isolated too. Degradation kinetics study was also performed to check which order of reaction the alectinib drug follows when it is degraded in oxidative degradation condition. Alectinib was found to generate sixteen degradation products in oxidative stress conditions. Initially, four degradation products (DP-1 to DP-4) was isolated and extensively characterized using LC-MS, MS-MS, NMR and FTIR spectroscopy. Later on, the stressed samples were also exposed to high resolution mass spectrometry, the MS and MS-MS data of other minor peaks (DP-5 to DP-16) were also detected and therefore, detailed structure elucidation of DP-5 to DP-16 were also carried out. Even though DP-1, DP-2, and DP-3 have the same molecular mass of 498, they are different molecules identified as N-oxide, epoxide, and N-hydroxy impurity respectively. The characteristic differences in their structures were confirmed through LC-MS, NMR, and FTIR spectra. Amongst all the DPs, DP-2 (epoxide impurity) was the most significant degradation product which can be easily produced when the drug substance was exposed to oxidative stress condition. Moreover, DP-4 (epoxide impurity) was having a different molecular mass than the previous three and confirmed as amide impurity. Moreover, during HRMS study, five other peaks (DP-9, DP-12, DP-13, DP-14 and DP-15) were identified with same molecular mass of 498 which also characterized based on MS and MS-MS spectra and discussed in individual DP section. The remaining seven degradation products namely DP-5, DP-6, DP-7, DP-8, DP-10, DP-11 and DP-16 were having molecular ion peaks at 515.2649, 503.2647, 533.2755, 517.2803, 362.1170, 377.1087, 358.1145 respectively which were also structurally elucidated based on MS and MS-MS spectra and elution pattern on the HRMS spectra as discussed in individual DP section.

SECTION-D: 3.8 QUANTITATIVE ESTIMATION AND VALIDATION OF ALECTINIB DRUG SUBSTANCE USING QUANTITATIVE NUCLEAR MAGNETIC RESONANCE SPECTROSCOPY

3.8.1 Introduction

Since alectinib is a recently approved anti-cancer drug, it is not official in many pharmacopoeias and therefore primary reference standard of alectinib is not available by them. The main advantage of a quantitative NMR method for the estimation of this drug is that this does not require primary reference standard. The quantitative estimation by NMR was reported as early as in 1963 by Forbes and Hollis [33-34], since then many reports have been published involving this concept. Nonetheless, even after that the quantitative estimation was not widely accepted until two decades ago when thorough demonstration of validation of Q-NMR method was proposed by G. Maniara et. al.[35]. Soon after that, the potential of NMR as quantitative tool in organic substances was proposed to Consultative Committee for Amount of Substance (CCQM) 1998 [36-37]. Since then, many reports were published in this realm using various nucleuses such as ^1H , and ^{31}P and accepted as a tool for quantitative estimation [38-39]. In ^1H quantitative NMR estimation technique, the proton signals of the known weighed compound are to be compared with the proton signals of known weighed internal standard. The basic principle of the estimation by Q-NMR is that the intensity of the ^1H NMR signal of the analyte is directly proportional to number of nuclei generating the response [40]. By applying correction factors of exact weights, molecular weights, theoretical proton values, obtained proton signal values, and potency of internal standard, the exact assay of a compound can be calculated.

As per literature search, many analytical methods are available for estimation of alectinib which involves lengthy chromatographic procedures and sample preparation [41-44]. To the best of our knowledge, no any method of quantitative NMR for estimation of assay of alectinib was available in literature hence this novel method was developed which comply well within the criteria of method validation as per ICH guidelines.

3.8.2 Experimental

3.8.2.1 Chemicals, reagents and Materials

The active pharmaceutical ingredient alectinib was procured from Sun Pharmaceuticals Industries Limited., Vadodara, India. The internal reference standard

ethyl 4-(dimethyl amino) benzoate was procured from Sigma-aldrich.

3.8.2.2 Instrumentation and analytical condition

3.8.2.2.1 Nuclear magnetic resonance spectrometry

The proton NMR experiments were performed on Bruker AVANCE 500 MHz NMR instrument. The probe temperature was set as 298K throughout experiment cycle. The chemical shifts of ^1H and ^{13}C spectra were recorded on delta scale in ppm with reference to tetra methyl silane (TMS). The axis of the scale was calibrated as 2.56 ppm for DMSO-d₆ peak in ^1H spectra and at 39.5 ppm for DMSO-d₆ peak in ^{13}C NMR spectra. 48 scans were collected for each sample with 66560 data points using a 30° pulse length; the spectral width 10000.00 Hz; pre-acquisition delay 6 ms and acquisition time 3.3280001 s. A delay time of 10 s between pulses was used to ensure full T1 relaxation of protons. High precision NMR tubes (5 mm diameter and 7-inch length) were used for all the experiments.

3.8.2.3 Sample preparation

3.8.2.3.1 Ethyl 4-(dimethyl amino) benzoate IS standard preparation for specificity

An accurately weighed 5.0 mg of ethyl 4-(dimethyl amino) benzoate standard was transferred in to NMR tube and dissolved in 0.6 mL of DMSO-d₆ diluent.

3.8.2.3.2 Alectinib sample preparation for specificity

An accurately weighed 10.0 mg of alectinib drug substance was transferred into NMR tube and dissolved in 0.6 mL of DMSO-d₆ diluent.

3.8.2.3.3 Alectinib sample preparation in presence of ethyl 4-(dimethyl amino) benzoate IS

An accurately weighed 2.0 mg of ethyl 4-(dimethyl amino) benzoate standard IS and 3.0 mg of alectinib drug substance were transferred into NMR tube and dissolved in 0.6 mL of DMSO-d₆ diluent.

3.8.2.3.4 Alectinib sample preparation in presence of ethyl 4-(dimethyl amino) benzoate IS for method validation parameters

An accurately weighed 2.0 mg of ethyl 4-(dimethyl amino) benzoate standard IS and varied quantity of alectinib drug substance (as shown in Table-4.20 and Table-4.21) were transferred into NMR tube and dissolved in 0.6 mL of DMSO-d₆ diluent.

3.8.2.3.4.1 System suitability

Although NMR instrument is very sensitive and specific, the proton signals peak shape and splitting pattern itself suggest the proper shimming and other appropriateness in NMR. However, as part of quantitative estimation, some instrumental observations could be set as system suitability parameters which must be within the limit for legitimate NMR spectra results. Such instrumental observations which could be considered as system suitability criteria are % relative standard deviation of the proton signal values obtained from replicate spectra should be not more than 2.0%, signal to noise ratio should be not more than 150, and the difference of delta ppm value of the analyte signal value should be not more than 0.2 ppm [45].

3.8.2.3.4.2 Linearity, LOD and LOQ

Triplicate sample solutions were prepared for each of 25%, 50%, 75%, 100%, 125% and 150% level of alectinib concentration.

3.8.2.3.4.3 Accuracy and Method precision

Triplicate sample solutions were prepared for each of 50%, 100% and 150% level of alectinib concentration. Sample weights were changed to achieve 50% and 150% level of alectinib concentration keeping IS weight constant so that change in proton signal value can be recorded and further calculation of changed assay can be done.

3.8.2.3.4.4 Robustness

Robustness study was carried out by challenging the different peak integration of the analyte as well as of the IS. In ¹H NMR spectra, all the proton signals vary slightly in terms of producing intensity of the proton signal. This slight variation in the proton signal should not affect the quantitation of the analyte. Hence, 1H signal at 3.9 ppm was integrated instead of 8.4 ppm for the analyte and 1H signal at 4.3 ppm was integrated instead of 6.7 ppm for the IS.

3.8.2.4 Estimation of alectinib by Q-NMR method

The amount of alectinib obtained and assay of the alectinib was calculated as per following equations [13]:

$$WtAna = \frac{I_{Ana} N_{Std} MW_{Ana}}{I_{Std} N_{Ana} MW_{Std}} WtStd \quad \text{----- (1)}$$

$$\%Assay = \frac{I_{Ana} N_{Std} MW_{Ana} WtStd}{I_{Std} N_{Ana} MW_{Std} WtAna} PStd \quad \text{----- (2)}$$

where WtAna= Weight of alectinib drug (mg), WtStd = Weight of internal standard (IS) (mg), IAna = Integral value of 1H signal due to analyte, IStd = Integral value of 1H signal due to internal Standard (IS) (2.0000), NAna = Theoretical integral value of 1H signal due to analyte (1.0000), NStd = Theoretical integral value of 1H signal due

to internal standard (IS) (2.0000), MW_{Ana} = Molecular weight of analyte (519.10 g/mole), MW_{Std} = Molecular weight of internal standard (193.24 g/mole), P_{Std} = Potency of internal standard (IS) (99.98%)

3.8.3 Results and discussion

3.8.3.1 Spectroscopic aspects of alectinib and ethyl 4-(dimethyl amino) benzoate (IS) with respect to proposed Q-NMR method

Even though ¹H NMR spectrum and assignment of proton signals to the various protons in the molecular structure is reported in the literature [46], Proton ¹H NMR spectrum was recorded for alectinib in diluent of DMSO-d₆ and the proton signals of ¹H spectrum of alectinib were tried to be correlated with its structure which is in agreement with the reported results [Figure-3.78, Figure-3.79], [Table-3.19]. Although many internal standards were available, ethyl 4-(dimethyl amino) benzoate (IS) was selected for this method due to (i) its high solubility in DMSO-d₆ solvent in which alectinib is also soluble, (ii) there are multiple ¹H signal peaks available separate from analyte signal which gives multiple choice of selection of different IS and analyte peaks, (iii) this IS not reactive with analyte or with the diluent. The crucial point that needs to be addressed while optimizing the Q-NMR method is that the signals due to analyte and internal standard must not be overlapped with each other at least in the region where both the peaks are to be selected for the calculation [47]. If this separation is not achieved in the ¹H NMR spectrum, the easiest way to achieve is to select alternative internal standard with similar solubility pattern so that difference in molecular structure can easily resonate ¹H signals in the different isolated regions in the spectrum. For identification of ¹H signals of ethyl 4-(dimethyl amino) benzoate (IS), certificate of analysis provided by Sigma-aldrich was referred which indicates that there are total 5 distinct ¹H signals observed in its ¹H NMR spectrum [48]. Each of these signals were tried to be correlated with its structure [Figure-3.80, Figure-3.81]. Although there are many separate ¹H NMR signals of analyte and IS, signals at 8.4 ppm and 6.7 ppm corresponding to analyte proton of alectinib and ethyl 4-(dimethyl amino) benzoate internal standard respectively were used for calculation of assay [Figure-3.82]. As per the ¹H NMR spectrum and molecular structure of alectinib, there are 5 aromatic protons available in the structure designated as 1, 4, 15, 16, and 18 which resonated between 7.0 ppm to 8.5 ppm. Furthermore, from the spectrum of Q-NMR it also evident that each of these proton peaks are clearly isolated

from the IS peak in the nearby region. In general, protons from clear aromatic and aliphatic regions are preferred choice as it is easy to identify and integrate such peaks due to their specific splitting pattern and resonance in specific region in the spectrum. Although the resonances between 1.2 ppm to 4.5 ppm were observed to be more or less overlapped with internal standard peaks and not chosen as the candidates for calculation by Q-NMR, selection of other potential proton signals were challenged in robustness study during method validation and found satisfactory.

Figure-3.78: Molecular structure of alectinib

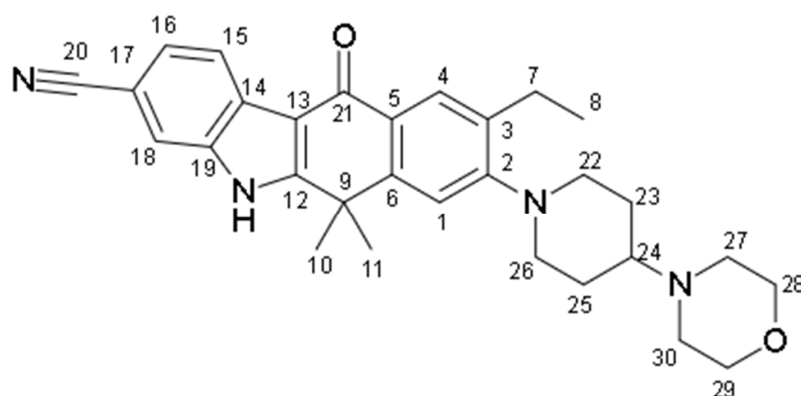
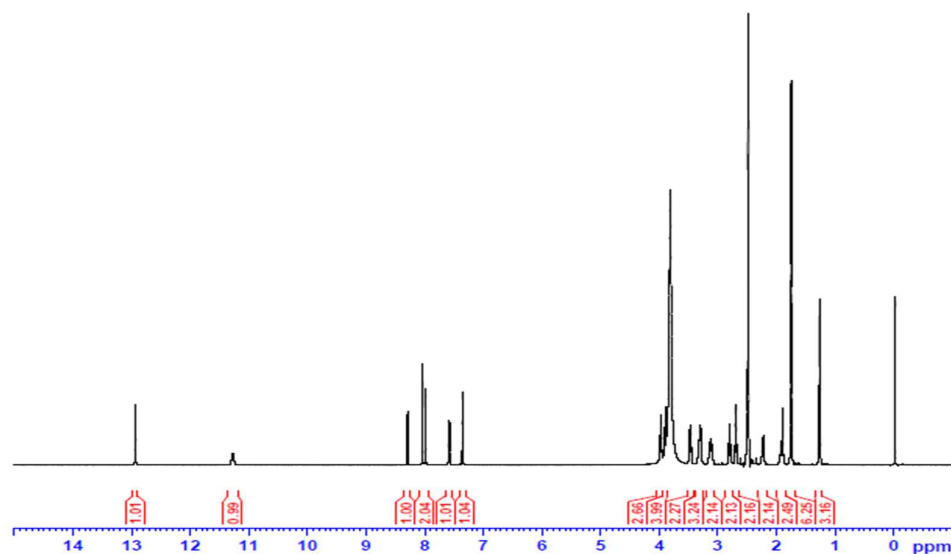
Figure-3.79: ^1H NMR spectrum of alectinib

Table-3.19: Spectroscopic aspects of ^1H NMR of alectinib

| Chemical shift (ppm) | Multiplicity | No. of protons | Assignment in structure |
|----------------------|--------------|----------------|-------------------------|
| 1.34 | Triplet | 3 | 8 |
| 1.82 | Singlet | 6 | 10, 11 |
| 1.90-4.20 | Multiplet | 19 | 7, 22 to 28, 29, 30 |
| 7.35-8.45 | Multiplet | 5 | 1, 4, 15, 16, 18 |
| 10.79 | Singlet | 1 | Hydrochloride |
| 12.88 | Singlet | 1 | NH |
| Total no. of protons | | 35 | - |

Figure-3.80: Molecular structure of ethyl 4-(dimethylamino) benzoate

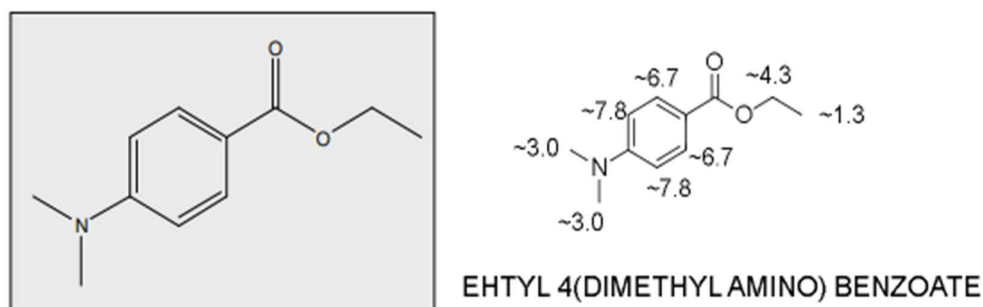
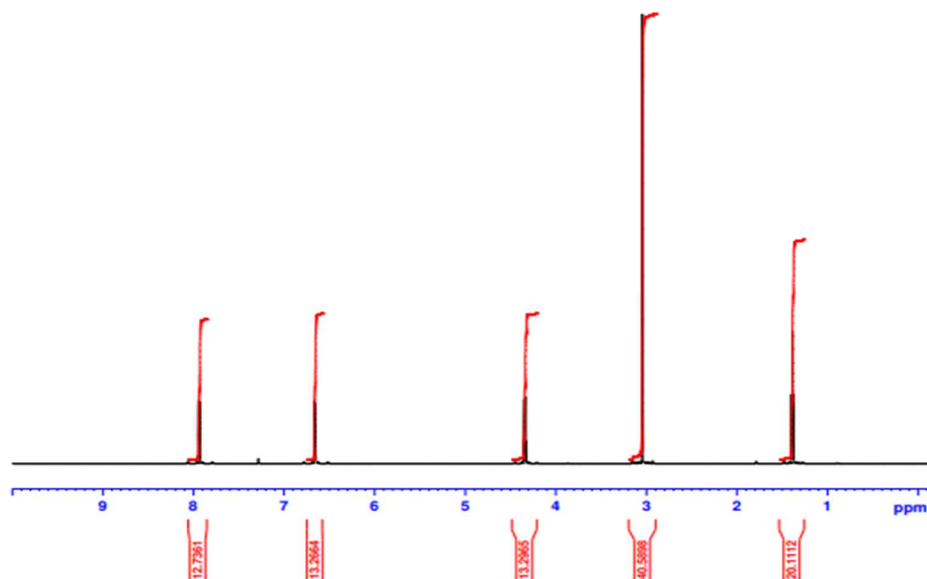
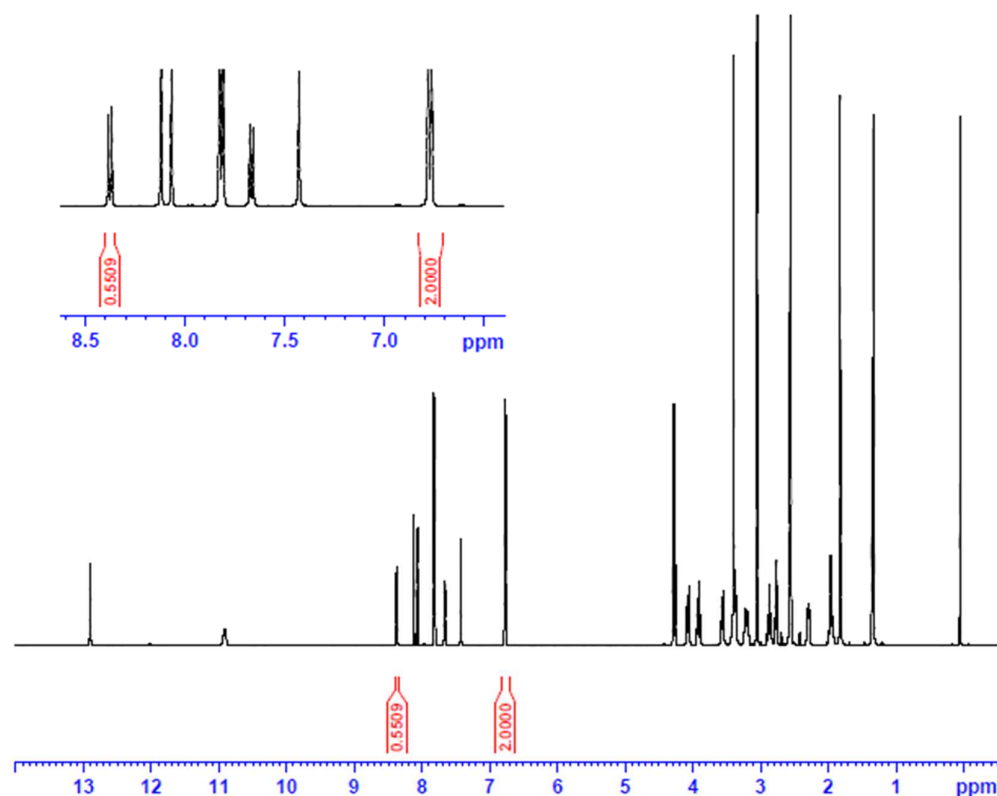
Figure-3.81: ^1H -NMR spectrum (600MHz, ethyl 4-(dimethyl amino) benzoate in CDCl_3) from certificate by Sigma aldrich

Figure-3.82: ^1H NMR spectrum of alectinib in presence of IS for Q-NMR at 100% level



3.8.3.2 Method validation

The method was validated as per International Conference on Harmonization (ICH) guidelines and following parameters were covered: system suitability, linearity, LOD, LOQ, accuracy, method precision, intermediate precision, range and robustness.

3.8.3.2.1 System suitability

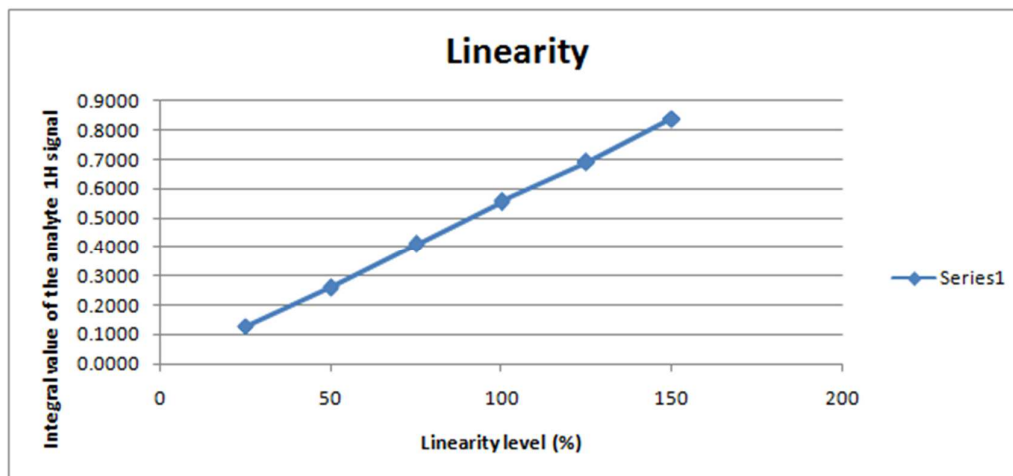
System suitability criteria of % relative standard deviation of all the applicable replicates were obtained less than 2.0% throughout all the validation parameter study. Moreover, the delta ppm value of the target signals of analyte as well as IS were also recorded and did not deviate more than 0.2 ppm.

3.8.3.2.2 Linearity

Linearity was performed by analyzing sample solutions containing alectinib concentration from 25% to 150% range each in triplicate. Linearity curve was plotted between weight of alectinib taken and the integral value of ^1H NMR signal at 8.4 ppm from the level of 25% to 150%. The equation of the curve was obtained as $y = 0.18220x - 0.00962$ and the correlation coefficient was found to be 0.9997 indicating

good linear response of the analyte proton signal [Table-3.20][Figure-3.83].

Figure-3.83 Calibration curve for linearity



3.8.3.2.3 LOD and LOQ

LOD and LOQ were determined by the value of standard deviation of the response (σ) and slope (S) from the linearity curve plotted from 25% to 150% level. The standard deviation (σ) and slope (S) was obtained to be 0.250568 and 0.18220 respectively, hence LOD and LOQ were calculated as per equation (1) and (2) and obtained as 4.54% and 13.75% level respectively.

$$\text{LOD} = \frac{3.3 * \sigma}{S} \quad \text{----- (3)}$$

$$\text{LOQ} = \frac{10 * \sigma}{S} \quad \text{----- (4)}$$

Table 3.20: Linearity results

| Linearity level | Sample weight (mg) | Integral value of the analyte 1H signal |
|-----------------|--------------------------------------|-----------------------------------------|
| 25% | 0.7550 | 0.1275 |
| 25% | 0.7561 | 0.1294 |
| 25% | 0.7521 | 0.1280 |
| 50% | 1.5070 | 0.2598 |
| 50% | 1.4810 | 0.2568 |
| 50% | 1.5125 | 0.2611 |
| 75% | 2.2440 | 0.4076 |
| 75% | 2.2612 | 0.4115 |
| 75% | 2.2589 | 0.4101 |
| 100% | 3.0990 | 0.5509 |
| 100% | 3.1250 | 0.5590 |
| 100% | 3.1514 | 0.5569 |
| 125% | 3.8600 | 0.6888 |
| 125% | 3.8972 | 0.6920 |
| 125% | 3.8200 | 0.6902 |
| 150% | 4.7030 | 0.8389 |
| 150% | 4.6159 | 0.8414 |
| 150% | 4.5985 | 0.8348 |
| | Standard deviation | 0.2506 |
| | Slope (S) | 0.18220 |
| | Intercept | -0.00962 |
| | Correlation Coefficient (r) | 0.9997 |

3.8.3.2.4 Accuracy and Method precision

As per ICH guidelines, accuracy and precision was established by analyzing nine different sample preparation of triplicate sample preparation at three different concentrations of 50%, 100% and 150%. Amount of drug added and amount of drug obtained was calculated and thereby %assay was calculated which were found to be well within the range between 96.54 to 97.68% and %RSD was also found to be

0.40% indicating the analytical method found to be accurate and precise [Table-3.21].

Table 3.21: Accuracy and Method precision test results

| Accuracy level | Amount of drug added (mg) | Amount of drug obtained (mg) | % Assay |
|---------------------------|---------------------------|------------------------------|---------|
| 50% Set-1 | 1.51 | 1.46 | 96.54 |
| 50% Set-2 | 1.48 | 1.43 | 96.79 |
| 50% Set-3 | 1.51 | 1.47 | 96.97 |
| 100% Set-1 | 3.10 | 3.02 | 97.35 |
| 100% Set-2 | 3.13 | 3.04 | 97.29 |
| 100% Set-3 | 3.15 | 3.07 | 97.35 |
| 150% Set-1 | 4.70 | 4.59 | 97.54 |
| 150% Set-2 | 4.62 | 4.51 | 97.68 |
| 150% Set-3 | 4.60 | 4.49 | 97.59 |
| Mean | | | 97.23 |
| Standard deviation | | | 0.39 |
| %RSD | | | 0.40 |

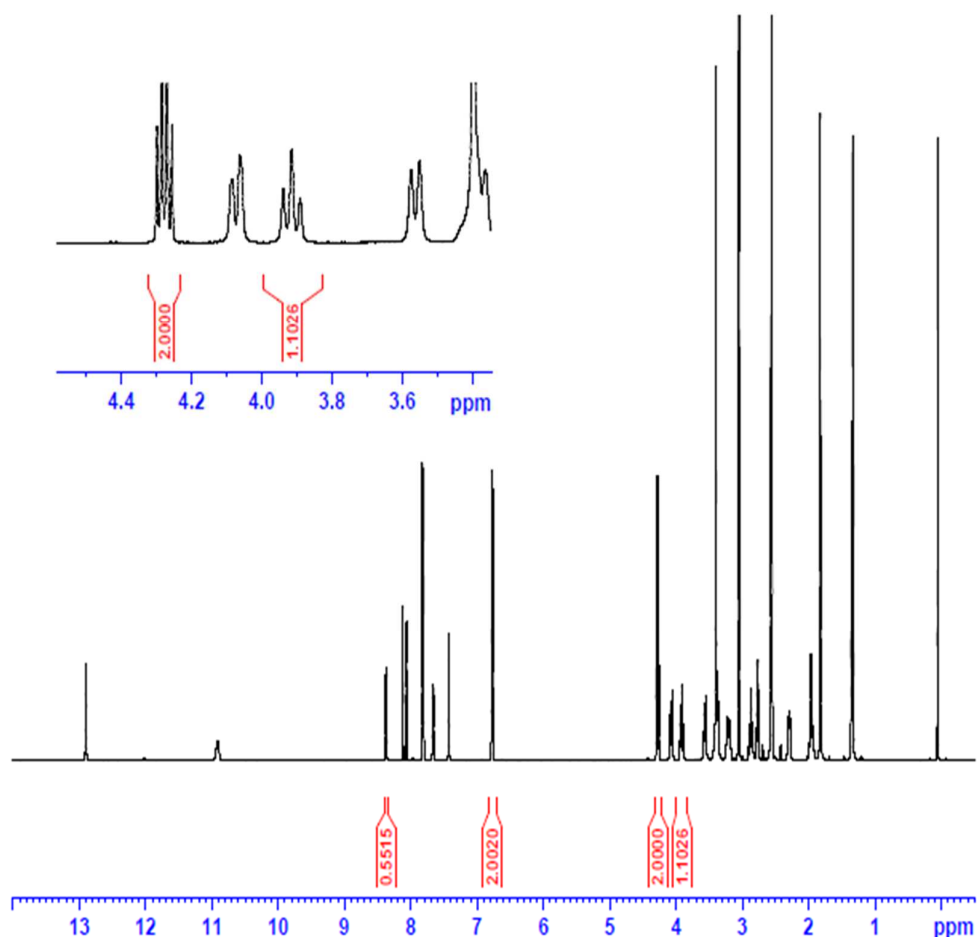
3.8.3.2.5 Range

From the results obtained from linearity, LOD, LOQ, accuracy, method precision, the range of the analytical method was obtained from 13.75% to 150% level concentration of alectinib.

3.8.3.2.6 Robustness

Even after selecting different 1H signal peak for the analyte as well as IS, the %assay was obtained 97.42% which is almost comparable to 97.33% as per initial analysis which indicates the different peak integration of the 1H peaks do not have major impact on quantitation of the alectinib [Figure-3.84].

Figure-3.84: ^1H NMR spectrum of alectinib in presence of IS for Q-NMR at 100% level but showing different peaks which can be integrated as part of robustness study



3.8.4 Conclusion

The analytical method for estimation of alectinib by quantitative NMR satisfied all the validation requirements as per ICH guideline such as linearity, method precision, accuracy, and robustness which proves that this method would be a good alternative to previously reported analytical methods of chromatography and other spectroscopy. Some advantages of the method are that Q-NMR is very rapid and does not require extensive solution preparation procedures as solid samples can directly be analyzed by the method and also does not involve costly and difficult to available primary reference standard of the analyte. These merits of this method make it really useful for the pharmaceutical industry to utilize this method in quality control and other pharmaceutical applications.

Note: Some content of this chapter has been published in the journal of separation

science plus by the authors [49].

3.9 REFERENCES:

1. WHO, factsheets details on cancer, <https://www.who.int/news-room/factsheets/detail/cancer>, (last time accessed: October 20, 2020).
2. The American Cancer Society medical and editorial content team, About lung cancer, https://www.cancer.org/cancer/lung-cancer/about/what-is.html#written_by, (last time accessed: October 20, 2020).
3. Fan J., Xia Z., Zhang X., Chen Y., Qian R., Liu S., You D., Zhang J., Luo P., The efficacy and safety of alectinib in the treatment of ALK+ NSCLC: a systematic review and meta-analysis. *OncoTargetsTher.* 2018, *11*, 1105–1115.
4. Huang X., Li Y., Li X., Hu X., Tang P., Hu G., An UPLC–MS/MS method for the quantitation of alectinib in rat plasma. *J. Pharm. Biomed. Anal.* 2017, *132*, 227-231.
5. <https://www.fda.gov/drugs/resources-information-approved-drugs/alectinib-approved-alk-positive-metastatic-non-small-cell-lung-cancer-nsclc>, (last time accessed: December 04, 2020).
6. McKeage K., Alectinib: a review of its use in advanced ALK-rearranged non-small cell lung cancer. *Drugs*, 2015, *75*, 75-82.
7. I.C.H. Q1A (R2), Stability testing of new drug substances and products. ICH harmonised tripartite guideline, International conference on harmonisation of technical requirements for registration of pharmaceuticals for human use, 2003.
8. I.C.H. Q1B, Stability testing: photo-stability testing of new drug substances and products. ICH harmonised tripartite guideline, International conference on harmonisation of technical requirements for registration of pharmaceuticals for human use, 1996.
9. Bommuluri V., Vajjha S., Rumalla C., Doddipalla R., Kaliyaperumal M., Korupolu R., Choppela V., Isolation, identification and structural interpretation of degradation impurities in idelalisib. *Sep. Sci. plus.* 2020, *3*, 330-339.
10. I.C.H. Q3A (R2), Impurities in new drug substances, ICH harmonised tripartite guideline, International conference on harmonisation of technical requirements for registration of pharmaceuticals for human use, 2006.
11. I.C.H. Q3B (R2), Impurities in new drug product, ICH harmonised tripartite guideline, International conference on harmonisation of technical requirements

- for registration of pharmaceuticals for human use, 2006.
12. I.C.H. Q6A, Specifications: Test procedures and acceptance criteria for new drug substances and new drug products: Chemical substances, ICH harmonised tripartite guideline, International conference on harmonisation of technical requirements for registration of pharmaceuticals for human use, 1999.
 13. Belide P., Mounica P., RP-HPLC method development and validation for estimation of alectinib in bulk and pharmaceutical dosage form. *International J. of Pharmacy and Analytical Research*, 2019, 8, 293-300.
 14. Y P., Rao T.N., Srinivas Y., Method development and validation of alectinib drug by RP-HPLC in bulk and pharmaceutical dosage form. *Asian J. Pharm. Ana.* 2018; 8, 186-190.
 15. Lee S., Nath C.E., Balzer B.W.R., Lewis C.R., Trahair T.N., Anazodo A.C., Shaw P.J., An HPLC–PDA method for determination of alectinib concentrations in the plasma of an adolescent. *ActaChromatogr.* 2019, 32, 166-169.
 16. Srikanth, Rani P., HPLC-MS/MS method development and validation for determining stability of alectinib in human plasma samples. *Int. J. Curr. Res.* 2017, 9, 51506-51511.
 17. Ara S., Al-Qudah E., Alzweiri M., Sweidan K., New forced degradation products of vildagliptin: identification and structural elucidation using LC-MS, with proposed formation mechanisms. *J. Liq. Chromatogr. Relat. Technol.* 2020, 43, 633-644.
 18. Leite H.O.A, Kassab N.M., Prado M.S.A., Singh A.K., Stability-indicating methods applied in the separation and characterization of the main degradation product of propafenone. *Sep. Sci. plus.* 2018, 1, 490-497.
 19. Katakam L.N.R., Dongala T., Quality by design with design of experiments approach for the development of a stability-indicating LC method for benzonatate and its impurities in liquid oral dosage form. *Sep. Sci. plus.* 2020, 3, 276-285.
 20. Parmar P.J., Patel V.B., Shah D.A., Stability indicating LC method for estimation of valbenazine and its degradation kinetic study. *Sep. Sci. plus.* 2020, 3, 94-101.
 21. Baghel M., Rajput S., Degradation and impurity profile study of ciclopiroxolamine after pre-column derivatization: a risk based approach. *J. Chromatogr. Sci.* 2017, 55, 899-910.
 22. Sato-Nakai M., Kawashima K., Nakagawa T., Tachibana Y., Yoshida M.,

- Takanashi K, Morcos P., Binder M., Moore D., Yu Li., Metabolites of alectinib in human: their identification and pharmacological activity. *Heliyon*. 2017, 3, 1-18.
23. https://www.ema.europa.eu/en/documents/assessment-report/alecensa-epar-public-assessment-report_en.pdf (last time accessed: December 15, 2020).
24. https://www.accessdata.fda.gov/drugsatfda_docs/label/2017/208434s003lbl.pdf (last time accessed: December 15, 2020).
25. Ibrahim H., Couderc F., Perio P., Collin F., Nepveu F., Behavior of N-oxide derivatives in atmospheric pressure ionization mass spectrometry. *Rapid Commun. Mass Spectrom.* 2013, 27, 621–628.
26. Kalariya P.D., Talluri M.V.N.K., Patel P.N., Srinivas R., Identification of hydrolytic and isomeric N-oxide degradants of Vilazodone by on line LC-ESI-MS/MS and APCI-MS. *J. Pharm. Biomed. Anal.* 2015, 102, 353-365.
27. Ma S., Chowdhury S.K., Alton K.B., Thermally induced n-to-o rearrangement of tert-n-oxides in atmospheric pressure chemical ionization and atmospheric pressure photoionization mass spectrometry: differentiation of n-oxidation from hydroxylation and potential determination of n-oxidation site. *Anal. Chem.* 2005, 77, 3676-3682.
28. Ramanathan R., Su A.-D., Alvarez N., Blumenkrantz N., Chowdhury S. K., Alton K., Patrick J., Liquid Chromatography/Mass Spectrometry Methods for Distinguishing N-Oxides from Hydroxylated Compounds. *Anal. Chem.* 2000, 72, 1352–1359.
29. Ramulu K., Thilak Kumar T., Radha Krishna S., Vasudev R., Kaviraj M., Rao B. M., Someswara Rao N., Identification, isolation and characterization of potential degradation products in pioglitazone hydrochloride drug substance. *Pharmazie*, 2010, 65, 162–168.
30. Kamata K., Ishimoto R., Hirano T., Kuzuya S., Uehara K., Mizuno N., Epoxidation of alkenes with H₂O₂ catalyzed by selenium-containing dinuclearperoxotungstate and kinetic, spectroscopic, and theoretical investigation of the mechanism. *Inorg. Chem.* 2010, 49, 2471-2478.
31. Takakusa H., Wahlin M.D., Zhao C., Hanson K.L., New L.S., Chan E.C.Y., Nelson S.D., Metabolic intermediate complex formation of human cytochrome p450 3a4 by lapatinib. *Drug Metab. Dispos.* 2011, 39, 1022-1030.
32. McIsaac J.E., Ball R.E., Behrman E. J., Mechanism of the base-catalyzed

- conversion of nitriles to amides by H_2O_2 . *J. Org. Chem.* 1971, **36**, 3048-3050.
33. J. L. Jungnickel, J. W. Forbes, Quantitative Measurement of Hydrogen Types by integrated Nuclear Magnetic Resonance Intensities, *Anal. Chem.*, 1963, **35**, 938–942.
34. D. P. Hollis., Quantitative Analysis of Aspirin, Phenacetin, and Caffeine Mixtures by Nuclear Magnetic Resonance Spectrometry, *Anal. Chem.*, 1963, **35**, 1682–1684.
35. Maniara G, Rajamoorthi K, Rajan S and Stockton G W, Method performance and validation for quantitative analysis by $(1)H$ and $(31)P$ NMR spectroscopy. Applications to analytical standards and agricultural chemicals, *Anal. Chem.*, 1998, **70**, 4921, DOI: 10.1021/ac980573i
36. Report of the 4th Meeting (Feb 1998), Consultative Committee for Amount of Substance (CCQM) (<https://www.bipm.org/utils/common/pdf/CC/CCQM/CCQM4.pdf>)
37. Takeshi Saito , Taichi Yamazaki and Masahiko Numata, Development of nuclear magnetic resonance as a tool of quantitative analysis for organic materials, *Metrologia*, 2019, **56(5)**, DOI: <https://doi.org/10.1088/1681-7575/ab348d>
38. Wells R J, Hook J M, Al Deen T S and Hibbert D B, Quantitative Nuclear Magnetic Resonance (QNMR) Spectroscopy for Assessing the Purity of Technical Grade Agrochemicals: 2,4-Dichlorophenoxyacetic Acid (2,4-D) and Sodium 2,2-Dichloropropionate (Dalapon Sodium), *Agric. Food Chem.*, 2002, **50**, 3366–3374, DOI: 10.1021/jf0114379
39. Saito T, Nakaie S, Kinoshita M, Ihara T, Kinugasa S, Nomura A and Maeda T, Practical guide for accurate quantitative solution state NMR analysis, *Metrologia*, 2004 , **41**, 213–218, DOI: 10.1088/0026-1394/41/3/015
40. Pedro Henrique Cavalcanti Franco, SauloFehelberg Pinto Braga, Renata Barbosa de Oliveira, Isabela Costa César, Purity determination of a new antifungal drug candidate using quantitative 1H NMR spectroscopy: Method validation and comparison of calibration approaches, *MagnReson Chem.*, 2019, 1–9, DOI: 10.1002/mrc.4936
41. Xiang-xin Huang; Yun-xuan Li; Xiang-yu Li; Xiao-xia Hu; Peng-fei Tang; Guo-xin Hu. An UPLC–MS/MS method for the quantitation of alectinib in rat plasma, *A J. of Pharm. and Biomed. Analysis*, 2017, **132**, 227-231. DOI

- 10.1016/j.jpba.2016.10.010
42. Pavanibelide; P.Mounica. RP-HPLC method development and validation for estimation of alectinib in bulk and pharmaceutical dosage form, *International J. of Pharmacy and Analytical Research*, 2019, **8(3)**, 293
43. Samiuela Lee; Christa E. nath; Ben W. R. Balzer; Craig R. Lewis; Toby N. Trahair; Antoinette C. Anazodo; and Peter J. Shaw. An HPLC–PDA method for determination of alectinib concentrations in the plasma of an adolescent, *ActaChromatographica*, 2019, **32**, 166, DOI 10.1556/1326.2019.00578
44. Y Prashanthi; TentuNageswara Rao; Yellapu Srinivas, Method Development and Validation of Alectinib Drug by RP-HPLC in Bulk and Pharmaceutical Dosage Form, *Asian Journal of Pharmaceutical Analysis*, 2018, **8(4)**, 186-190, DOI: 10.5958/2231-5675.2018.00034.0
45. Hemant Gadape and Kalpesh Parikh, Quantitative determination and validation of Carvedilol in pharmaceuticals using quantitative nuclear magnetic resonance spectroscopy, *Analytical methods*, 2011, **3**, 2341-2347, DOI: 10.1039/c1ay05247k
46. Mika Sato-Nakai, Kosuke Kawashima, Toshito Nakagawa, Yukako Tachibana, Miyuki Yoshida, Kenji Takanashi, Peter N. Morcos, Martin Binder, David J Moore, Li Yu. Metabolites of alectinib in human: their identification and pharmacological activity. *Heliyon*, 2017, **3 (2017)**, e00354. doi: 10.1016/j.heliyon.2017. e00354
47. Xianrui Liang, Liping Du, Feng Su, Harendra S. Parekh and Weike Su, The application of quantitative NMR for the facile, rapid and reliable determination of clindamycin phosphate in a conventional tablet formulation, *Magn. Reson. Chem.*, 2014, **52**, 178–182, DOI: DOI 10.1002/mrc.4048
48. [https://www.sigmaaldrich.com/catalog/CertOfAnalysisPage.do?symbol=42582&LotNo=BCBH6276V&brandTest=FLUKASUPPORTING INFORMATION](https://www.sigmaaldrich.com/catalog/CertOfAnalysisPage.do?symbol=42582&LotNo=BCBH6276V&brandTest=FLUKASUPPORTING_INFORMATION), accessed on 22-Nov-2020.
49. Parmar, R, Rajput, S, Mohan, A. Identification, isolation and structure elucidation of novel forced degradation products of alectinib hydrochloride. *Sep Sci plus*. 2021; 4: 174– 184. <https://doi.org/10.1002/sscp.202000104>